THE BIOCHEMICAL ANALYSIS OF MUCUS AND MUCINS IN RESPIRATORY DISEASES WITH A FOCUS ON TUBERCULOSIS

Thesis Presented for the Degree of

DOCTOR OF PHILOSOPHY

Department of Surgery

UNIVERSITY OF CAPE TOWN

February 2016

Supervisor: Prof. Anwar Suleman Mall

Declaration

I, **Henrietta Refiloe Mofokeng**, hereby declare that the work on which this dissertation/thesis is based is my original work (except where acknowledgements indicate otherwise) and that neither the whole work nor any part of it has been, is being, or is to be submitted for another degree in this or any other university.

I hereby grant the University of Cape Town free licence to reproduce this thesis in whole or in part, for the purpose of research.

Signature: Signed by candidate

Signature removed

Date: 15 February 2016

Dedication

I dedicate this thesis to my mom (Domina),

my dad (Anthony), my sister (Antoinette)

and my brother (Bashi).

With much love!

Acknowledgements

First and foremost, I would like to thank my heavenly Father for the strength He has given me to complete the project. It really has been a long journey.

I would like to express my sincere gratitude to the following people for their contribution towards the success of the project.

I am grateful mainly to the National Research Foundation for financial assistance they provided for the project and the Health and Welfare SETA (HWSETA) for financial assistance to complete the project.

I express my gratitude to my supervisor Prof. Anwar Suleman Mall, for accepting my request to do the research. I thank him for his constant guidance, wisdom, support and encouragement. I extend my gratitude to Prof. Delawir Kahn, for his support, encouragement and giving ideas around the project. According to his classification, we have passed gold stage to platinum.

To my fellow lab family, I have no words. Thanks to Mrs. Zoe Lotz, Mrs. Marilyn Tyler and Mrs. Lizette Fick for the assistance with techniques around the lab. I am a better person because of you. Not only did I learn lab techniques but I discovered by passion for cooking and baking, and picked up some life lessons. To my fellow lab mates, Julia, Yolanda, Sam, Rufaro and Baxolele, you made each day in the lab worthwhile. One thing I do miss about the lab is the company and Friday tea sessions.

I thank Groote Schuur hospital, DP Marais hospital, Gugulethu clinic, Seeisoville clinic and Thusanong clinic for granting access to their facilities for the collection of sample. To Prof. Keertan Dheda, for assistance with sample collection and advice. To the staff at respective facilities, thank you. A big thank you to the department of anaesthesia, especially Dr. Marcus Rademeyer, for the collection of tracheal aspirates from patients who underwent surgery.

To Prof. Bongani Ndimba from the University of the Western Cape, thank you for the permission to use your lab for the proteomics part of project. To Dr. Salome Smit from the Central Analytical Facility at the Stellenbosch University, for assisting me in obtaining the identities of the proteins and assisting with the troubleshooting of O-glycan release. A very big thank you to Dr. Jeronimo (Jerry) Rodriguez for assisting with the amino acid analysis; and Prof. Dhiren Govender for assisting with the analysis of the work on immunohistochemistry. His expertise advice as a pathologist was high appreciated. A heartfelt thank you to Dr. Niclas Karlsson and Dr. Chunsheng Jin at Gothenburg University in Sweden, for conducting the O-glycan analysis. Without your assistance the O-glycan analysis would be at the optimising stages. To Dr. Jackson Marakalala and Dr. Claudius Marondedze, for proofreading the work.

Last but not least, I'm grateful for the support I have received from my family throughout this long journey. To my friends for their continued support and encouragement. The time we lost shall be regained.

Table of Contents

List of Figures

List of Tables

List of abbreviations

1D SDS PAGE	One dimensional sodium dodecyl sulphate polyacrylamide gel electrophoresis
2D SDS PAGE	Two dimensional sodium dodecyl sulphate polyacrylamide gel electrophoresis
AB	Alcian Blue
AgPAGE	Agarose polyacrylamide gel electrophoresis
APS	Ammonium Persulphate
BALs	Bronchoalveolar lavages
CHAPS	3-[(3-Cholamidopropyl) dimethylammonio]- 1-propanesulfonate
CsCl	Caesium chloride
DAB	Diaminobenzidine
Et al	et alia
ddH20	Double distilled water
DTT	Dithiothreitol
ECL	Enzyme chemiluminescence
EDTA	Ethylenediaminetetraacetic acid
ELISA	Enzyme-linked immunosorbent assay
FBS	Fetal bovine serum
GalNAc	N-acetyl galactosamine
GlcNAc	N-acetyl glucosamine
GuHCl	Guanidinium hydrochloride
H & E	Haematoxylin and eosin
HID	High iron diamine
HCl	Hydrochloric acid
HIV	Human immunodeficiency virus

HPLC	High performance liquid chromatography
HRP	Horseradish peroxidase
IEF	Isoelectric focusing
IPG	Immobilized pH gradient
kDa	Kilo Daltons
kVh	Kilo Volt-hours
LC-ESI-MS	Liquid chromatography electrospray ionisation – mass spectrometry
M	Molar
M.tb	Mycobacterium tuberculosis
MALDI-TOF	Matrix assisted laser desorption ionization time of flight
MW	Molecular Weight
m/z	Mass per charge
ml	Millilitre
mm	Millimetre
mM	Millimolar
MUC	Mucin
MW	Molecular weight cut-off
NaCl	Sodium chloride
NaOH	Sodium hydroxide
NaBH4	Sodium borohydride
OPA	O-phthalaldehyde
P	Proline
PAS	Periodic acid Schiff
pI	Isoelectric point
PMSF	Phenylmethanesulfonylfluoride
PVDF	Polyvinyl difluoride

RT	Room temperature
S	Serine
SDS	Sodium dodecyl sulphate
SSC	Saline sodium citrate buffer
T	Threonine
TAE	Tris base, acetic acid
TB	Tuberculosis
TBS	Tris-buffered saline
TBST	Tris-buffered saline and Tween-20
TCA	Trichloroacetic acid
Tris	Tris (hydroxymethyl) aminomethane
Tris-HCl	Tris hydrochloric acid
TEMED	N, N, N1,N1- Tetra methylethelene-diamine
µg	Microgram
µg/µl	Microgram per microlitre
µl	Microlitre
V	Volts
v/v	Volume per volume
w/v	Weight per volume
WHO	World Health Organisation

Abstract

Respiratory diseases are a major cause of death in South Africa, with TB being one of the major respiratory illnesses. The respiratory tract is lined by a layer of mucus which protects the airways and lungs against injury by foreign agents. The main constituents of this layer of mucus are mucins. MUC5AC and MUC5B are the predominant respiratory tract mucins. However, little is known of the association between respiratory mucins and TB. This study aimed at describing the types and role of respiratory mucins in TB.

Fifty six sputum samples, 17 tracheal aspirates and 95 bronchoalveolar lavages (BALs) were collected in 6M guanidinium hydrochloride and inhibitors. The airway mucus was divided into TB and non-TB groups. Mucins were reduced and alkylated with DTT and iodoacetamide and purified by density gradient ultracentrifugation in caesium chloride. Identification of MUC5AC, MUC5B, MUC2 and MUC7 were determined by western blotting and confirmed by immunohistochemistry.

Western blot data proved the dominance of MUC5AC and MUC5B mucins in airway mucus. In comparison to the non-TB group, a higher secretion of MUC5AC than MUC5B in patients with TB was observed. MUC5AC also showed distinct behavioural characteristics in its fractionation in a caesium gradient compared to MUC5B. The presence of MUC5AC and MUC5B in different fractions suggests varying glycosylation of the mucin. Varying populations of MUC5B were observed in sputa with 3 new glycoforms shown in TB. A small group of TB patients had MUC7 in the sputa (and not in the lavage) and there were varying amounts of MUC2 in some TB samples and non-TB mucus. At tissue level, MUC5B was found to be the main secreted gel-forming mucin. MUC5B and MUC7 were found to play a role in the protection again infection by Mycobacterium tuberculosis in tuberculous granulomas. Using proteomics it was demonstrated that respiratory mucus protein expression differs in, tracheal aspirates, BALs and sputa. Although inter-individual variations were observed in all samples, similar proteins were expressed in relation to the functioning of the lung. O-glycan analysis showed that the majority of the O-glycans detected were sialylated and that core 3 and 4 O-glycan structures diminished in the presence of HIV.

CHAPTER 1 : INTRODUCTION AND LITERATURE REVIEW

1.1 Background

Mucus is a slippery secretion that coats the epithelial surfaces of the eyes, middle ear, the respiratory, gastrointestinal and urogenital tracts (Linden *et al.*, 2008). It is produced and secreted by mucous membranes, typically the mucous glands distributed in the body. Mucus serves as a lubricant as it keeps the epithelium hydrated and for the transportation and passage of food (Ali and Pearson, 2007). Additionally, it is a permeable gel layer for the exchange of gases and nutrients (Almutairi *et al.*, 2016). The mucus is the body's primary barrier against inhaled particles including pathogens and other infectious agents.

In the respiratory tract, the body produces mucus in an attempt to expel the microbes and inhaled particles (Bansil and Turner, 2006) The respiratory tract is generally exposed to dust, toxic gases and microorganisms through air that has been inhaled. Injury or damage to the respiratory tract as a result of these inhaled particles may result in respiratory infections and diseases. The attachment of microbes to the respiratory tract can present the initial step in the development of lung infection.

Studying the composition of respiratory mucus in disease will ultimately lead to understanding the pathogenesis of diseases. Respiratory diseases are one of the major causes of morbidity and mortality in the world with South Africa experiencing a rapid increase in tuberculosis epidemic (Mayosi *et al.*, 2009; Nie *et al.*, 2013; van Zyl Smit *et al.*, 2010). In 2014, South Africa recorded a high incidence rate of TB with 834 cases per 100 000 population recorded by the World Health Organisation (WHO) (WHO, 2015). In addition, the number of deaths attributable to TB among human immunodeficiency virus were 59 per 100 000 population. The high mortalities related to TB have increased the urgency in the understanding of the properties of respiratory mucus in TB.

1.2 Lower respiratory tract mucus

The lower respiratory tract epithelium extends from the trachea and terminates at the bronchioles. It is lined by basal, clara, ciliated, goblet, neuroendocrine (kulchitsky), brush and serous cells (Colby et al., 2007). The airway mucus is produced by the goblet cells and submucosal glands containing serous and mucous cells. Furthermore, ciliated cells and goblet cells decrease in number as the terminal bronchioles are approached.

The lower airway mucus is continuously secreted, utilized by the body and then discarded or recycled. Proposed by Lucas and Douglas in 1934, mucus is composed of two layers. The first layer which is approximately 7 μm in depth is the periciliary fluid layer (also known as the sol phase) that is situated on top of the epithelial cilia (Kim, 1997; Rubin, 2010a; Rubin, 2010b). The second layer overlies the sol phase and is called the mucus layer, also known as the gel phase (Kim *et al.*, 1997; Lai *et al.*, 2009). The mucus gel generally has a neutral pH with a thickness varying between 5 μm and 50 μm (Evans *et al.*, 2009; Lai *et al.*, 2009). The function of the periciliary fluid layer is to protect the underlying epithelium and keeps the mucus gel hydrated.

The mucus has a short lifespan as it is replaced every 10 to 20 minutes (Lai *et al.*, 2009). The lower respiratory mucus is a complex mixture mainly composed of water, approximately 97% (Lu and Zheng, 2013). The remaining 3% of solids is composed of enzymes, lysozymes, defensins, cytokines, inorganic salts, proteins, immunoglobulins, glycoproteins (known as mucins), lipids and cellular debris (Bansil and Turner, 2006; Fahy and Dickey, 2010; Vareille *et al.*, 2011). The mucus is formed in the Golgi apparatus and secreted in vesicles.

1.3 Mucus as a barrier

The main and most crucial function of the lower respiratory mucus is to be the first line of defense against inhaled particles. In addition to the ciliated cells and goblet cells, the respiratory mucus contains lactoferrins, lysozyme, collectins and defensins (Kato *et al.*, 2015; Vareille *et al.*, 2011). Activation of these proteins upon infection, elicit an innate immune response.

Although airway mucus is mainly composed of water, it has viscoelastic and adhesive properties. These properties are conferred by the cross-linked and entangled mucus glycoproteins (mucins) secreted by goblet cells and submucosal glands (Lai *et al.*, 2009). Mucins play a pivotal role in the mucosal defense by trapping inhaled particles and binding bacteria through the adhesions on the bacterial membranes (Sonawane *et al.*, 2012; Widdicombe, 1995). The trapped particles are cleared from the airways through constant coordinated ciliary beating and airflow, a mechanism known as mucociliary clearance, towards the larynx (Ali and Pearson, 2007; Curran and Cohn, 2010; Randell and Boucher, 2006). Mucus clearance is essential for respiratory health as it allows for the expulsion of inhaled particles and pathogens from the airways. Healthy mucus has low viscosity and elasticity which is essential in mucociliary clearance, which is dependent on the thickness of mucus (Ali and Pearson, 2015; Fahy and Dickey, 2010).

1.4 Mucins

1.4.1 Mucin definition and nomenclature

Mucins are the major components of mucus largely responsible for its biological properties (Andersch-Bjorkman *et al.*, 2007; Bansil and Turner, 2006; Thornton *et al.*, 1990). They are high molecular weight glycoproteins ranging between 2 to 50 MDa and they contain up to 80% carbohydrate by weight (Bansil and Turner, 2006; Ridley *et al.*, 2014; Thornton *et al.*, 2008). Mucins, also called MUCs, acquired their name from the gene that encodes their protein backbone (apomucin). They are named according to their order of discovery (Ali and

Pearson, 2007). According to the HUGO Gene Nomenclature Committee (HGNC) 21 genes encoding mucins have been identified through cDNA cloning. Mucin genes have long stretches of variable number of tandemly repeated nuclucleotides, a region known as variable number of tandem repeats (VNTR) (Rose and Voynow, 2006). Owing to the latter characteristic, mucins are highly polymorphic.

Two classes of mucins have thus far been reported based on their chromosomal localization and amino acid sequence. The first class is located at the cell surface and is known as membrane bound or transmembrane mucins. The other class is secreted and is subdivided into gel forming and non-gel forming. The locations of the MUC genes are outlined in Table 1.1. (HGNC, 2013; Rose and Voynow, 2006).

Table 1.1: Location of the human mucin genes on the chromosome

MUC Gene	Chromosome Locus
MUC1	1q21
MUC13	3q13.3
MUC4	3q29
MUC20	3q29
MUC7	4q13.3
MUC21	6p21.33
MUC22	6p21.33
MUC3A	7q22.1
MUC3B	7q22
MUC11	7q22
MUC12	7q22
MUC17	7q22
MUC15	11p14.3
MUC2	11p15.5
MUC5AC	11p15.5
MUC5B	11p15.5
MUC6	11p15.5
MUC18	11q23.3
MUC19	12q12
MUC8	12q24.3
MUC16	19q13.2

(Compiled from Corfield, 2015; HGNC, 2015; Rose and Voynow, 2006)

1.4.2 Membrane bound mucins

Membrane bound mucins are intercalated in the plasma membrane through a transmembrane domain (Hattrup and Gendler, 2008). This type of mucin is thought to be monomeric. They comprise of an extracellular domain mainly composed of glycosylated tandem repeat region, a single membrane-spanning domain and a short cytoplasmic tail (Hattrup and Gendler, 2008). Furthermore, the cytoplasmic domain is thought to play a role as a molecular sensor and is involved in signal transduction pathways (Backstrom *et al.*, 2013). To date this group consists of MUC1, MUC3A, MUC3B, MUC4, MUC11, MUC12, MUC13, MUC15, MUC16, MUC17 and MUC20.

1.4.3 Secreted mucins

This group of mucins is subdivided into two groups, namely, the secreted gel-forming and secreted non gel-forming. Eight mucin glycoproteins have been reported to be secreted. MUC2, MUC5AC, MUC5B, MUC6 and MUC19 are classified as secreted polymeric gel-forming mucins rich in cysteine residues (Kreda *et al.*, 2012; Rose and Voynow, 2006). Gel-forming mucins are vital for the formation of the mucus gel and their main functions are to protect and lubricate the epithelium (Backstrom *et al.*, 2013). The other three mucins, MUC7, MUC8 and MUC9, are secreted non-gel-forming mucins with no cysteine residues. Secreted mucins form major components of salivary, bronchial and cervical mucus (Backstrom *et al.*, 2013).

1.4.4 Mucin structure

Mucins are heavily glycosylated molecules with a size between 2 and 50 MDa (Thornton *et al.*, 2008). Mucins are also described as polydisperse and heterogeneous in nature. Considerable efforts have been devoted to the analysis of the structure of the mucin. However its properties such as size, polydispersity, extensive glycosylation, heterogeneity and high viscosity have limited these efforts (Harding, 1989; Thornton *et al.*, 1997b). As a result there are disagreements in the reporting of conformations of the tertiary structure of the mucins. Two models were thus proposed for the structure of mucins.

The first model, the windmill model, was proposed by Allen, Pain and their colleagues (Harding, 1989). Their model described four high molecular weight protein subunits linked at the naked or non-glycosylated region to a 70 000 molecular weight protein in the centre by disulphide bridges, in a shape of a windmill (Harding, 1989; Pearson *et al.*, 1981). On the other hand, Carlstedt and Sheehan proposed the second model which was linear, flexible, random coil model (Carlstedt *et al.*, 1983; Carlstedt and Sheehan, 1984). Subsequent studies have described the gel-forming mucins to behave as random coils in dilute solution and to appear linear under the electron microscope (Thornton *et al.*, 1997a). Recently, Ridley and coworkers have assessed the intracellular assembly and packaging of MUC5B in secretory granules and discovered that the N-terminal domains form dimers through disulfide-linkage between D3 domains (Ridley et al., 2014). Their findings thus support a linear model. However, these two models had a consensus regarding the molecular weight of the mucin which was between 2 and 50 MDa as a result of their polydispersity. Moreover, the random coil has been widely described as the structure of the gel-forming respiratory tract mucins (Almutairi *et al.*, 2016).

1.4.5 The structure of mucin monomers

Through light scattering Carlstedt and Sheehan, and later using electron microscopy with Thornton and their colleagues, have demonstrated that mucins are polydisperse linear polymers that are fragmented into monomers upon reduction (Thornton *et al.*, 1997a). The reduction process only disrupts the disulphide bonds and has led to the understanding of the mucin monomers. These monomers have a molecular weight of 2 – 3 MDa.

The mucins are fragmented into elongated, rod-like molecules with a molecular weight of 2-3 MDa. The amino (N-) and carboxy (C-) terminal regions of the apomucins are reported to be non-glycosylated and rich in cysteine residues. Furthermore, situated at the N-terminal regions are D1, D2, D’ and D3 structural domains and situated at the C-terminal regions are D4, B, C, CK structural domains which are similar to Von Willebrand Factor (vWF) domains (Figure 1.1) (Backstrom *et al.*, 2013; Bansil and Turner, 2006; Ridley *et al.*, 2014). These domains are essential for disulphide mediated polymerization. The glycosylated regions are

situated at the centre of the apomucins characterized by a high number of serine, threonine and proline residues commonly referred to as STP residues. The sequences that encode the STP residues are tandemly repetitive and encoded by a single central exon of the MUC gene (Rose and Voynow, 2006). However, these repeat units differ from one mucin to another in sequence and size. Figure 1.1 illustrates the differences in the organization of the structure of mucin monomers. The hydroxyl groups of the serine and threonine residues are linked to oligosaccharides through an O-glycosidic bond (Rose and Voynow, 2006; Thornton *et al.*, 1996). The high number of the carbohydrates distinguishes mucins from other glycoproteins.

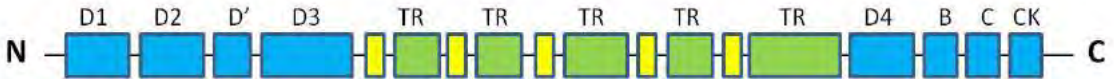

Figure 1.1: A schematic diagram of a gel forming mucin monomer.

The organization of the mucin monomer into the N- terminal region containing domains similar to von Willebrand Factor (vWF) denoted in blue; the central region containing cysteine residues denoted in yellow and tandem repeats of serine, threonine and proline residues denoted in green; and the C- terminal region containing domains similar to (vWF) denoted in blue. (Adapted from (Backstrom *et al.*, 2013).

1.4.6 Glycosylation of mucin subunits

Mucins from different organs display different patterns of O-glycans. Carbohydrates make up 70-80 % of the mucin weight (Sellers *et al.*, 1988). Glycosylation of the mucins is initiated in the Golgi apparatus by α-N-acetylgalactosaminyltransferases that facilitate the attachment of the N-acetylgalactosamine (GalNAc) to the hydroxyl of the serine and threonine residues to form the simplest O-glycan called the Tn antigen (Brockhausen *et al.*, 2009; Gerken, 2012; Hanisch *et al.*, 2009). Complex core O-glycan structures are achieved by elongating the Tn antigen through the addition of galactose, N-acetylglucosamine (GlcNAc), fucose and sialic acid. The structures of the O-glycan cores and antigenic epitopes found in mucins are shown in Table 1.2 (Brockhausen *et al.*, 2009). The O-glycans terminate with fucose, sialic acid and sulfated GlcNAc or blood group determinants making mucins negatively charged (Harrop *et al.*, 2012; Rose and Voynow, 2006).

Table 1.2: Structures of O-glycan cores and antigenic epitopes found in mucins

O-Glycan	Structure
Core	
Tn antigen	GalNAcαSer/Thr
Sialyl-Tn antigen	Siaα2-6GalNAcαSer/Thr
Core 1 or T antigen	Galβ1-3GalNAcαSer/Thr
Core 2	GlcNAcβ1-6(Galβ1-3)GalNAcαSer/Thr
Core 3	GlcNAcβ1-3GalNAcαSer/Thr
Core 4	GlcNAcβ1-6(GlcNAcβ1-3)GalNAcαSer/Thr
Core 5	GalNAcα1-3GalNAcαSer/Thr
Core 6	GlcNAcβ1-6GalNAcαSer/Thr
Core 7	GalNAcα1-6GalNAcαSer/Thr
Core 8	Galα1-3GalNAcαSer/Thr
Epitope	
Blood groups O, H	Fucα1-2Gal-
Blood group A	GalNAcα1-3(Fucα1-2)Gal-
Blood group B	Galα1-3(Fucα1-2)Gal-
Linear B	Galα1-3Gal-
Blood group i	Galβ1-4GlcNAcβ1-3Gal-
Blood group I	Galβ1-4GlcNAcβ1-6(Galβ1-4GlcNAcβ1-3)Gal-
Blood group Sd(a), Cad	GalNAcβ1-4(Siaα2-3)Gal-
Blood group Lewis^a	Galβ1-3(Fucα1-4)GlcNAc-
Blood group Lewis^x	Galβ1-4(Fucα1-3)GlcNAc-
Blood group sialyl-Lewis^x	Siaα2-3Galβ1-4(Fucα1-3)GlcNAc-
Blood group Lewis^y	Fucα1-2Galβ1-4(Fucα1-3)GlcNAc-

1.5 Mucin production in the respiratory tract

Studies that led to the characterisation of respiratory mucins have demonstrated that MUC1, MUC2, MUC4, MUC5AC, MUC5B, MUC7, MUC8, MUC11, MUC13, MUC15, MUC16, MUC18, MUC19, MUC20, MUC21 and MUC22 are expressed in the respiratory tract (Kato *et al.*, 2015). Figure 1.2 illustrates some of the membrane bound mucins and the secreted mucins in the respiratory tract. Mucin content changes in the respiratory tract under different conditions. Using antibodies developed in their laboratories, a number of researchers have demonstrated that gel-forming mucins are the main mucins found in the airways in order to entrap foreign particles (Hovenberg *et al.*, 1996; Kirkham *et al.*, 2002; Thornton *et al.*, 1996; Wickstrom *et al.*, 1998). They further showed that MUC5AC and

MUC5B are the major populations of polymeric mucins secreted in the respiratory airways. In addition MUC5AC was shown to be produced in goblet cells and MUC5B to be produced in mucous cells in the submucosal glands. However, some evidence suggests that MUC5B is also produced in the goblet cell (Rose *et al.*, 2001).

MUC2 has been shown to be expressed in small amounts in the surface epithelium of 'irritated' and diseased airways. It was demonstrated that MUC2 was up-regulated by *P. aeruginosa*, inflammatory mediators and tobacco smoke components (Davies *et al.*, 2002). The other secreted mucins are MUC7 and MUC8 which are shown to respectively be expressed by the serous cells and the mucosal cells of the submucosal gland of the respiratory tract.

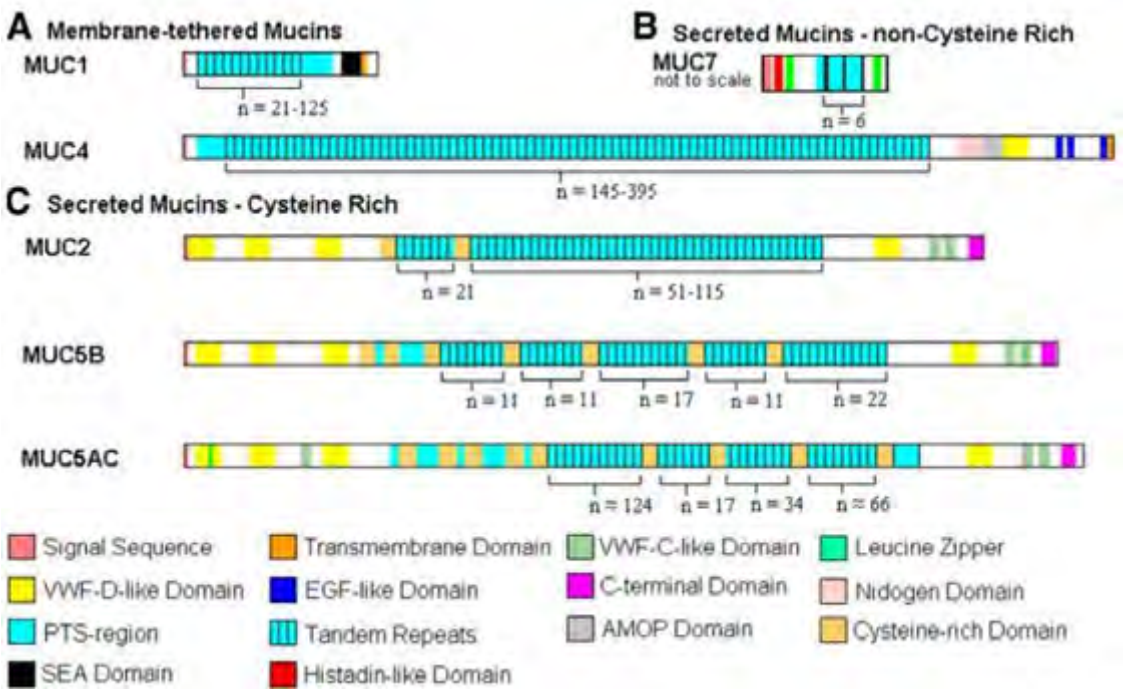

Figure 1.2: An illustration of some respiratory mucins.

A: MUC1 and MUC4 membrane bound mucins. B: MUC7 lacking cysteine domains. C: MUC2, MUC5B, and MUC5AC mucins. The number of tandem repeats (TR) is indicated as 'n' below each MUC. Other domains that are shown are the proline, threonine, serine-rich (PTS) domains; an extracellular domain associated with O-glycosylation, SEA domain; and von Willebrand D like domains. (Adapted from Rose and Voynow, 2006).

With the membrane-bound mucins identified in the respiratory tract, MUC1 has been shown to be produced in the microvilli and MUC4 has been associated with the cilia. MUC13 on the other hand is expressed on the surface of the trachea. Interestingly, MUC16 has been shown to be expressed by the submucosal gland and as a membrane-bound mucin on the epithelium of the tracheal surface (Davies *et al.*, 2007).

In addition, glycosylation studies on respiratory mucins have demonstrated that O-glycan core 3 and core 4 structures are found in the bronchial epithelium (Hanisch *et al.*, 2009). The carbohydrates of the mucin domain attract water creating a hydrophilic environment thereby hydrating and lubricating the epithelia.

1.6 Respiratory mucus and mucins in disease

The hypersecretion of mucus is the major cause of morbidity and mortality in respiratory tract diseases. Mucus hypersecretion is a prominent feature in asthma, chronic obstructive pulmonary disease (COPD) and cystic fibrosis where respiratory mucus and mucins have been extensively studied (Fahy and Dickey, 2010). Mucus hypersecretion is a characteristic of inflammation and epithelial diseases. Therefore mucociliary clearance plays an important role in disease development. Mucus hypersecretion is reported to be caused by the expansion of the goblet cells and the increased size of the submucosal glands (Bergeron and Boulet, 2006). Studies on the hypersecretion of mucus have shown that mucin content increases with increased mucus secretion. This hypersecretion leads to poor mucus clearance. Moreover, cough is employed to complement the mucociliary clearance (Rubin, 2010b). However failure to clear mucus results in mucus retention and colonization by microbes (Hauber *et al.*, 2006).

The presence of microbes in the lungs triggers a respiratory defense involving the mucociliary clearance, antimicrobial proteins and alveolar macrophages (Mizgerd, 2008). Furthermore, the virulent microbes elicit an inflammatory response. However, this inflammation may injure the lungs and contribute towards respiratory infections and diseases leading to airway obstruction and ultimately leading to the loss of pulmonary function. This may be seen in respiratory diseases such as asthma, COPD and cystic fibrosis

where mucus accumulates in the airways as a result of poor mucus clearance leading to narrow airways, as illustrated in Figure 1.3. The presence of increased inflammatory cells in the lumen and airway wall is indicative of airway diseases which can lead to airway remodeling. However airway remodeling is mainly observed in asthma.

In addition to mucus hypersecretion, mucins are associated with the regulation of inflammation and immune response. Alterations in the sequence of mucin glycosylation, and terminal sialylation and sulfation have been found to play a role in the development of and susceptibility to diseases.

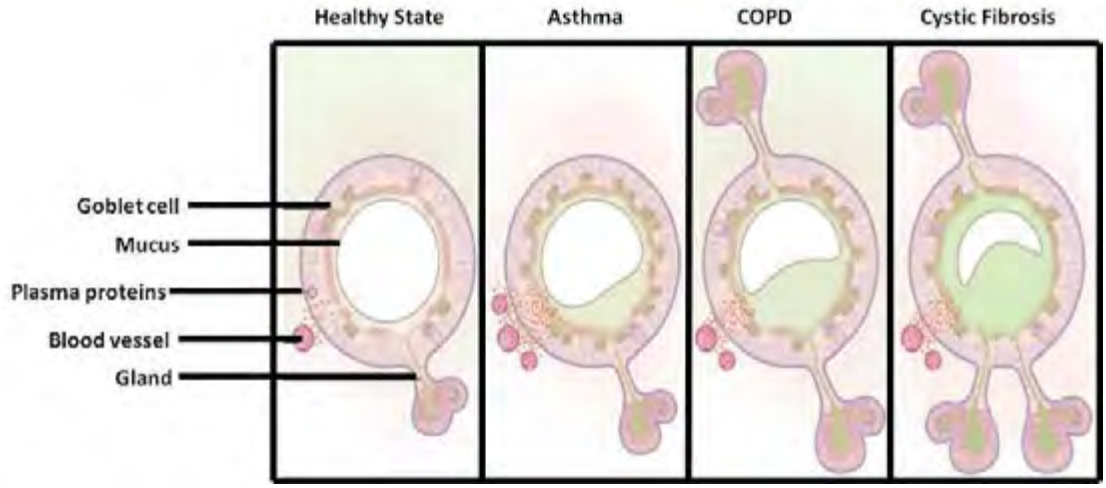

Figure 1.3: An illustration of the airway mucus in healthy and disease states.
In a healthy state the airways consist of low levels of mucus. However, disease states are characterised by accumulation of mucus in the airways. In asthma, increase number of subepithelial bronchial microvessels can be noticed. In both chronic obstructive pulmonary disease (COPD) and cystic fibrosis, increased and prominent mucosal glands have been noticed. (Adapted from Fahy and Dickey, 2010).

1.6.1 Asthma

Asthma is a common respiratory disease characterized by inflamed and narrow airways, airway hyper-responsiveness and airflow limitation. Affected people are sensitive to environmental allergens (Amin *et al.*, 2014). It was estimated that 235 million people suffered from asthma in 2013 (WHO, 2013). The extrinsic asthma and intrinsic asthma are two forms of asthma that have been identified. Extrinsic asthma presents onset in childhood. This type of asthma is episodic and is occasionally caused by an external allergic trigger though infections have also been reported as a trigger. The intrinsic asthma presents onset in adult life and is commonly caused by an infection. This type of asthma is commonly referred to as non-allergic.

Symptoms associated with the disease include coughing, chest tightness, shortness of breath, mucus hypersecretion and sputum production (Morcillo and Cortijo, 2006). Recurrent episodes of wheezing have also been reported. The narrowing and inflammation of the airways increases the susceptibility to allergic reactions as they make the airways sensitive to irritations. Airway mucus plugs are an important cause of airway obstruction in asthma. In addition, airway remodeling has been considered to be central in mucus dysfunction (Fahy and Dickey, 2010; Morcillo and Cortijo, 2006).

The airway mucus in asthma is characterized by high concentrations of mucins, plasma proteins that have been leaked from the bronchial blood vessels (Figure 1.3) and inflammatory cells (Innes *et al.*, 2009). The high concentration of mucins contributes to the elasticity and viscosity of the airway mucus. This thus hampers the clearance of mucus from the airways. Groneberg and his colleagues have shown that the expression of MUC5AC and MUC5B increased in asthma and that the respective mucins were expressed by different types of airway cell (Groneberg *et al.*, 2002). Their results further indicated that changes in the level of mucus production in fatal asthmaticus and mild asthma were not as a result of metaplasia of the goblet cells and glandular mucous cells. They concluded that the hypersecretion of mucus in asthma resulted from the up-regulation of mucin gene expression.

Genetic studies on mucins in asthma have shown varying lengths of the MUC5B alleles during severe asthma (Vinall *et al.*, 2000). Another study has shown that the short VNTR allele of MUC7 ($MUC7^5$) was found to be less frequent in asthmatic individuals as compared to the non-asthmatic individuals. It was thus deduced that $MUC7^5$ plays a role in the protection of the respiratory tract of asthmatic individuals (Kirkbride *et al.*, 2001; Rousseau *et al.*, 2004; Watson *et al.*, 2003).

1.6.2 COPD

COPD is a chronic inflammatory disease characterized by chronic bronchitis, airway thickening (Figure 1.3) and emphysema. The World Health Organization estimates that COPD will be the third leading cause of death in the world by 2030. COPD is understood to be caused by smoking, post-tuberculous lung damage, occupational exposures and domestic air pollution (Ehrlich and Jithoo, 2006). It affects the small airways and the alveoli. The pathogenesis of COPD is attributed to perpetual inflammation and oxidative stress.

The risk factors of COPD include tobacco smoke, occupational dusts, indoor and outdoor air pollution. Inhaled smoke has been reported to lead to the dysfunction of the cilia thus resulting in poor mucus clearance. Smoking has also been reported to cause hyperplasia. Smoking also leads to the development of emphysema as a result of the expansion of the alveoli. The inflammation causes airflow limitations in the bronchioles and reduction in the elasticity of the lung tissue thereby entrapping air in the lungs. Brashier and Kodgule (2012) have highlighted that TB is increasingly becoming recognized as a risk factor for COPD.

Bacterial and viral infections cause exacerbation of COPD in airway disease (Lu and Zheng, 2013). The presence of the latter leads to mucin up-regulation in COPD. MUC5AC and MUC5B have been shown to be up-regulated in COPD. Caramori *et al.* (2009) have found increased expression of MUC5AC in the submucosal glands of stable COPD patients. Work by (Kirkham *et al.*, 2008)has shown MUC5B to be the prominent secreted mucin in COPD. MUC16 has been shown to be elevated in the blood of COPD patients (Yilmaz *et al.*, 2011). In addition, the increased MUC16 levels have been associated with the right ventricular failure in COPD patients.

1.6.3 Cystic Fibrosis

Cystic Fibrosis (CF) is a genetic disorder characterized by recurrent airway infections. CF is caused by mutations in the gene encoding the cystic fibrosis transmembrane conductance regulator (CFTR). The mutation leads to CFTR dysfunction causing events that will ultimately result in the deterioration of the lungs. The CFTR failure causes isotonic absorption of sodium chloride leading to the dehydration of mucus (Fahy and Dickey, 2010; Perez-Vilar and Boucher, 2004). The latter causes mucus retention as a result of poor mucus clearance and initiates bacterial colonization. Subsequently, bacterial infections persist, biofilm is formed and mucus is overproduced resulting in inflammation and bronchiectasis (Perez-Vilar and Boucher, 2004)Symptoms include wheezing, phlegm, shortness of breath, persistent cough, abdominal pain and greasy stools (Sloane *et al.*, 2005).

Studies on CF have demonstrated that MUC5AC and MUC5B mucin are decreased in the disease. However, increased levels of MUC5B were recorded in comparison with the MUC5AC mucin levels (Henke *et al.*, 2004; Kirkham *et al.*, 2002). Henke and colleagues subsequently showed that MUC5AC and MUC5B mucins increase during pulmonary exacerbation (Henke et al., 2007). In another study, small amounts of MUC2 were identified in CF (Davies *et al.*, 1999).

Microbes associated in recurrent airway infections mainly present as biofilms on the surface of the epithelium. These include *P. aeruginosa*, *Staphylococcus aureus* and aspergillus species (Fahy and Dickey, 2010). *P. aeruginosa* is the most common and potent cause of airway infection reported in CF. The microbe produces lipopolysaccharide (LPS) which initiates the defense response in the respiratory tract (Li *et al.*, 2006). A study by Li *et al.* (2006) examined the expression and regulation of MUC7 gene in the lung and trachea of transgenic mice upon stimulation with LPS. MUC7 was shown to be highly expressed in the serous cells and within the respiratory epithelium. LPS has also been shown to up-regulate MUC2 gene in epithelial cells (Hauber *et al.*, 2006).

1.6.4 Tuberculosis (TB)

TB is a major global health problem that accounted for 1.5 million deaths out of 9.6 million new cases in 2014 (WHO, 2015). TB is a disease caused by *Mycobacterium tuberculosis* (*M.tb*), a pathogenic rod-shaped bacillus that was discovered by Robert Koch in the 19thcentury. The bacilli are trapped in mucus droplets and transmitted from one person to another by inhalation of aerosol from sneezing and coughing into the terminal bronchi and pulmonary alveoli (Kruh *et al.*, 2010; Mehta *et al.*, 2012). Pulmonary TB is characterised by a productive cough, expectoration of blood, chest pain, loss of appetite, weight loss, night sweats, fatigue, chills and fever (Middleton *et al.*, 2004). However, *M.tb* not only invades the pulmonary alveoli, extrapulmonary TB has also been reported in highly vascular areas such as lymph nodes, meninges, kidney, spine and growing end of bones (Swaminathan and Narendran, 2005)

Upon inhalation, *M.tb* is transported across the alveolar epithelium into the lung tissue and activates innate immune response. Cells of the innate immune response express pattern recognition receptors (PRRs), through which they engage the bacteria and secrete host defence factors such as cytokines and chemokines (Hazlett and Wu, 2011; Marakalala *et al.*, 2011). This response then activates phagocyte antimicrobial activities and result in the recruitment of additional mononuclear leukocytes into the site of infection forming a tuberculous granuloma (Guirado and Schlesinger, 2013). The structure of a tuberculous granuloma is illustrated in Figure 1.4. The main function of the granuloma is to contain and neutralise *M.tb.* However, the *M.*tb pathogen has developed strategies to persist within the tuberculous granuloma through the evasion of the host defence. This strategy is achieved by subverting the killing effects of macrophages through its ability to block the fusion of phagosomes with the lysosome (Bajaj and Batra, 2012; Sonawane *et al.*, 2012). Furthermore, the glycan structures in the cell wall of *M.tb* are reported to play a crucial role in the pathogenesis of TB.

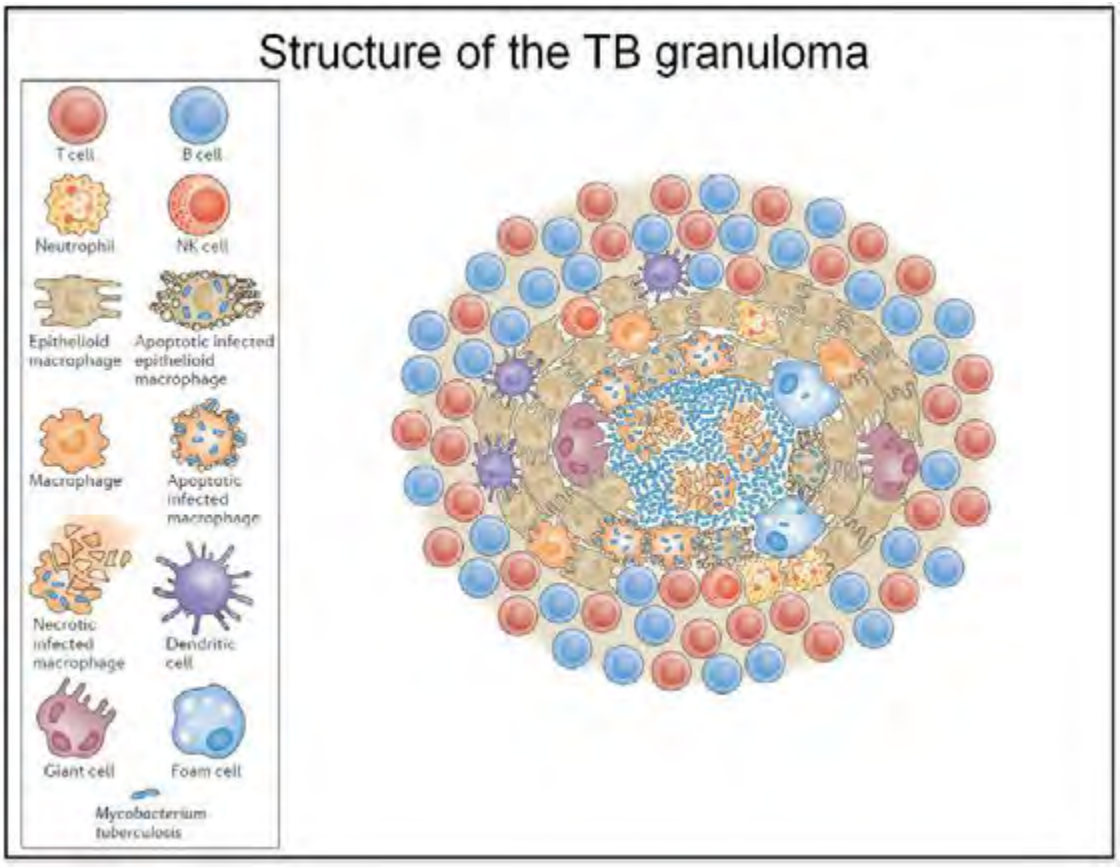

Figure 1.4: A schematic of the structure of a tuberculous granuloma

An illustration of the organisation of the granuloma found in tuberculosis which is composed of epithelioid cells, macrophages, foam cells, neutrophils, dendritic cells, natural killer (NK) cells, B and T cells. The *M.tb* pathogen in shown localised within the tuberculous granuloma. (Adapted from Ramakrishnan, 2012).

Considerable efforts have been taken to control TB. However, in 1993, the high incidence rate led WHO to declare TB a 'global emergency' (Jordan *et al.*, 2010). Subsequently, in 2005, the WHO committee for Africa declared TB to be an African regional emergency (Lawn *et al.*, 2006). In 2014, South-East Asia and Western Pacific Regions recorded the highest number of new TB cases which accounted for 58% of the new cases globally. Africa had the greatest proportion burden with 281 cases per 100 000 people recorded by WHO (WHO, 2015). In 2014, South Africa had a high incidence of TB with 834 cases per 100 000 people (WHO, 2015). The high incidence rate has been attributed to co-infection with human immunodeficiency virus (HIV), and the emergence of the drug-resistant strains of TB such as the multidrug resistant (MDR-TB) and extensively drug resistant (XDR-TB) have contributed to the progression of the TB epidemic (Karim *et al.*, 2009; Streicher *et al.*, 2012).

Co-infection with HIV causes susceptibility to opportunistic infections with TB being the prominent infection. The presence of HIV has been shown to promote TB by decreasing macrophages, activating lymphocytes, increasing tissue destruction and decreasing CD4 cells (Swaminathan and Narendran, 2005). TB has been shown to enhance HIV replication by secreting TNF alpha and through the destruction of CD4 cells (Swaminathan and Narendran, 2005).

Prolonged periods are required in the treatment of TB as the bacilli differ in metabolic activity (Bajaj and Batra, 2012). The recommended TB treatment is isoniazid, rifampicin, pyrazinamide and ethambutol for the first 2 months and the continuation of isoniazid and rifampicin from months 4 – 6 (WHO, 2009). The bacterium has developed resistance to some of the drugs in an attempt to evade the host defence. The resistance to TB drugs is caused by genetic mutations (that either occur in the target or the activator of the drug) which result in a heritable loss of susceptibility to antibiotics (Sacchettini *et al.*, 2008). MDR-TB is the strain of *M.tb* that is resistant to at least two drugs, isoniazid (INH) and rifampicin. XDR-TB refers to the strain of bacteria that is resistant to isoniazid, rifampicin and fluoroquinolones (Sacchettini *et al.*, 2008).

1.7 Interaction of TB and the respiratory mucosa

In 2002, Middleton and co-workers initiated a study into the interaction of mycobacteria species with the human respiratory mucosa using an organ culture with air interface model (Middleton *et al.*, 2002). Their study showed two distinct morphologies of mucus, fibrous and globular mucus. In addition, their study showed that mycobacteria species adhered specifically to the fibrous mucus matrix and to epithelial cells called M-cells that transport particles across the mucosa. The study further showed that *M.tb* adhered mainly to fibronectin in the extracellular matrix in mucosal damage but not to ciliated cells. In their subsequent study, still using an organ culture with air interface model, the team illustrated the invasion of the human bronchial tissue by *M.tb* and the increased numbers of *Mycobacterium avium* on the mucosal surfaces (Middleton *et al.*, 2003).

These studies led the investigators to hypothesize that the difference between fibrous and globular mucus could be attributed to their mucin content. They therefore investigated the role of mucins in mycobacterial interactions with the respiratory mucosa (Middleton *et al.*, 2004). The addition of purified mucins to the organ culture air interface model showed increased fibrous mucus. However, this study could not determine whether the presence of mycobacteria of the respiratory mucosa stimulated mucus production or not.

1.8 Previous studies in our laboratory

A pilot study by Govender (2006) initiated the investigation into the association between respiratory mucins and TB at a biochemical and molecular level. The study involved the collection of sputum from healthy individuals, post mortem cadavers and suspected TB positive adults and children. MUC5B was identified in both the healthy controls and TB positive adults and children. In contrast MUC5AC was barely evident in the controls but presented in both the TB positive adults and children. MUC2 barely featured in the control group but was identified in the TB positive adults and children.

In addition, genetic investigations were undertaken for the presence of known polymorphisms in the mucin genes, MUC2 and MUC5B, in a small number of samples, and using a European study as a comparison. Both a MUC2/PvuII polymorphism in exon 11 of the MUC2 gene and a VNTR of intron 36 of MUC5B were identified in the study sample. Generally the C allele of MUC2/PvuII occurred less frequently than the G allele. Categorisation of the sample on the basis of TB status showed a higher C allele frequency in TB positive cases and revealed that allele C homozygotes were found only amongst TB positive cases (30%). However the data set was small and the study needed to be expanded.

The MUC5B alleles represented variable numbers of the 59 bp repeat sequence within intron 36. This differed from the European study as a greater number of alleles were identified in the Western Cape population. In comparison to the European study of Desseyn *et al.* (1999), it appeared that the frequency of the 8 repeat allele was higher in the Western Cape population whereas the 7 repeat allele dominated in the European population. Furthermore the 10 and 3 repeat alleles found in this study did not present in the European study, and the 4 repeat alleles of the European study was absent in this study group. The 10 repeat allele was of interest as it was seen only in a TB negative individual and not in the TB positive group. The 8/8 allele combination common to the study group presented predominantly in the TB positive individuals.

1.9 Rationale of the study

The increase in the TB incidence rate has reawakened efforts in identifying biomarkers that could serve as targets for drug and vaccine design (Gupta et al., 2012). Furthermore, Sonawane *et al.* (2012) have highlighted that the glycans on the *M.tb* cell wall could be essential in the development of drug targets. In addition, it has been established that the respiratory mucus provides the first line of defence by acting as a barrier through adhering pathogens through to mucins. However, there is limited information regarding the interaction of *M.tb* with respiratory mucins. Therefore a need arose in understanding of the properties of respiratory mucus in TB. This study thus expanded on the pilot study by Govender (2006) to be able to verify its findings and to throw further light on the role of respiratory mucus and mucins in the pathogenesis of TB.

1.10 Aims and objectives

Aims:

Our aim was to isolate and characterise mucins from respiratory mucus in order to elucidate the role of the dominant secreted mucins in patients with TB.

Objectives:

The specific objectives and proposed experiments of the study were to:

- Determine the respiratory mucins secreted in non-TB and TB mucus and to verify their identity using Western blotting.
- Determine the composition of the respiratory apomucin in non-TB and TB by HPLC analysis of amino acid.
- Release oligosaccharides and determine the alterations in glycosylation.
- To determine the expression of mucins in lung tissue infected with TB through analysis by immunohistochemistry.
- To generate 2D proteome profile maps of respiratory mucus from non-TB and TB mucus.
- To identify the expressed proteins between non-TB and TB through mass spectrometry analysis.

CHAPTER 2 : MATERIALS AND METHODS

2.1 Materials and suppliers

The materials used in this study and their sources are tabulated below:

Table 2.1: Chemicals and reagents used for the study

Materials (Chemical, reagents)	Suppliers (company details in Appendix)
Acetone	Merck
Acrylamide (40 % 37.5:1 acylamide:bisacrylamide)	BioRad
AG50WX8 cation-exchange resin	BioRad
Agarose	Sigma
Agarose (low electrosomotic flow grade)	Sigma
Ampholytes pH 3-10	BioRad
Ammonium persulfate (APS)	Sigma
AquaStain	Vacutec
B-Mercaptoethanol	BDH
Bradford Quickstart dye reagent	BioRad
Bromophenol blue sodium salt	Merck
Bovine Serum Albumin (BSA)	Sigma
Caesium Chloride (CsCl)	Sigma
CHAPS	Sigma
Coomassie Brilliant Blue R-250	Sigma
Dialysis tubing	Sigma-Aldrich
Direct Blue	Sigma
Dithiolthreitol (DTT)	Fermentas
EDTA	Merck
Fat free milk powder	Spar brand
Glacial Acetic acid	Merck
Glycerol	BDH
Glycine	BioRad

Guanidine Hydrochloride (GuHCl)	Sigma
HRPO-linked goat anti-rabbit	Dako
HRPO-linked rabbit anti-mouse	Dako
Iodoacetamide	Sigma-Aldrich
IPG Strips	BioRad
***N-Ethylmaleimide* (*NEM*)**	Sigma-Aldrich
Nitrocellulose membrane	PALL Corp (Whitehead Scientific)
PageRuler^{TM} Prestained Protein Ladder	Fermentas (Whitehead Scientific)
Period acid solution	Merck
PlusOne Drystrip cover fluid	GE Healthcare
PMSF	Sigma-Aldrich
Poly-L-lysine	Sigma-Aldrich
Precast 4-20% gradient gels	Vacutec
Propan-2-ol	Merck
Sodium dodecyl sulfate (SDS)	BioRad
Sodium metabisulphite	Merck
TEMED	Sigma-Aldrich
Tris	Merck
Thiourea	Sigma
Tween-20	Merck
Urea	Argon Lab suppliers

Table 2.2: Antibodies used in the study for Western Blot analysis

Antibody	Suppliers	Mono/Polyclonal	Location
MUC7	Abcam (AB55542)	Monoclonal	Recombinant fragment: 36-136 human MUC7
MUC16 [X325]	Abcam (AB10033)	Monoclonal	
LUM2-3 (MUC2)	EU consortium	Polyclonal	C-terminus
MAN5ACI	EU consortium	Polyclonal	
MAN5BI	EU consortium	Polyclonal	N-terminus
EU-MUC5Bb2-2	EU consortium	Monoclonal	Cysteine in tandem repeat
EU-MUC7a	EU consortium	Monoclonal	N-terminus
HRP-linked goat anti-rabbit	Dako(P0488)		
HRP-linked rabbit anti-mouse	Dako(P0260)		

Antibodies from the EU consortium donated by Prof. Dallas Swallow from University College London, UK.

2.2 Research ethics and permissions

This study was conducted at the Surgical Research Laboratory, Department of Surgery, Groote Schuur Hospital between May 2010 and August 2013. Work done for this project was approved by the Ethics Committee of Research at the Health Sciences Faculty of the University of Cape Town (UCT). Ethics reference number REC: REF 142/2009.

Further permission was obtained from the Western Cape (Western Cape DoH reference: 2011 RP 42) and Free State provincial Department of Health (DoH) for the collection of sputa at the facilities in the respective provinces. No reference number was supplied by the Free State DoH.

2.3 Sample collection

2.3.1 Healthy or uninfected sample collection (n=17)

Tracheal aspirates were collected from patients with no history of respiratory diseases who underwent surgery at Groote Schuur Hospital (Cape Town, Western Cape). Tracheal aspirates were collected after induction of anaesthesia and intubation. These samples were called uninfected controls. Tracheal aspirates were collected into 6 M GuHCl pH 6.5, containing a cocktail of protease inhibitors (10 mM EDTA, 5 mM NEM and 1 mM PMSF). Samples were collected and transported on ice and then stored at -20 ˚C until further analysis.

2.3.2 Bronchioalveolar lavage (BAL) collection (n=95)

BAL samples were collected from patients who underwent bronchoscopy as part of a specific treatment protocol at Groote Schuur Hospital (Cape Town, Western Cape). BAL samples were collected in PBS at pH 7.4 and were transported on ice. A protease inhibitor, 1 mM PMSF, was added to each sample and kept at -80 ˚C in order to be freeze dried. Freeze dried BALs were stored at -20 ˚C until further use.

2.3.3 Sputum collection (n=56)

Sputa from TB positive patients were collected from Gugulethu Clinic and DP Marais Hospital in the Western Cape and Leseding, Thusanong and Seeisoville Clinics in the Free State. Prior to sample collection, patients were encouraged to rinse their mouths with water. Sputa were collected into 6M guanidinium hydrochloride (GuHCl) pH 6.5, containing a cocktail of protease inhibitors (10 mM EDTA, 5mM NEM and 1 mM PMSF). Samples were collected and transported on ice and stored at -20 ˚C until further use.

2.4 Sample preparation

Samples were prepared individually and no samples were pooled.

2.4.1 Mucus sample preparation

Mucus was homogenized with a Junkel and Kunkel Ultra-Turrax at high burst for 30 seconds at room temperature to solubilize the sputa in GuHCl. Insoluble debris was separated from mucus by centrifugation in a Hitachi HIMAC centrifuge at 3 000 rpm for 30 minutes at 4 ˚C. The supernatants were collected into clean tubes.

2.4.2 Preparation of crude mucus

Following mucus sample preparation, the mucus was reduced in 6 M GuHCl and 10 mM DTT for 5 hours at 37 ˚C to break the disulphide bonds in the mucus. The thiol groups (-SH) resulting from reduction were alkylated with 25 mM iodoacetamide overnight in the dark at room temperature. Iodoacetamide binds the sulfhydryl/thiol groups of the cysteine residues so that the disulphide bonds cannot be reformed. Samples were then placed in the dialysis tubing and dialysed against three changes of distilled water at 4 ˚C with constant stirring. Dialysed samples were then freeze dried according to 2.4.6.

2.4.3 Purification of mucins with caesium chloride

Mucins were purified using caesium chloride (CsCl) density gradient ultra-centrifugation (Creeth and Denborough, 1970). The density of the mucus was adjusted to 1.39 to 1.40g/ml by the addition of CsCl at a final concentration of 3.5M CsCl. Density gradient ultracentrifugation was performed using a Beckman ultra-centrifuge at 40 000 rpm for 48 hours at 4 ˚C. Mucin-rich fractions were identified using a PAS assay to determine the glycoprotein and the Bradford assay to determine the concentration of proteins. The absorbance of the PAS assay was read at 540 nm and the Bradford assay was read at 595 nm. The glycoprotein-rich fractions were pooled and subjected to a second CsCl spin at

40 000 rpm for 48 hours at 4 ˚C. PAS assay and Bradford assay were performed following the second spin. Dialysis tubing was prepared by boiling distilled water with a tinge of EDTA and sodium carbonate. The mucin-rich fractions from each patient was pooled and dialysed against three changes of 6M GuHCl at 4 ˚C.

2.4.4 Reduction and alkylation of samples

Purified fractions were reduced in 6M GuHCl and 10 mM DTT for 5 hours at 37 ˚C to break the disulphide bonds in the mucus. The thiol groups resulting from reduction were alkylated with 25 mM iodoacetamide overnight in the dark at room temperature. Iodoacetamide binds the sulfhydryl/thiol groups of the cysteine residues so that the disulphide bonds cannot be reformed.

2.4.5 Dialysis of samples

It was essential to remove GuHCl from the samples prior to analysis. Samples were placed in the dialysis tubing and dialysed against three changes of distilled water at 4 ˚C with constant stirring. Dialysed samples were then freeze dried.

2.4.6 Freeze drying

Following dialysis the samples were placed in plastic containers with holes in the lids. Samples were frozen in liquid nitrogen and placed in flasks of the freeze dryer (Christ ALPHA1-5, Lasec Laboratory). Samples were freeze dried at -80 ˚C until the samples were completely lyophilised and stored at -20 ˚C for analysis.

2.5 Amino acid analysis

The amino acid content of respiratory mucins was determined by amino acid analysis. This involves four basic steps namely: the hydrolysis of the protein to its individual amino acid content, labelling of amino acid with a detectable marker, high pressure liquid chromatography (HPLC) separation of mucins and data interpretation. The amino acid

content of purified breast milk mucins was analysed using an HPLC system according to the methods of Klapper (1982). The samples were vacuum-dried and placed in a hydrolysis vessel containing some constantly boiling hydrochloric acid (HCl) and 1% (v/v) phenol. The vessel was purged with nitrogen gas and sealed under vacuum. The samples were then hydrolyzed in the gas phase at 110 °C for 24 hours. Following hydrolysis, the vessel tip was cooled and vacuum dried to remove the residual HCl. The dried samples were re-dissolved in citrate buffer pH 2.2 and injected into a high-pressure liquid chromatography column packed with a cation exchange resin (sulfonated polystyrene cross-linked with divinylbenzene) and eluted with a series of buffers ranging from a low (0.25M trisodium citrate, pH 3.05) to high (0.25M sodium nitrate, pH 9.5) pH. Detection was carried out using post-column derivatization with o-phthalaldehyde, a fluorescent reagent that reacts with all the amino acids except proline. For proline detection, the samples were treated with sodium hypochlorite ahead of post column derivatization with OPA. The relative ratios of the individual amino acids for each sample were determined and compared.

2.6 Agarose gel electrophoresis

Agarose gel electrophoresis was used to effectively separate proteins larger than 200 kDa. To prepare samples for the electrophoresis, 1 mg of the lyophilized sample was weighed out and dissolved in 100 µl of sample buffer (2% sodium dodecyl sulfate (SDS), 10% glycerol, 0.01% bromophenol blue, 5% β-mercaptoethanol). The mixture was boiled in the heating block, Dri Block (Stuart Scientifica) at 95 °C for 5 minutes. The samples were cooled at room temperature then pulse spun in the microcentrifuge. The samples, 25 µl, were loaded onto 0.7% (w/v) agarose gels. The proteins were separated by electrophoresis at 65 V and 400 mA for 2.5 hours in 40mM Tris/acetate and 1mM EDTA at pH 8.0 (1 X TAE) containing 0.1% (w/v) SDS.

2.7 Western Blot analysis

Following agarose gel electrophoresis, the gels were soaked in 0.6M sodium chloride/ 60 mM sodium citrate (4 X SSC) for 3 minutes. Nitrocellulose membrane with a 0.2 µm pore size were soaked in running buffer for approximately 5 minutes and subsequently rinsed in

4 X SSC. The membrane was placed onto the vacuum blot apparatus (Pharmacia LKB Vacugene XL) and 4 X SSC containing 10 % Poly-L-Lysine was vacuum blotted onto the membrane. The gels were carefully placed on the membranes, ensuring no air bubbles were present between the gels and the membranes. The gels were vacuum blotted for 1 hour at a constant pressure of 40 mbars at room temperature. The gels were kept wet with 4 X SSC throughout the transfer of proteins. Once the transfer of proteins was complete, the membranes were rinsed in water and then incubated in 5% (w/v) low fat milk powder in TBS and 0.05% Tween-20 (TBST) for 30 minutes at room temperature on the shaker in order to block non-specific binding to antibody. The blocking buffer was discarded and the membranes were incubated in primary antibody at 4 ˚C overnight.

Following probing with the primary antibody, the membranes were washed with 1 X TBST for 3 x 5 minutes. The membranes were incubated with secondary antibody for 1 hour at room temperature on the shaker. The membranes were then washed with 1 X TBST for 3 x 10 minutes and rinsed with distilled water.

Table 2.3: Concentrations of primary and secondary antibodies used for Western blotting

Primary antibody	Recognition site	Secondary antibody
LUM2-3(MUC2) (1:2000)	C-terminus	HRP-linked goat anti-rabbit (1:2000)
MAN5ACI (1:5000)		HRP-linked goat anti-rabbit (1:2000)
MAN5BI (1:2000)	N-terminus	HRP-linked goat anti-rabbit (1:2000)
EU-MUC7a (1:1000)	N-terminus	HRP-linked rabbit anti-mouse (1:1500)

2.7.1 Mucin detection

Enhanced chemiluminuscence (ECL) solution was prepared according to the manufacturer's instructions. The ECL solution was poured over the membranes and exposed for 30 seconds. The ECL solution was removed with filter paper. The membrane was placed in the viewer/imager and bands detected for 10 minutes at 1 minute intervals.

2.7.2 Membrane stripping

After detection the membranes were incubated with stripping buffer (62.5 mM Tris, 0.5 M NaCl, 100 mM Mercaptoethanol and 2% SDS) for 1 hour at 37 ˚C. The membranes were washed with 1 X TBST for 3 x 15 minutes. Once the membranes were stripped, the membranes were incubated in blocking buffer for 30 minutes on the shaker and subsequently probed with the primary antibody and secondary antibody as in section 2.7.

2.8 Immunohistochemistry

Formalin fixed paraffin wax embedded lung tissue blocks were from post mortem patients. Serial sections (2 µm) were cut from the tissue blocks of each patient and heat fixed at 60 ˚C for 1 hour. The sections were dewaxed in xylol for 15 minutes with 3 changes, rehydrated through graded alcohols (absolute and 96% two changes) at 2 minutes intervals and rinsed with water. The sections were then divided for Histochemical staining: haematoxylin and eosin (H & E) staining for diagnosis, high iron diamante (HID) to identify sulfomucins and sialomucins, periodic acid Schiff/alcian blue (PAS/AB) staining to identify neutral mucins and sialomucins, and Immunohistochemistry: MUC2,MUC5AC,MUC5B,MUC7,MUC16 and MUC7 to identify the mucins expressed in the lungs.

2.8.1 H & E Staining

The tissue sections were dewaxed and rehydrated through the alcohols to water and stained with haematoxylin for 9 minutes. The tissue was rinsed for 3 minutes under running tap water, blued in Scott's Tap Water Substitute (a blueing reagent designed for minimising loss of tissue sections) for 3 minutes and rinsed again with water for 3 minutes. The tissue was stained with 1% eosin for 3 minutes followed by a quick rinse under running tap water. The slides were dehydrated through the alcohols to xylol, cover slipped and mounted using entellan.

2.8.2 HID Staining

Following dewaxing and rehydration through the alcohols to distilled water, the tissue was treated with HID solution for 18 hours. The sections were rinsed in distilled water and stained with 1% Alcian blue. Once stained, the sections were rinsed under running water for 5 minutes, dehydrated through the alcohols to xylol cover slipped and mounted using entellan.

2.8.3 PAS/AB Staining

The sections were dewaxed and rehydrated through the alcohols to tap water, then treated with Alcian blue solution for 5 minutes. The sections were rinsed in 3 changes of distilled water and treated with periodic acid solution for 2 minutes. The sections were rinsed again with 3 changes in distilled water followed by staining with Schiff reagent for 8 minutes and then rinsed in running tap water for 10 minutes. The nuclei were stained with Mayers haematoxylin for 35 seconds then rinsed under tap water, blued in Scott's Tap Water Substitute for 2 minutes, rinsed again under running water for 5 minutes, dehydrated through the alcohols to xylol, cover slipped and mounted using entellan.

2.8.4 Mucins detection

The sections were dewaxed in xylol, rehydrated through graded alcohols to tap water. Endogenous peroxidase was blocked with 1% hydrogen peroxide in distilled water for 15 minutes followed by rinsing under tap water. Antigens were retrieved with 0.01M citrate buffer for 2 minutes in a pressure cooker on full pressure. The sections were cooled under running water for 15 minutes and then rinsed with 1 X PBST. Non-specific binding sites were blocked with normal goat serum (1:20 in 1 X PBS) for 10 minutes. The normal goat serum was drained off the slides (not rinsed) and then probed with primary antibodies according to Table 2 below. The sections were rinsed twice with 1 X PBST at 5 minutes intervals followed by incubation with the secondary antibody (Envision Monoclonal goat anti Mouse). The secondary antibody was rinsed off with 1 X PBST and the colour developed with diaminobenzidine (DAB) substrate chromogen system for 8 minutes. The DAB was rinsed off

with 1 X PBS and then water. The colour was enhanced by incubating the tissue in 1% Copper Sulfate for 10 minutes. The tissue was counterstained with haematoxylin for 2 minutes followed by a quick rinse under running tap water, blued in Scott's water for 2 minutes and rinsed in running tap water for 10 minutes. The tissue was dehydrated through the alcohols to xylol, cover slipped and mounted using entellan.

Table 2.4: Concentrations of primary antibodies for immunohistochemistry for detecting mucin expression in lung tissue

Antibody	Supplier	Dilution	Incubation time
MUC2	Leica (NL-MUC2)	1:100 in 1 X PBS	1 hour
MUC5AC	Leica (NL-MUC5AC)	1:100 in 1 X PBS	30 minutes
MUC5Bb2-2	EU Consortium	1:100 in 1 X PBS	1 hour
MUC7	Abcam (AB55542)	1:100 in 1 X PBS	1 hour
MUC16 [X325]	Abcam (AB10033)	1:100 in 1 X PBS	30 minutes

***** Antibodies from the EU consortium donated by Prof. Dallas Swallow from University College London, UK.

2.9 Proteomic analysis

2.9.1 Sample preparation

5mg of each sample was weighed out and dissolved in 2 ml of 1 X PBS. Precipitation of respiratory mucus proteins with acetone was carried out as described by Khan and Packer (Khan and Packer, 2006).

To prepare the samples for acetone precipitation, a 1:5 mucus-to-acetone ratio was used to precipitate respiratory mucus proteins according to Khan and Packer, 2006. The mucus proteins were precipitated overnight at -20 ˚C. Following overnight precipitation, the samples were centrifuged at 13 200 rpm for 15 minutes at 4 ˚C. The supernatants were stored at -20 ˚C for later use and the pellets were resuspended in 1 ml of solubilisation

buffer. Protein concentrations were determined using the BioRad assay according to the manufacturer's instructions. Protein quantification was done in triplicate using bovine serum albumin (BSA) as a standard.

2.9.2 One dimensional (1D) SDS Polyacrylamide Gel Electrophoresis (PAGE) analysis

Equal volumes of the samples prepared in section 2.9.1 and the sample buffer were mixed and boiled in the heating block at 95 °C for 5 minutes. The samples were cooled at room temperature then pulse spun in the microcentrifuge. The samples were loaded on 12% and 4-20% gradient gels respectively. The proteins were separated by electrophoresis at 100 V for 2 hours. The gels were stained with a protein stain, AquaStain (Vacutec) for 10 minutes.

2.9.3 Two dimension (2D) SDS PAGE analysis

2.9.3.1 Sample solubilisation

A 100 μg of each sample was added to 1.25 μl of ampholytes, 2 μl of 50% DTT and 8 M urea solubilisation buffer to the final volume of 125 μl.

2.9.3.2 In-gel rehydration

The samples were loaded in the grooves of the rehydration tray (GE Healthcare). The gel sides of the 7 cm long IPG strips pH 4-7 (BioRad) were immersed in the prepared samples in the rehydration tray and the IPG strips were covered with mineral oil (GE Healthcare). The respective IPG strips were re-hydrated overnight at room temperature.

2.9.3.3 Isoelectric focusing (IEF)

Following the overnight rehydration of IPG strips, the strips were loaded on the Ettan IPGphorII IEF machine (GE Healthcare), aligned and overlaid with mineral oil. The IEF

machine was programmed for a three-step long run. For the first step, 250 V were applied for 10 minutes. For the second step, 4 000 V were applied for an hour. For the final step, 4 000 V were applied until 12 000 V-hours were reached. The IEF was carried out at 20 ˚C.

2.9.3.4 Equilibration of the IPG strips

Equilibration buffers 1 and 2 were prepared fresh by adding 2% (w/v) DTT (buffer 1) and 2.5% (w/v) iodoacetamide (buffer 2) to equilibration base buffer (6M Urea, 2% SDS, 0.05 M Tris-HCl and 20% glycerol at pH 8.8) respectively. Buffer 1 containing DTT reduces disulphide bonds and maintains monothiols in the reduced state. Buffer 2 contains iodoacetamide which covalently binds cysteines so that the protein cannot form disulphide bonds.

Following the IEF, the strips were rinsed with water and placed in each channel of the rehydration/equilibration tray. Each channel was filled with 2.5ml of equilibration buffer 1 and incubated with gentle agitation for 15 minutes. After 15 minutes, the equilibration buffer 1 was decanted and each channel was refilled with 2.5 ml of equilibration buffer 2. The strips were then incubated with gentle agitation for 15 minutes. The strips were rinsed with 1 X SDS buffer in preparation for the second dimension.

2.9.3.5 Second dimension of 2D PAGEs

Following equilibration, the strips were placed on top of 12% SDS PAGE gels. The gels were assembled using the Mini-Protean III Cell (BioRad). To secure the strips, 1% low melting agarose gel was overlaid on top of the strips. The gels were run at 100 V for 1.5 hours.

2.9.3.6 SDS PAGE Staining

Following electrophoresis, the gels were stained using the three-step Coomassie staining. The gels were first placed in the Coomassie I stain solution (10% glacial acetic acid, 0.025% (w/v) Coomassie Brilliant blue R-250 and 25% propan-2-ol dissolved in distilled water) then heated in a microwave for 1 minute and incubated overnight at room temperature with agitation. The stain was decanted, replaced with Coomassie II stain solution (10% glacial

acetic acid and 0.003125% (w/v) Coomassie Brilliant blue R-250 dissolved in distilled water) and heated in a microwave for 1 minute. The gels were incubated with the stain for 30 minutes with agitation. Following staining with Coomassie II staining solution, the stain was decanted, replaced with Coomassie III staining solution (10% glacial acetic acid and 0.003125% (w/v) Coomassie Brilliant blue R-250 dissolved in distilled water) then heated in a microwave for about 1 minute. The gels were incubated with the stain for 30 minutes with agitation. The stain was decanted and the gels were destained with the destaining solution (10% glacial acetic acid and 1% glycerol dissolved in distilled water) until the desired protein bands or spots were achieved. The images were taken with the Molecular Imager PharoxFS Plus System (BioRad).

2.9.4 Comparative analysis of 2D gel images

Comparative analysis of 2D SDS-PAGE gels within defined experiments was done using the BioRad PDQuest Advanced 2D Analysis Software version 8.0.1. Background was subtracted and peaks were located. Quantification of resolved proteins was normalized according to the total density of the valid spots.

2.9.5 In gel trypsin digestion

All gel pieces were cut into smaller cubes and washed twice with water followed by 50% (v/v) acetonitrile for 10 minutes. The acetonitrile was replaced with 50 mM ammonium bicarbonate and incubated for 10 minutes, and repeated two more times. All the gel pieces were then incubated in 100% acetonitrile until they turned white, after which the gel pieces were dried in the speedivac. Proteins were reduced with 10 mM DTT for 1 hour at 57 °C. This was followed by brief washing steps of ammonium bicarbonate followed by 50% acetonitrile before proteins were alkylated with 55 mM iodoacetamide for 1 hour in the dark. Following alkylation the gel pieces were washed with ammonium bicarbonate for 10 minutes followed by 50% acetonitrile for 20 minutes, before being dried in vacuo. The gel pieces were digested with 20 µl of a 10 ng/µl trypsin solution at 37 °C overnight. The resulting peptides were extracted twice with 70% acetonitrile in 0.1% formic acid for 30 minutes, and then dried and stored at -20 °C. All peptides were cleaned using stage tips

before injection. Dried peptides were dissolved in 5% acetonitrile in 0.1% formic acid and 10 µl injections were made for nano-LC chromatography. Mass spectrometry was carried out as in section 2.9.7.

2.9.6 Filter-aided sample preparation (FASP)

Samples were mixed 40 µl sample with 40 µl SDT lysis buffer (4% SDS, 100 mM Tris-HCl pH 7.6, 0.1 M DTT that was added freshly just before use). The 80 µl sample was then mixed with 100 µl UA buffer (8 M urea, 100 mM Tris-HCl, pH 8.5) and placed on the filter (Amicon ultra 0.5 centrifugal filter, 10 kDa, Millipore). The device was centrifuged for 40 minutes at 14 000 ×g. This was followed by the addition of 200 µl UA and centrifugation at 14 000 ×g for 40 minutes. The proteins were then alkylated by the addition of 100 µl of 0.05 M iodoacetamide UA buffer. This was then mixed and incubated for 5 minutes before centrifugation at 14 000 ×g for 30 minutes. This was followed by the addition of 100 µl of UB (8 M urea, 0.1 M Tris-HCl pH 8.0), centrifuged for 30 minutes at 14 000 ×g and repeated once more. After centrifugation 100 µl of a 50 mM ammonium bicarbonate solution was added, centrifuged at 14 000 ×g for 30 minutes and repeated once more. This was followed by the addition of 40 µl trypsin and then incubated at 37 °C for 17 hours in a wet chamber. Following incubation, the filter was placed in a clean eppendorf tube and centrifuged for 40 minutes at 14 000 ×g, followed by the addition of 40 µl of a 0.5 M sodium chloride solution and centrifuged for 20 minutes at 14 000 ×g. Finally, the solution was acidified by the addition of 4 µl FA. The filtrate was then desalted using C18 StageTips. The desalted solution was dried in the speedivac and stored at -20 °C. Dried peptides were dissolved in 5% acetonitrile in 0.1% formic acid and 10 µl injections were made for nano-LC chromatography.

2.9.7 Mass spectrometry

All experiments were performed on a Thermo Scientific EASY-nLC II connected to a LTQ Orbitrap Velos mass spectrometer (Thermo Scientific, Bremen, Germany) equipped with a nano-electropsray source. For liquid chromatography, separation was performed on an

EASY-Column (2 cm, ID 100 µm, 5 µm, C18) pre-column followed by an XBridge BEH130 NanoEase column (15 cm, ID 75 µm, 3.5 µm, C18) column with a flow rate of 300 nl/minutes. The gradient used was from 5-40 % B in 20 minutes, 40-80% B in 5 minutes and kept at 80% B for 10 minutes. Solvent A was 100% water in 0.1 % formic acid, and solvent B was 90% acetonitrile in 0.1% formic acid. For 120 minutes gradient: The gradient used was from 5-17% B in 5 minutes, 17-25% B in 90 minutes, 25-60% B in 10 minutes, 60-80% B in 5 minutes and kept at 80% B for 10 minutes. Solvent A was 100% water in 0.1 % formic acid, and solvent B was 90% acetonitrile in 0.1% formic acid.

The mass spectrometer was operated in data-dependent mode to automatically switch between Orbitrap-MS and LTQ-MS/MS acquisition. Data were acquired using the Xcaliber software package. The precursor ion scan MS spectra (m/z 400 – 2000) were acquired in the Orbitrap with resolution R = 60000 with the number of accumulated ions being 1 x 106. The 20 most intense ions were isolated and fragmented in linear ion trap (number of accumulated ions 1.5 x 104) using collision induced dissociation. The lock mass option (polydimethylcyclosiloxane; m/z 445.120025) enabled accurate mass measurement in both the MS and MS/MS modes. In data-dependent LC-MS/MS experiments, dynamic exclusion was used with 60 seconds exclusion duration. Mass spectrometry conditions were 1.5 kV, capillary temperature of 200 °C, with no sheath and auxiliary gas flow. The ion selection threshold was 500 counts for MS/MS and an activation Q-value of 0.25 and activation time of 10 ms were also applied for MS/MS.

2.9.8 Data analysis

Thermo Proteome Discoverer 1.3 (Thermo Scientific, Bremen, Germany) was used to identify proteins via automated database searching (Mascot, Matrix Science, London, UK and Sequest) of all tandem mass spectra against the UNIPROT Homo Sapiens database. Carbamidomethyl cysteine was set as fixed modification, and oxidized methionine, N-acetylation and deamidation (NQ) was used as variable modifications. The precursor mass tolerance was set to 10 ppm, and fragment mass tolerance set to 0.8 Da. Two missed tryptic cleavages were allowed. Proteins were considered positively identified when they were identified with at least 2 tryptic peptides per protein, a Mascot or Sequest score of more

than p<0.05 as determined by Proteome Discoverer 1.3. Percolator was also used for validation of search results. In Percolator a decoy database was searched with a false discovery rate (FDR) (strict) of 0.02 and FDR (relaxed) of 0.05 with validation based on the q-value.

2.10 Oligosaccharide analysis

This section of the work was conducted by Dr. Chunsheng Jin and Dr. Niclas Karlsson at Medicinaregatan, University of Gothenburg in Sweden.

Liquid-chromatography-Mass spectrometry was performed to analyse the O-linked oligosaccharides from the mucin glycoproteins separated by gel electrophoresis. Freeze dried mucus was separated on composite gel for AgPAGE with a gradient of 0-6% polyacrylamide, 0.5%-1% agarose (low electrosomotic flow grade) and 0-10% glycerol within the gel, made up in a 0.375 M Tris-HCl buffer, pH 8.1., 40% ammonium persulfate and TEMED. The gel was poured using a BioRad miniprotein system at 50 °C and allowed to set for 30minutes at this temperature followed by additional time at room temperature. Sample buffer was made up 2X at a concentration of 0.75M Tris-HCl pH 8.1, 20% glycerol, bromophenol blue, 2% SDS. Unreduced sample was placed in the reducing sample buffer and boiled for 20 minutes. Iodoacetamide is added in excess (25 mM) and the solution was incubated in the dark at room temperature for 20 minutes. Running buffer was 192 mM borate, 1mM EDTA, 0.1% SDS and Tris, pH 7.6. Gel electrophoresis was at 40mAmp for 2-3 hours. A Kaleidoscope prestained marker was used. These enable observation of problems with polymerisation as high molecular weight standards will not separate. The electrophoresis was followed by electro-blotting of the glycoproteins to PVDF using a semi-dry method and staining with Direct Blue (DB71) for the glycoprotein bands. The gel was also stained with Coomassie Brilliant Blue. The identified bands were then removed.
The bands were wetted with methanol.

Oligosaccharide side-chains were separated by reductive alkaline β-elimination of sugar side-chains from the mucin glycoprotein. Samples from gel electrophoresis or purified sample (100 µl at a concentration of 1mg/ml in ddH_20), were incubated in eppendorfs, and

sealed to prevent evaporation, at 50˚C for 16h in 20 µl of 50 mM NaOH and 1.5 M $NaBH_4$. The resulting solutions were neutralized by the addition of 1ul of glacial acetic acid, before being desalted with 25 µl of AG50WX8 cation-exchange resin laid on top of a reversed-phase *u*-C18 ZipTip (Millipore), and dried in a Savant SpeedVac. Borate was then removed by repeated (5 times) addition and evaporation of 50ul of 1% acetic acid in methanol. The samples were resuspended in 10 µl of MilliQ water for liquid chromatography coupled to electrospray mass spectrometry (LC/ESI-MS) analysis.

The desalted oligosaccharide alditols were then analysed by liquid chromatography coupled to electrospray tandem mass spectrometry (LC/ESI-MS/MS) on a graphitized carbon column (7-*í*m Hypercarb particles (Thermo-Hypersil) in a 100 × 0.25mm column) or a 150 × 0.32mm Hypercarb column (Thermo-Hypersil). A solvent rate through the column of 5ul/minutes was provided by a Surveyor LC pump (ThermoFinnigan) with flow splitting from 100 µl/minutes. Oligosaccharides were eluted with an H_2O/acetonitrile gradient (0-40% acetonitrile in 30 minutes, followed by a 3 minutes wash with 90% acetonitrile) containing 10 mM NH_4HCO_3. Mass spectrometry was performed using an LCQ Deca (ThermoFinnigan) in negative ion mode, with three scan events: full scan with mass range 320-2000 *m*/*z*, dependent zoom scan of the most intense ions in each scan, and dependent MS/MS scan after collision-induced fragmentation. The capillary temperature was 180 ˚C, the capillary voltage was 32.0V, and the electrospray voltage was 2.5kV. Dynamic exclusion of ions for zoom scan for 30 seconds was introduced after three selections within 30 seconds. For MS/MS, the normalized collision energy was 35%, with an activation time of 30 minutes. Oligosaccharide structure and linkage were determined using a combination of analysis of LC/ESI-MS/MS data and the GlycoSuiteDB sugar database (http://www.glycosuite.com).

CHAPTER 3 : CLINICAL DATA AND SAMPLE COLLECTION

3.1 Clinical recruitment

A total of 168 adults were recruited from primary health clinics in suburban Kroonstad in the Free State Province and suburban Cape Town in the Western Cape Province. In addition to the primary health clinics, adults were also recruited from the Respiratory Clinic at Groote Schuur Hospital and at the DP Marais Hospital in the Western Cape Province. DP Marais Hospital is a TB/HIV hospital in the Western Cape.

Of the 168 recruited for the study, 64 were definite tuberculosis (TB) and 104 adults without TB. Table 3.1 demonstrates the breakdown of the diagnoses from patients without TB within the non-TB group and the uninfected controls for the study. Both males and females were recruited. The ages of the recruited patients ranged for 21 to 75 years. The recruited patients presented with wheezing, weight loss, coughing and/or a productive cough, chest pains, and shortness of breath.

3.2 Diagnostic classification

Uninfected controls – This group was composed of patients who underwent surgery for various reasons besides lung disease. An exclusion criterion was set to exclude patients with prior history of TB.

Non-TB – This group was composed of patients with other respiratory infections and diseases and patients with no evidence of active TB based on direct sputum smear microscopy and radiology.

TB – Patients positively diagnosed with active pulmonary TB by either x-ray showing abnormalities consistent with active TB or 2 sputum smears positive for acid-fast bacilli (AFB). This group also included drug resistant TB strains such as multidrug-resistant (MDR)-TB patients and extensive drug-resistant (XDR)-TB.

Table 3.1: Diagnoses of patients without TB

Diagnosis	Number of patients
Uninfected controls	17
Sarcoidosis	53
Lung Cancer	4
Pulmonary Alveolar Proteinosis	4
Asthma	1
Bronchiectasis	6
Pneumonitis	5
COPD	1
Asbestosis	1
Silicosis	2
Interstitial Lung Disease	7
LIP	3

3.3 Co-infection with HIV

It was difficult to recruit patients who were infected with TB only, since the incidence of TB is strongly associated with HIV infection in this region. Of the 104 patients without TB, 47 were infected with HIV. Out of the 63 TB patients 56 were co-infected with HIV.

3.4 Choice of samples

Initially the project was aimed at analysing respiratory mucus in bronchoalveolar lavage (BAL) samples obtained by bronchoscopy from patients who routinely underwent the procedure for diagnostic and therapeutic purposes. The BALs are usually assessed for the composition of the extracellular luminar spaces of airways during respiratory diseases (Plymoth *et al.*, 2003). The BALs were chosen as a sample of choice to limit the possibility of contamination of respiratory mucus by salivary secretions during expectoration. However, the majority of patients who underwent the bronchoscopy procedure were not TB positive.

In addition to the BALs, sputum was thus selected as the second sample of choice for TB positive mucus. Patients were encouraged to rinse their mouths in order to limit contamination of the respiratory mucus by salivary secretions during expectoration. All of the sputa collected (n=56) were from TB positive patients with a productive cough as it proved difficult to get sufficient sample from those who did not. The TB positive patients were all on medication.

In an attempt to collect sputum from recruits without TB and other respiratory diseases, sputum was induced with 5% saline. However there was no sputum production from these individuals. Therefore tracheal aspirates were collected from patients who underwent surgery for conditions other than respiratory diseases (n=17).

3.5 Discussion

Significant research has been done to find quicker and reliable techniques for diagnosing TB. However, direct sputum smear microscopy is the most common and widely used technique in diagnosing TB. Recently, a confirmed diagnosis of TB is given upon isolating *M.tb* or upon identifying the specific DNA sequence of the bacteria from the sputum or BAL mucus (Majeed and Bukhari, 2011).

The collection of mucus from the recruited patients proved to be a huge limitation to the study. Firstly individuals without respiratory diseases did not produce mucus even after sputum induction. Secondly, individuals without respiratory diseases do not undergo bronchoscopy as it is an invasive procedure. Thirdly, with the complication of HIV, some definite TB positive patients were sputum-scarce as they did not have a productive cough (Peter *et al.*, 2014). This factor decreased the collection of sputum from patients with definite TB. Another limiting factor was the inadequate amount of mucus extracted from the sputa and tracheal aspirates for analyses.

Collection of mucus from individuals without respiratory diseases was very difficult. Therefore better methods are necessary for inducing sputum from these individuals.

CHAPTER 4 : PROTEIN ANALYSIS OF RESPIRATORY SECRETIONS IN UNIFECTED CONTROLS, BALS AND SPUTA

4.1 Introduction

Proteomics is a tool used to study proteins in a biological sample. As the proteome differs from cell to cell, expression proteomics was introduced to compare proteins expressed under certain conditions. To date, expression proteomics remains the most used methodology to compare proteins in the diseased and healthy state. The lung proteome has been widely studied to give information towards understanding the mechanisms leading to lung dysfunction, and to finding biomarkers for diagnostic and prognostic purposes (Lindahl *et al.*, 2001; Wattiez *et al.*, 1999). Knowledge of the lung proteome has been acquired through the analysis of samples such as the epithelial lining fluid, sputum, plasma/serum, lung tissue and the bronchoalveolar lavage fluid (BALF) (Kriegova *et al.*, 2006; Magi *et al.*, 2006).

Owing to its ability to separate hundreds of proteins at a time, the two-dimensional (2D) SDS-PAGE technique remains the method of choice in expression proteomics for separating proteins in complex mixtures (Gorg *et al.*, 2000). The principle of 2D electrophoresis is based on separating the extracted proteins firstly according to their isoelectricpoint (pI) followed by the second dimension where proteins are separated according to their relative molecular mass (Scott *et al.*, 2005).

Gel-based and shotgun proteomic techniques have been employed in the development of the lung proteome (Issa *et al.*, 2011; Plymoth *et al.*, 2003; Wattiez *et al.*, 2007). The 2D technique is widely used as it allows for the separation and visualisation of the lung proteins under various physiological conditions. However, the separation of mucins and glycoconjugates using the gel-based techniques is limited due to their large size (Kesimer and Sheehan, 2012). Recent advances in shotgun proteomics by (Kesimer *et al.*, 2009), has led to the identification of mucins using a high performance liquid chromatography coupled to tandem mass spectrometry (LC-MS/MS).

The aim of this chapter was to identify protein expressed in uninfected controls and TB respiratory mucus. To identify the proteins expressed in the respiratory mucus, proteins were reduced with DTT and alkylated with iodoacetamide. The resulting proteins were precipitated with acetone and their concentrations determined using the Bradford assay. The results were divided into uninfected controls which were collected from healthy tracheal aspirates, TB BALs and TB sputum. The TB group was divided into 2 groups (BALs and sputum) in order to give protein information from the different sources of mucus in TB.

4.2 Results

4.2.1 Separation of respiratory mucus proteins by 1D SDS PAGE

The 1D SDS PAGE was carried out to evaluate the abundance of extracted proteins, the quality of the extracted proteins and their loading quantities prior to separation using the 2D technique. The staining of proteins at the top of the wells was observed in all samples. The detection of these proteins indicated the presence of high molecular weight proteins that could not penetrate the 4% polyacrylamide gel. The protein band intensities varied between samples indicating inter-individual variations as equal amounts of protein were loaded.

Multiple protein bands were observed in the uninfected controls group (Figure 4.1). Similarities in the pattern of the expressed proteins were observed in the biological replicates within the group. Proteins were highly expressed at approximately 72 kDa, above 55 kDa, between 34 kDa and 26 kDa, and at approximately 17 kDa.

Similar protein expression patterns between samples in the TB BALs group in lanes 1 – 4 (Figure 4.2) were noticed. Moreover, more proteins were expressed in lanes 3 and 4 (Figure 4.2) in comparison to lanes 1 and 2. These proteins were highly expressed between 72 kDa and 55 kDa, between 34 kDa and 26 kDa, and at approximately 17 kDa. Interestingly, 2 protein bands were observed in TB BALs at approximately 17 kDa.

Lanes 5 – 9 (Figure 4.2) illustrate protein expression patterns in the TB sputum group. One case of MDR-TB was included in the TB sputum group, lane 9 (Figure 4.2). Protein expression varied between samples indicating inter-individual variation. Highly expressed proteins were noted in lanes 6 and 8. These highly expressed proteins were noted between 95 and 55 kDa, between 34 kDa and 26 kDa, and at approximately 17 kDa. A protein band was observed at approximately 17 kDa in sputa in comparison to TB BALs. Interestingly, the number of protein bands was decreased in the MDR-TB when compared to other TB groups.

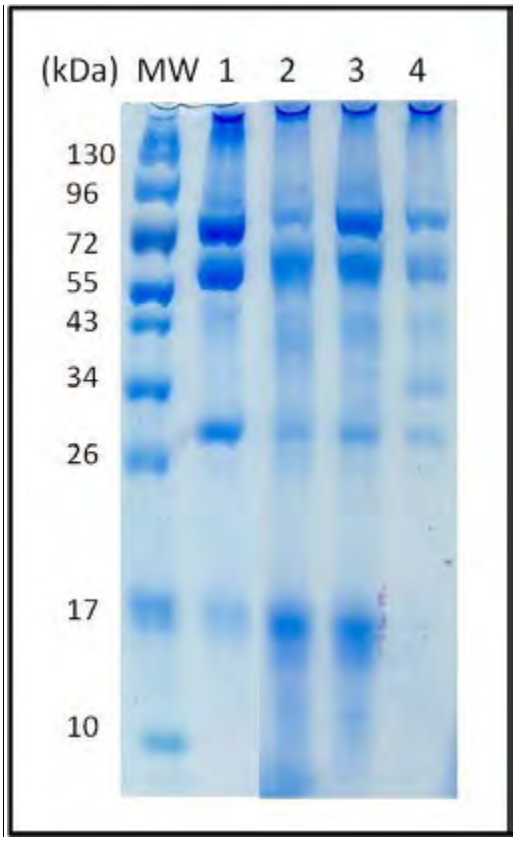

Figure 4.1: A 1D SDS PAGE analysis of proteins from the uninfected controls group.

Approximately 15 µg of protein from healthy tracheal aspirates (uninfected controls) was loaded onto 4-20% SDS polyacrylamide gels. MW is the molecular weight marker lane. Lanes 1-4 represent biological replicates of the proteins extracted from non-TB mucus.

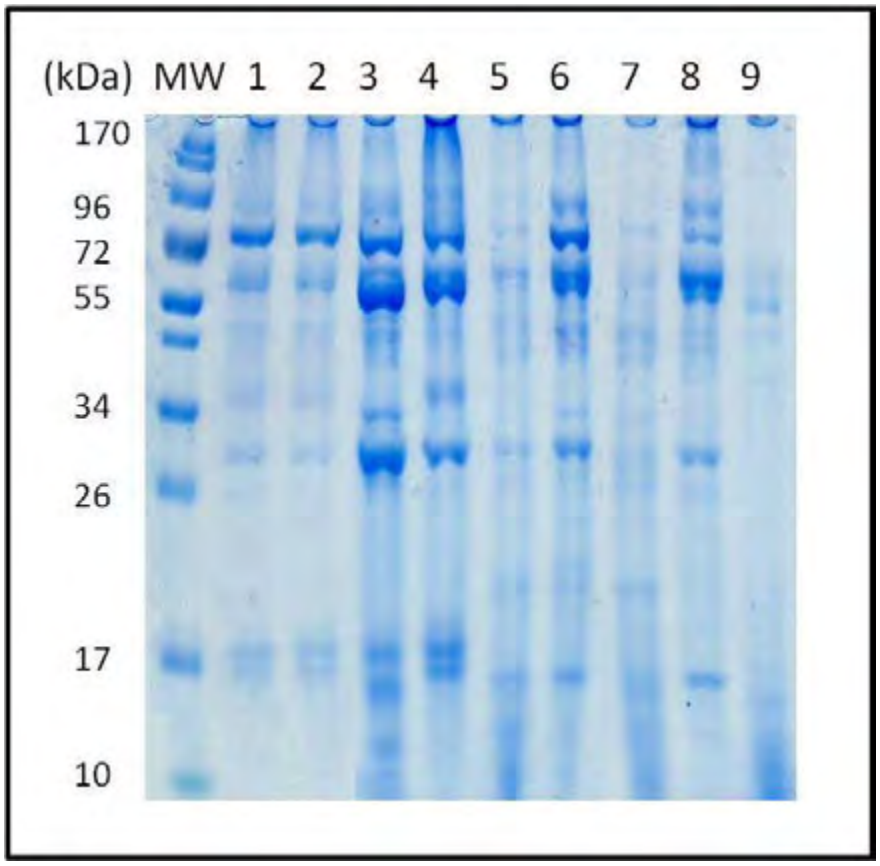

Figure 4.2: A comparative 1D SDS PAGE analysis of proteins from TB BALs and TB sputum groups.

Approximately 15 µg of protein respectively from BAL and sputa of patients with TB was loaded onto 4-20% SDS polyacrylamide gels. MW is the molecular weight marker lane. Lanes 1-4 represent biological replicates of proteins extracted from BALs. Lanes 5-8 represent biological replicates of proteins extracted from sputa. Lane 9 represents proteins extracted from the MDR-TB sample.

4.2.2 Protein identification using mass spectrometry

Proteins were identified from 1D SDS polyacrylamide gels. Gel pieces from 1D SDS polyacrylamide gels were trypsinised and the peptide digests were analysed with mass spectrometry. The mass spectrometer was operated in data-dependent mode to automatically switch between Orbitrap-MS and LTQ-MS/MS acquisition. Proteins were considered positively identified with at least 2 tryptic peptides per protein. A Mascot or Sequest score of more than $p<0.05$ as determined by Proteome Discoverer 1.3 Percolator was also used for validation of the search results.

The names of the proteins from the uninfected controls group, the TB sputum group and TB BALs group are listed as assigned on the database. Proteins with a mascot score above 24 were usually considered significant. Proteins with sequence coverage of 5% were considered good. The total number of peptides detected for each protein and those that were unique to the protein were assigned by the databases. The tables below give a summary of the identified proteins, their score, the number of unique peptides identified, the number of peptides identified, the number of amino acids of the identified proteins, their molecular weight and calculated isoelectric points (pI) as assigned by the databases. A total of 122 proteins were identified from the uninfected controls group (Table 4.1), 79 proteins (Table 4.2) and 74 proteins (Table 4.3) were identified from the TB BALs and TB sputum groups respectively.

Table 4.1: Proteins identified using mass spectrometry from the uninfected controls group following separation by 1D SDS PAGE

Accession No.	Protein	Score	No. of Unique Peptides	No. of Peptides	No. of Amino Acids	MW [kDa]	calc. pI
P63104	14-3-3 protein zeta/delta	26.86	1	1	245	27.7	4.79
P11021	78 kDa glucose-regulated protein	38.80	2	2	654	72.3	5.16
P60709	Actin, cytoplasmic 1	121.12	5	5	375	41.7	5.48
P40394	Alcohol dehydrogenase class 4 mu/sigma chain	36.73	1	1	386	41.5	7.85
P30838	Aldehyde dehydrogenase, dimeric NADP-preferring	42.59	2	2	453	50.4	6.54
P01023	Alpha-2-macroglobulin	120.57	7	7	1474	163.2	6.46
P01019	Angiotensinogen	51.41	1	1	485	53.1	6.32
P04083	Annexin A1	64.83	1	1	346	38.7	7.02
P03973	Antileukoproteinase	47.88	2	2	132	14.3	8.75
P01008	Antithrombin-III	41.03	1	1	464	52.6	6.71
P02730	Band 3 anion transport protein	38.03	2	2	911	101.7	5.19
Q8TDL5	BPI fold-containing family B member 1	122.01	3	3	484	52.4	7.23
P04003	C4b-binding protein alpha chain	64.83	2	2	597	67.0	7.30
Q9NZT1	Calmodulin-like protein 5	39.24	1	1	146	15.9	4.44
P04040	Catalase	218.64	5	5	527	59.7	7.39
P49913	Cathelicidin antimicrobial peptide	50.68	2	2	170	19.3	9.41
O43866	CD5 antigen-like	31.37	1	1	347	38.1	5.47
P00450	Ceruloplasmin	35.91	2	2	1065	122.1	5.72
P02452	Collagen alpha-1(I) chain	41.14	1	1	1464	138.9	5.80
P01024	Complement C3	138.94	6	6	1663	187.0	6.40
P08603	Complement factor H	104.89	3	3	1231	139.0	6.61
P31146	Coronin-1A	29.76	1	1	461	51.0	6.68
P81605	Dermcidin	73.36	2	2	110	11.3	6.54
Q02413	Desmoglein-1	74.58	1	1	1049	113.7	5.03
P13639	Elongation factor 2	35.12	1	1	858	95.3	6.83
P14625	Endoplasmin	27.80	1	1	803	92.4	4.84
Q96HE7	ERO1-like protein alpha	65.83	1	1	468	54.4	5.68
P02675	Fibrinogen beta chain	197.77	6	6	491	55.9	8.27
Q5D862	Filaggrin-2	59.77	1	1	2391	247.9	8.31
P04075	Fructose-bisphosphate aldolase A	31.66	2	2	364	39.4	8.09
P00738	Haptoglobin	75.67	3	3	406	45.2	6.58
P00739	Haptoglobin-related protein	80.98	1	1	348	39.0	7.09
P69905	Hemoglobin subunit alpha	83.60	2	2	142	15.2	8.68
P68871	Hemoglobin subunit beta	230.48	6	6	147	16.0	7.28
P69891	Hemoglobin subunit gamma-1	31.08	1	1	147	16.1	7.20
P22492	Histone H1t	34.01	1	1	207	22.0	11.71
O60814	Histone H2B type 1-K	40.07	1	1	126	13.9	10.32
P68431	Histone H3.1	50.53	2	2	136	15.4	11.12
P62805	Histone H4	30.63	1	1	103	11.4	11.36
Q86YZ3	Hornerin	38.47	3	3	2850	282.2	10.04
P01876	Ig alpha-1 chain C region	156.19	2	6	353	37.6	6.51
P01877	Ig alpha-2 chain C region]	145.50	1	5	340	36.5	6.10
P01880	Ig delta chain C region	80.96	1	1	384	42.2	7.93
P01857	Ig gamma-1 chain C region	77.58	2	5	330	36.1	8.19
P01859	Ig gamma-2 chain C region	126.02	1	4	326	35.9	7.59
P01860	Ig gamma-3 chain C region	88.02	1	5	377	41.3	7.90
P01742	Ig heavy chain V-I region EU	40.96	1	1	117	12.5	6.57

P01743	Ig heavy chain V-I region HG3	30.08	1	1	117	12.9	8.92
P01765	Ig heavy chain V-III region TIL	61.48	1	1	115	12.3	9.13
P01834	Ig kappa chain C region	169.49	2	2	106	11.6	5.87
P01616	Ig kappa chain V-II region MIL	38.40	1	2	112	12.0	9.29
P0CG05	Ig lambda-2 chain C regions	80.08	1	1	106	11.3	7.24
P0CF74	Ig lambda-6 chain C region	32.05	1	1	106	11.3	7.24
P01871	Ig mu chain C region	145.01	5	5	452	49.3	6.77
Q9Y6R7	IgGFc-binding protein	212.75	12	12	5405	571.6	5.34
P01591	Immunoglobulin J chain	48.05	1	1	159	18.1	5.24
P19827	Inter-alpha-trypsin inhibitor heavy chain H1	24.93	1	1	911	101.3	6.79
Q13835-2	Isoform 1 of Plakophilin-1	74.12	1	1	726	80.4	8.97
P02751-10	Isoform 10 of Fibronectin	87.37	2	2	2176	239.5	5.88
P01009-2	Isoform 2 of Alpha-1-antitrypsin	103.67	2	2	359	40.2	5.47
P12814-2	Isoform 2 of Alpha-actinin-1	40.07	2	2	887	102.6	5.50
P35222-2	Isoform 2 of Catenin beta-1	59.67	1	1	88	9.5	4.92
Q00610-2	Isoform 2 of Clathrin heavy chain 1	49.53	3	3	1639	187.8	5.69
P0C0L4-2	Isoform 2 of Complement C4-A	124.44	1	1	1698	187.6	7.12
P0C0L4-2	Isoform 2 of Complement C4-A	41.96	1	1	1698	187.6	7.12
Q96KP4-2	Isoform 2 of Cytosolic non-specific dipeptidase	36.82	1	1	391	43.8	6.48
P02671-2	Isoform 2 of Fibrinogen alpha chain	31.90	1	1	644	69.7	8.06
P06396-2	Isoform 2 of Gelsolin	33.38	1	1	731	80.6	5.85
P14314-2	Isoform 2 of Glucosidase 2 subunit beta	41.06	2	2	525	59.1	4.42
P04406-2	Isoform 2 of Glyceraldehyde-3-phosphate dehydrogenase	51.78	1	1	293	31.5	7.61
Q8TC59-2	Isoform 2 of Piwi-like protein 2	24.03	1	1	937	105.7	9.04
P10909-3	Isoform 3 of Clusterin	47.83	1	1	274	32.3	6.65
P11277-3	Isoform 3 of Spectrin beta chain, erythrocytic	50.63	1	1	2106	242.7	5.35
Q9UGM3-7	Isoform 7 of Deleted in malignant brain tumors 1 protein	164.94	4	4	2532	273.3	5.44
Q15149-7	Isoform 7 of Plectin	36.58	1	1	4515	512.3	5.77
P15924-2	Isoform DPII of Desmoplakin	102.62	4	4	2272	260.0	6.96
P02679-2	Isoform Gamma-A of Fibrinogen gamma chain	39.53	3	3	437	49.5	6.09
P05164-2	Isoform H14 of Myeloperoxidase	150.81	7	7	650	73.8	9.11
P01042-2	Isoform LMW of Kininogen-1	34.10	1	1	427	47.9	6.65
P14923	Junction plakoglobin	68.09	1	1	745	81.7	6.14
P13645	Keratin, type I cytoskeletal 10	599.09	10	12	584	58.8	5.21
P13646	Keratin, type I cytoskeletal 13	423.63	6	10	458	49.6	4.96
P02533	Keratin, type I cytoskeletal 14	170.14	3	7	472	51.5	5.16
P08779	Keratin, type I cytoskeletal 16	179.14	2	6	473	51.2	5.05
Q04695	Keratin, type I cytoskeletal 17	61.30	2	4	432	48.1	5.02
P08727	Keratin, type I cytoskeletal 19	73.15	3	4	400	44.1	5.14
P04264	Keratin, type II cytoskeletal 1	496.40	12	13	644	66.0	8.12
P13647	Keratin, type II cytoskeletal 5	233.87	6	9	590	62.3	7.74
P02538	Keratin, type II cytoskeletal 6A	329.08	7	12	564	60.0	8.00
P02788	Lactotransferrin	328.50	15	15	710	78.1	8.12
P30740	Leukocyte elastase inhibitor	62.54	3	3	379	42.7	6.28
P23490	Loricrin	46.13	1	1	312	25.7	8.09
P61626	Lysozyme C	89.36	2	2	148	16.5	9.16
P14780	Matrix metalloproteinase-9	40.46	2	2	707	78.4	6.06
P26038	Moesin	72.88	2	2	577	67.8	6.40
P98088	Mucin-5AC (Fragments)	233.53	13	14	5030	526.3	6.90

Q9HC84	Mucin-5B	163.74	10	10	5762	596.0	6.64
P59665	Neutrophil defensin 1	61.82	2	2	94	10.2	6.99
Q06830	Peroxiredoxin-1	31.13	1	1	199	22.1	8.13
P03952	Plasma kallikrein	25.28	1	1	638	71.3	8.22
P00747	Plasminogen	52.89	1	1	810	90.5	7.24
P13796	Plastin-2	50.55	1	1	627	70.2	5.43
P01833	Polymeric immunoglobulin receptor	138.30	6	6	764	83.2	5.74
Q99623	Prohibitin-2	42.94	1	1	299	33.3	9.83
P12273	Prolactin-inducible protein	63.61	1	1	146	16.6	8.05
P02760	Protein AMBP	29.17	1	1	352	39.0	6.25
P05109	Protein S100-A8	60.41	1	1	93	10.8	7.03
Q08188	Protein-glutamine gamma-glutamyltransferase E	57.27	1	1	693	76.6	5.86
Q8IWL1	Pulmonary surfactant-associated protein A2	43.56	1	1	248	26.2	5.17
A6NMY6	Putative annexin A2-like protein	75.10	4	4	339	38.6	6.95
Q58FF6	Putative heat shock protein HSP 90-beta 4	35.69	2	2	505	58.2	4.73
P46940	Ras GTPase-activating-like protein IQGAP1	36.89	1	1	1657	189.1	6.48
P13489	Ribonuclease inhibitor	42.40	1	1	461	49.9	4.82
P02787	Serotransferrin	273.26	12	12	698	77.0	7.12
P02768	Serum albumin	1097.25	23	23	609	69.3	6.28
P22531	Small proline-rich protein 2E	22.45	1	1	72	7.8	8.31
Q9Y6N5	Sulfide:quinone oxidoreductase, mitochondrial	31.35	1	1	450	49.9	9.11
P08670	Vimentin	74.79	3	3	466	53.6	5.12
P02774	Vitamin D-binding protein	140.11	2	2	474	52.9	5.54
P04004	Vitronectin	34.09	1	1	478	54.3	5.80
P25311	Zinc-alpha-2-glycoprotein	32.60	2	2	298	34.2	6.05
Q96DA0	Zymogen granule protein 16 homolog B	53.98	1	1	208	22.7	7.39

Table 4.2: Proteins identified using mass spectrometry from the TB bronchoalveolar lavages group following separation by 1D SDS PAGE

Accession No.	Protein	Score	No. of Unique Peptides	No. of Peptides	No. of Amino Acids	MW [kDa]	calc. pI
P63104	14-3-3 protein zeta/delta	101.81	2	2	245	27.7	4.79
P52209	6-phosphogluconate dehydrogenase, decarboxylating	47.12	1	1	483	53.1	7.23
P60709	Actin, cytoplasmic 1	39.74	2	2	375	41.7	5.48
P01011	Alpha-1-antichymotrypsin	74.83	1	1	423	47.6	5.52
P01023	Alpha-2-macroglobulin	26.63	1	1	1474	163.2	6.46
P09525	Annexin A4	24.86	1	1	319	35.9	6.13
P02647	Apolipoprotein A-I	40.36	1	1	267	30.8	5.76
P02730	Band 3 anion transport protein	75.31	1	1	911	101.7	5.19
P04003	C4b-binding protein alpha chain	63.38	1	1	597	67.0	7.30
P04040	Catalase	153.38	3	3	527	59.7	7.39
P07339	Cathepsin D	53.26	1	1	412	44.5	6.54
P23528	Cofilin-1	53.30	1	1	166	18.5	8.09
P02745	Complement C1q subcomponent subunit A	29.45	1	1	245	26.0	9.11
P01024	Complement C3	109.15	2	2	1663	187.0	6.40
P01040	Cystatin-A	39.22	1	1	98	11.0	5.50
P81605	Dermcidin	69.12	2	2	110	11.3	6.54
P02675	Fibrinogen beta chain	33.48	1	1	491	55.9	8.27
Q5D862	Filaggrin-2	40.11	1	1	2391	247.9	8.31
P69905	Hemoglobin subunit alpha	106.51	1	1	142	15.2	8.68
P68871	Hemoglobin subunit beta	161.79	3	3	147	16.0	7.28
P02042	Hemoglobin subunit delta	41.50	1	2	147	16.0	8.05
P02790	Hemopexin	34.78	1	1	462	51.6	7.02
P62805	Histone H4	32.65	1	1	103	11.4	11.36
Q86YZ3	Hornerin	73.92	3	3	2850	282.2	10.04
P01876	Ig alpha-1 chain C region	99.38	2	2	353	37.6	6.51
P01877	Ig alpha-2 chain C region	47.48	1	1	340	36.5	6.10
P01857	Ig gamma-1 chain C region	99.58	3	6	330	36.1	8.19
P01859	Ig gamma-2 chain C region	82.95	1	3	326	35.9	7.59
P01860	Ig gamma-3 chain C region	132.88	2	5	377	41.3	7.90
P01768	Ig heavy chain V-III region CAM	65.11	1	2	122	13.7	9.63
P01781	Ig heavy chain V-III region GAL	43.85	1	1	116	12.7	8.48
P01771	Ig heavy chain V-III region HIL	60.55	1	1	121	13.6	9.36
P01834	Ig kappa chain C region	210.49	3	3	106	11.6	5.87
P01598	Ig kappa chain V-I region EU	39.54	1	1	108	11.8	8.44
P01616	Ig kappa chain V-II region MIL	75.74	1	2	112	12.0	9.29
P01620	Ig kappa chain V-III region SIE	105.90	1	1	109	11.8	8.48
P04433	Ig kappa chain V-III region VG (Fragment)	30.87	1	1	115	12.6	4.96
P01703	Ig lambda chain V-I region NEWM	73.79	1	1	103	10.9	9.29
P0CG05	Ig lambda-2 chain C regions	74.83	1	1	106	11.3	7.24
P01871	Ig mu chain C region	65.46	1	1	452	49.3	6.77
P01591	Immunoglobulin J chain	51.68	1	1	159	18.1	5.24
P02751-10	Isoform 10 of Fibronectin	56.59	2	2	2176	239.5	5.88
Q08554-2	Isoform 1B of Desmocollin-1	36.46	1	1	840	93.8	5.53
P35222-2	Isoform 2 of Catenin beta-1	61.57	1	1	88	9.5	4.92
P53675-2	Isoform 2 of Clathrin heavy chain 2	50.52	1	1	1583	180.2	5.78
P0C0L4-2	Isoform 2 of Complement C4-A	28.09	1	1	1698	187.6	7.12

P00751-2	Isoform 2 of Complement factor B	81.52	1	1	621	68.8	6.57
P02671-2	Isoform 2 of Fibrinogen alpha chain	32.86	2	2	644	69.7	8.06
P35579-2	Isoform 2 of Myosin-9	89.25	1	1	1382	159.8	5.97
P02549-2	Isoform 2 of Spectrin alpha chain, erythrocytic 1	24.31	1	1	2416	279.5	5.05
P60174-1	Isoform 2 of Triosephosphate isomerase	40.17	1	1	249	26.7	6.90
Q9Y3Z3-3	Isoform 3 of Deoxynucleoside triphosphate triphosphohydrolase SAMHD1	31.60	1	1	556	63.6	6.77
P55058-3	Isoform 3 of Phospholipid transfer protein	29.59	1	1	398	44.1	6.55
P11277-3	Isoform 3 of Spectrin beta chain, erythrocytic	188.21	5	5	2106	242.7	5.35
P02788-2	Isoform DeltaLf of Lactotransferrin	37.94	2	2	666	73.1	7.85
P02679-2	Isoform Gamma-A of Fibrinogen gamma chain	72.13	1	1	437	49.5	6.09
P05164-2	Isoform H14 of Myeloperoxidase	53.91	1	1	650	73.8	9.11
P14923	Junction plakoglobin	62.42	1	1	745	81.7	6.14
P13645	Keratin, type I cytoskeletal 10	374.91	10	11	584	58.8	5.21
P02533	Keratin, type I cytoskeletal 14	114.38	1	5	472	51.5	5.16
P08779	Keratin, type I cytoskeletal 16	108.59	3	4	473	51.2	5.05
P04264	Keratin, type II cytoskeletal 1	307.66	6	8	644	66.0	8.12
P13647	Keratin, type II cytoskeletal 5	169.18	4	6	590	62.3	7.74
P61626	Lysozyme C	29.34	1	1	148	16.5	9.16
P98088	Mucin-5AC (Fragments)	79.42	4	4	5030	526.3	6.90
Q9HC84	Mucin-5B	223.29	12	12	5762	596.0	6.64
P30041	Peroxiredoxin-6	54.48	1	1	224	25.0	6.38
P13796	Plastin-2	42.81	1	1	627	70.2	5.43
P01833	Polymeric immunoglobulin receptor	43.77	2	2	764	83.2	5.74
P05109	Protein S100-A8	55.61	1	1	93	10.8	7.03
Q08188	Protein-glutamine gamma-glutamyltransferase E	37.90	1	1	693	76.6	5.86
Q8IWL1	Pulmonary surfactant-associated protein A2	81.12	1	1	248	26.2	5.17
A6NMY6	Putative annexin A2-like protein	69.69	1	1	339	38.6	6.95
Q58FF6	Putative heat shock protein HSP 90-beta 4	46.02	1	1	505	58.2	4.73
P02787	Serotransferrin	139.57	5	5	698	77.0	7.12
P02768	Serum albumin	497.07	15	15	609	69.3	6.28
P11166	Solute carrier family 2, facilitated glucose transporter member 1	33.86	1	1	492	54.0	8.72
Q9Y6N5	Sulfide:quinone oxidoreductase, mitochondrial	38.65	2	2	450	49.9	9.11
P08670	Vimentin	48.38	3	3	466	53.6	5.12

Table 4.3: Proteins identified using mass spectrometry from the TB sputum group following separation by 1D SDS PAGE

Accession No.	Protein	Score	No. of Unique Peptides	No. of Peptides	No. of Amino Acids	MW [kDa]	calc. pI
P52209	6-phosphogluconate dehydrogenase, decarboxylating	34.07	1	1	483	53.1	7.23
P60709	Actin, cytoplasmic 1	99.96	3	3	375	41.7	5.48
P01023	Alpha-2-macroglobulin	121.75	4	4	1474	163.2	6.46
P04083	Annexin A1	126.97	1	1	346	38.7	7.02
P03973	Antileukoproteinase	58.33	3	3	132	14.3	8.75
P05090	Apolipoprotein D	44.09	1	1	189	21.3	5.15
P06731	Carcinoembryonic antigen-related cell adhesion molecule 5	65.33	1	1	702	76.7	5.92
P04040	Catalase	49.89	1	1	527	59.7	7.39
P49913	Cathelicidin antimicrobial peptide	28.36	1	1	170	19.3	9.41
P23528	Cofilin-1	47.78	1	1	166	18.5	8.09
P01024	Complement C3	91.91	2	2	1663	187.0	6.40
P81605	Dermcidin	54.57	1	1	110	11.3	6.54
Q92817	Envoplakin	48.37	1	1	2033	231.5	6.96
Q01469	Fatty acid-binding protein, epidermal	36.64	2	2	135	15.2	7.01
P02675	Fibrinogen beta chain	139.41	3	3	491	55.9	8.27
Q5D862	Filaggrin-2	63.11	1	1	2391	247.9	8.31
Q08380	Galectin-3-binding protein	37.30	1	1	585	65.3	5.27
P00738	Haptoglobin	67.70	2	2	406	45.2	6.58
P69905	Hemoglobin subunit alpha	34.20	1	1	142	15.2	8.68
P68871	Hemoglobin subunit beta	76.96	1	1	147	16.0	7.28
O60814	Histone H2B type 1-K	50.55	2	2	126	13.9	10.32
Q6NXT2	Histone H3.3C	46.40	1	1	135	15.2	11.11
Q86YZ3	Hornerin	58.11	3	3	2850	282.2	10.04
P01876	Ig alpha-1 chain C region	68.12	1	3	353	37.6	6.51
P01877	Ig alpha-2 chain C region	89.47	1	3	340	36.5	6.10
P01857	Ig gamma-1 chain C region	105.64	2	3	330	36.1	8.19
P01859	Ig gamma-2 chain C region	113.20	1	2	326	35.9	7.59
P01860	Ig gamma-3 chain C region	80.25	1	3	377	41.3	7.90
P01742	Ig heavy chain V-I region EU	68.29	1	1	117	12.5	6.57
P01768	Ig heavy chain V-III region CAM	67.52	1	1	122	13.7	9.63
P01772	Ig heavy chain V-III region KOL	48.63	1	1	126	13.7	5.87
P01834	Ig kappa chain C region	206.07	2	2	106	11.6	5.87
P01616	Ig kappa chain V-II region MIL	74.87	1	2	112	12.0	9.29
P0CG05	Ig lambda-2 chain C regions	111.59	2	2	106	11.3	7.24
P01871	Ig mu chain C region	83.50	2	2	452	49.3	6.77
P01591	Immunoglobulin J chain	48.26	1	1	159	18.1	5.24
Q13835-2	Isoform 1 of Plakophilin-1	96.89	1	1	726	80.4	8.97
Q8TDL5-2	Isoform 2 of BPI fold-containing family B member 1	49.99	1	1	160	17.7	9.72
P0C0L4-2	Isoform 2 of Complement C4-A	131.37	1	1	1698	187.6	7.12
P35579-2	Isoform 2 of Myosin-9	85.09	1	1	1382	159.8	5.97
P01009-3	Isoform 3 of Alpha-1-antitrypsin	46.22	1	1	306	34.7	5.19
Q9UGM3-4	Isoform 4 of Deleted in malignant brain tumors 1 protein	40.03	1	1	1527	166.4	5.43
P35241-4	Isoform 4 of Radixin	62.30	1	1	447	52.6	6.16
Q9UGM3-7	Isoform 7 of Deleted in malignant brain tumors 1 protein	136.03	1	1	2532	273.3	5.44
P02788-2	Isoform DeltaLf of Lactotransferrin	267.62	6	6	666	73.1	7.85
P15924-2	Isoform DPII of Desmoplakin	46.35	1	1	2272	260.0	6.96

P02679-2	Isoform Gamma-A of Fibrinogen gamma chain	59.79	1	1	437	49.5	6.09
P05164-2	Isoform H14 of Myeloperoxidase	56.09	3	3	650	73.8	9.11
P13645	Keratin, type I cytoskeletal 10	258.73	5	6	584	58.8	5.21
P13646	Keratin, type I cytoskeletal 13	525.97	5	7	458	49.6	4.96
P02533	Keratin, type I cytoskeletal 14	168.35	1	7	472	51.5	5.16
P08779	Keratin, type I cytoskeletal 16	171.70	1	7	473	51.2	5.05
Q7Z3Y8	Keratin, type I cytoskeletal 27	128.06	2	4	459	49.8	5.05
P04264	Keratin, type II cytoskeletal 1	211.20	3	4	644	66.0	8.12
P30740	Leukocyte elastase inhibitor	71.62	1	1	379	42.7	6.28
P61626	Lysozyme C	130.93	4	4	148	16.5	9.16
P98088	Mucin-5AC (Fragments)	272.16	11	12	5030	526.3	6.90
Q9HC84	Mucin-5B	190.68	6	7	5762	596.0	6.64
P59665	Neutrophil defensin 1	36.23	1	1	94	10.2	6.99
P80188	Neutrophil gelatinase-associated lipocalin	35.31	1	1	198	22.6	8.91
Q8WUA2	Peptidyl-prolyl cis-trans isomerase-like 4	36.45	1	1	492	57.2	5.92
P36955	Pigment epithelium-derived factor	51.92	1	1	418	46.3	6.38
P01833	Polymeric immunoglobulin receptor	197.34	3	3	764	83.2	5.74
P12273	Prolactin-inducible protein	61.96	1	1	146	16.6	8.05
P05109	Protein S100-A8	64.37	1	1	93	10.8	7.03
A6NMY6	Putative annexin A2-like protein	65.08	1	1	339	38.6	6.95
O95968	Secretoglobin family 1D member 1	35.20	1	1	90	9.9	9.25
P02787	Serotransferrin	182.03	6	6	698	77.0	7.12
P02768	Serum albumin	509.34	11	11	609	69.3	6.28
Q5T750	Skin-specific protein 32	34.01	1	1	250	26.2	7.97
P22531	Small proline-rich protein 2E	42.22	2	2	72	7.8	8.31
P02774	Vitamin D-binding protein	36.28	1	1	474	52.9	5.54
P25311	Zinc-alpha-2-glycoprotein	55.34	1	1	298	34.2	6.05
Q96DA0	Zymogen granule protein 16 homolog B	57.78	1	1	208	22.7	7.39

4.2.3 Classification of the functions of identified proteins

The functions of the identified proteins were classified using the Panther Classification System (http://www.pantherdb.org/). Panther is an acronym for **p**rotein **an**alysis **th**rough **e**volutionary **r**elationships. The functions of the proteins were first separated according to their protein classes then according to their family/subfamily that demonstrated similar functions. Figure 4.3 illustrates the classes of proteins identified from the uninfected controls group in a form of a pie chart. The classes of proteins found from the TB BALs group and the TB sputum group are represented in Figure 4.4 and Figure 4.5 respectively.

The figures show that more structural and cytoskeletal proteins were present in all three groups. Higher percentages of hydrolases, extracellular matrix, receptor proteins and proteins belonging to the protease family were noticed in the uninfected controls group when compared to the TB groups analysed from BALs and sputa. Defence proteins displayed similar percentages between the uninfected controls, the TB BALs and TB sputum groups. More calcium binding proteins were observed in uninfected controls and TB sputum groups than in TB BALs.

The protein classes could further be subdivided into 2 groups namely the molecular function (Table 4.4) and biological processes (Table 4.5) they are involved in. The molecular function also confirmed that more calcium binding proteins were observed in uninfected controls and TB sputum groups than in TB BALs. A higher number of proteins involved in antioxidant activity were noticed in the TB BALs group.

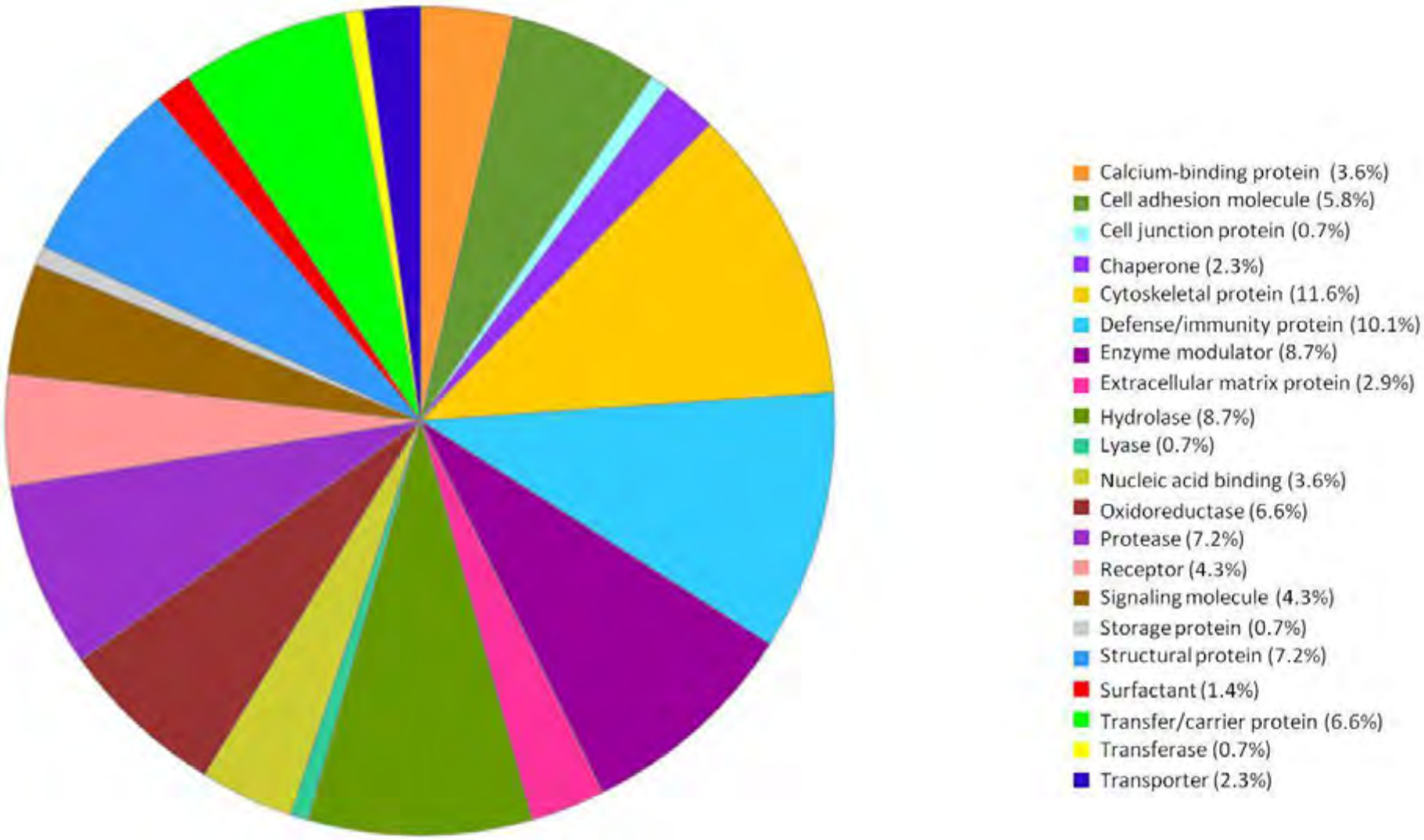

Figure 4.3: Proteins of the uninfected controls group classified according to their protein class.

The identified proteins were classified into their protein classes using the Panther Classification System (http://www.pantherdb.org/).

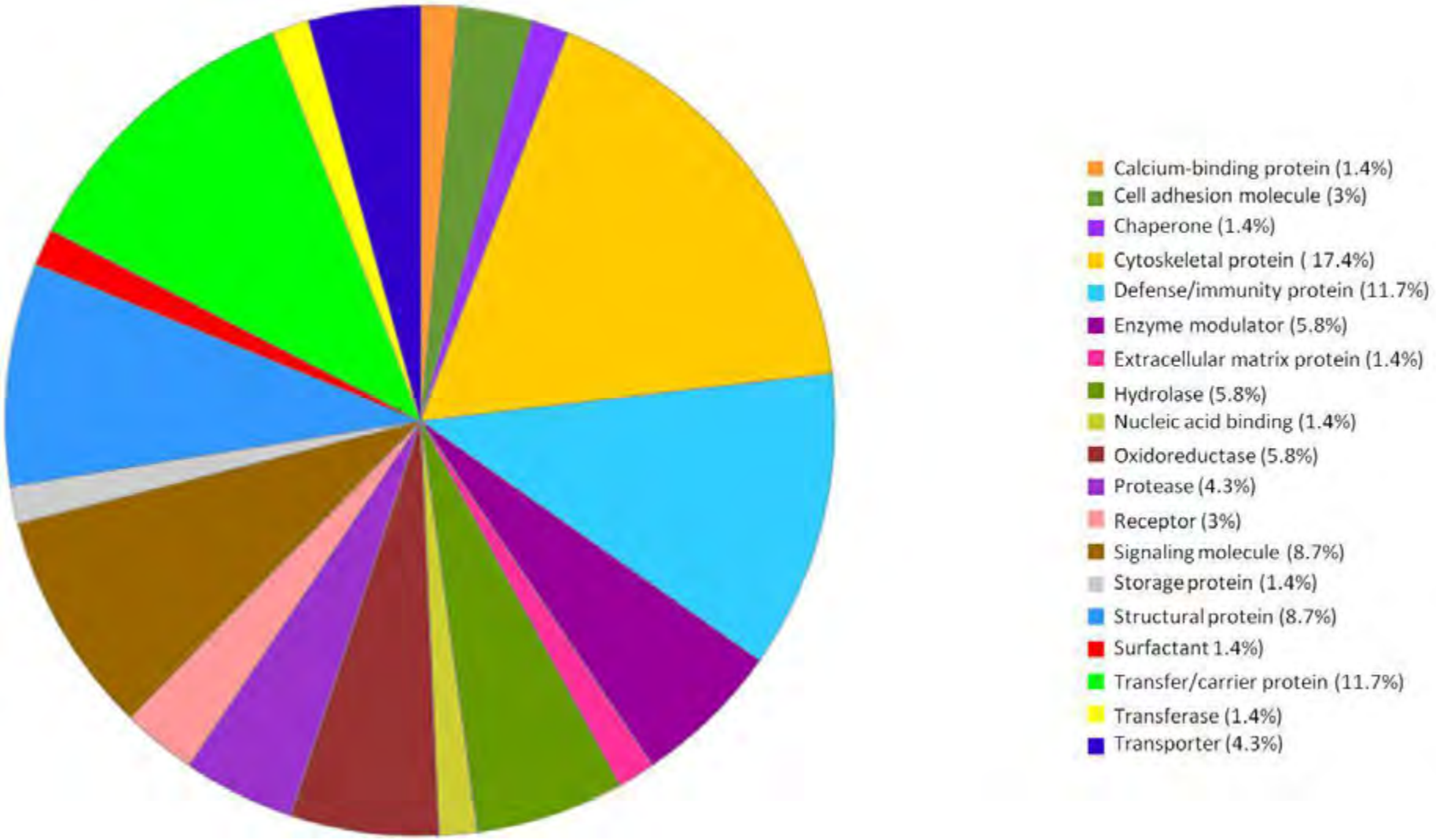

Figure 4.4: Proteins of the TB BALs group classified according to their protein class.

The identified proteins were classified into their protein classes using the Panther Classification System (http://www.pantherdb.org/).

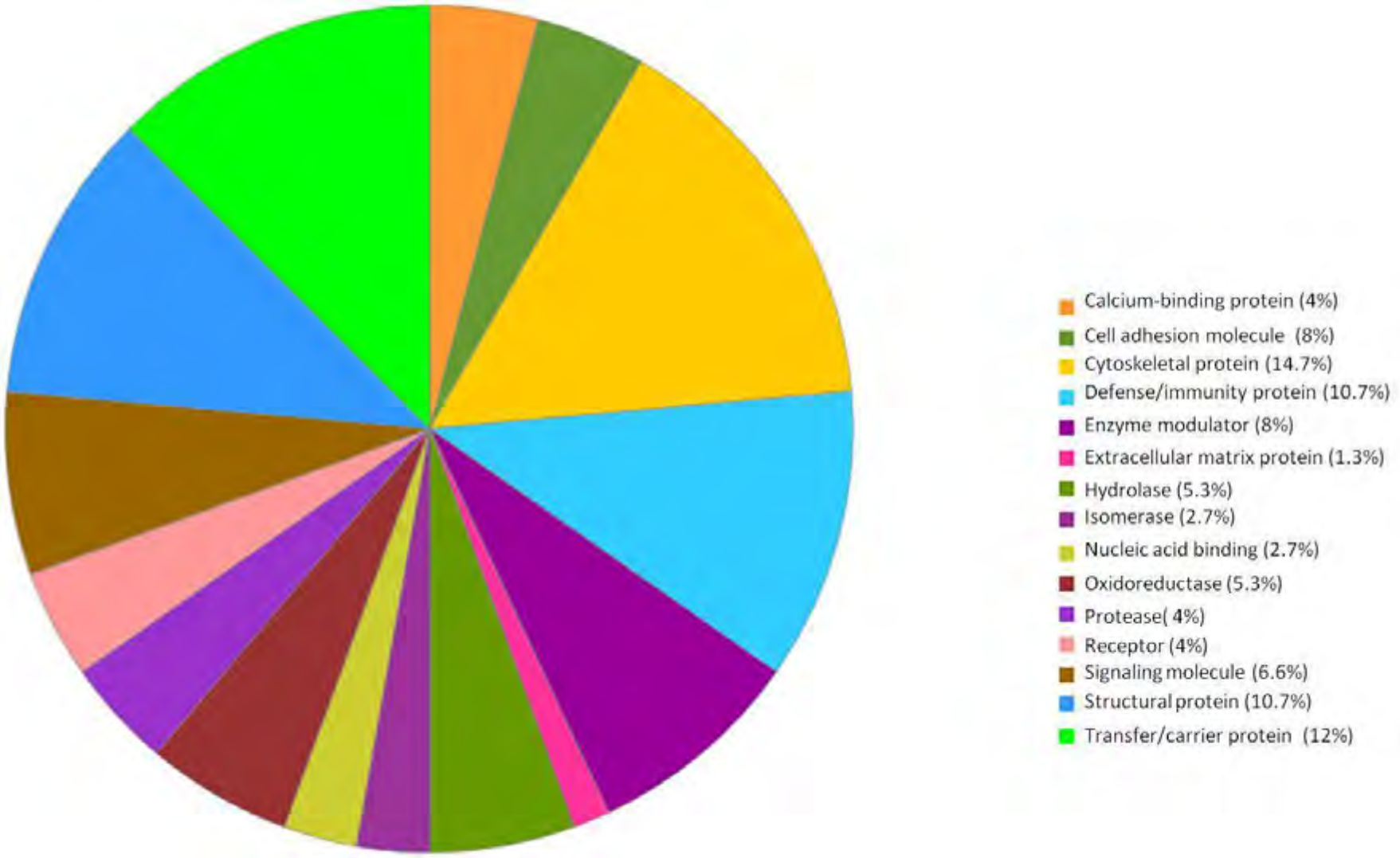

Figure 4.5: Proteins of the TB sputum group classified according to their protein class.

The identified proteins were classified into their protein classes using the Panther Classification System (http://www.pantherdb.org/).

Table 4.4: Classification of proteins according to their molecular function using the Panther Classification System

Molecular Function	Uninfected controls (%)	TB BALs (%)	TB Sputum (%)
Antioxidant activity	2.1	4.3	2.7
Binding	30.7	26.1	48.6
Catalytic activity	22	19.6	21.6
Enzyme regulator activity	12.1	8.7	16.3
Receptor activity	6.6	4.3	0
Structural molecule activity	20	28.3	8.1
Translation regulator activity	1	0	0
Transporter activity	5.5	8.7	2.7

Table 4.5: Classification of proteins according to their biological process using the Panther Classification System

Biological Process	Uninfected controls (%)	TB BALs (%)	TB Sputum (%)
Apoptosis	0.9	0	0.8
Cell adhesion	4.5	3.3	3.8
Cell communication	7.1	6.6	6.9
Cell cycle	3.1	2.5	1.5
Cellular component organisation	9.4	11.6	9.8
Cellular process	17.4	16.5	17.4
Developmental process	8.5	10.7	9.8
Generation of precursor metabolites and energy	0.9	0.9	0.8
Homeostasis process	0.9	0.9	0
Immune system process	9.8	9.1	9.8
Localization	0.4	0	15.9
Metabolic process	17	16.5	0
Reproduction	2.2	0	2.3
Response to stimuli	7.6	6.6	7.6
System process	3.6	4.1	4.5
Transport	6.7	10.7	9.1

4.3 Discussion

Proteins play crucial roles in the body with functions such as enzymes, transporters, structure creators, receptors, growth factors and antibodies among many others (Garrett and Grisham, 2005). The use of proteomics in the identification of proteins in the diseased and healthy state has been carried out for more than a decade. In 2005, Sloane and colleagues examined the expression of proteins during pulmonary exacerbations in cystic fibrosis (Sloane *et al.*, 2005). Similarly proteomic techniques were applied in other studies to determine proteins in diseases such as asthma (Haenena *et al.*, 2014), pulmonary sarcoidosis (Kriegova *et al.*, 2006) and tumor-associated glycoproteins (Li *et al.*, 2013). Recently, (Fu *et al.*, 2012) initiated an investigation into the expression of proteins in TB. However, the knowledge is far from complete and more information is required regarding TB. These studies have highlighted the importance of the extraction of the proteins from the sample and the reproducibility of the experiment.

Mucins are large polydisperse glycoproteins with molecular weights ranging between 200 kDa and 2 MDa (Issa *et al.*, 2011). It was thus essential to determine proteomic techniques that would lead to the identification of large proteins such as mucins. The protein extraction from the various sources of mucus was optimised using the acetone method. In an attempt to identify proteins using non gel-based techniques, the filter-aided sample preparation (FASP) method was employed. Using this technique, the samples were lysed, filtered with 10 kDa filter, detergents were removed with repeated washes and trypsinised in preparation for mass spectrometry. However, there was a limitation identifying proteins above 180 kDa. Therefore, this technique could not be used in the identification of proteins between the uninfected controls and TB groups, as large proteins, mucins in particular, could not be identified.

Gel-based techniques (1D SDS and 2D SDS polyacrylamide gels) were thus used in the identification of large proteins including mucins. However, proteins above 170 kDa we confined to the IPG strip and could not be resolved into the gel. Therefore these proteins could not be identified. The 1D protein profiles showed that the extracted proteins were of high quality. The 1D protein profiles also showed that proteins were expressed at different

concentrations in different samples indicative of inter-individual variations. The biological replicates from each group (uninfected controls, TB BALs and TB sputum) demonstrated high similarities in the protein expression pattern within each group. The consistency in the expression pattern across the replicates indicated the validity/reproducibility of the technique in separating mucus proteins.

The limitations of the 2D technique and the FASP technique led to the identification of proteins from the combination of 1D SDS polyacrylamide gels and mass spectrometry techniques. More proteins were identified from the uninfected controls group (122 proteins) in comparison to the TB BALs (79 proteins) and TB sputum groups (74 proteins). Although the Orbitrap mass spectrometry managed to identify the proteins, the identified proteins could not be quantified using this technique. Following protein identification, proteins were classified according to their protein classes, molecular function and biological processes using the Panther Classification System.

The most abundant protein class was cytoskeletal proteins which were higher in TB (BALs and sputum) when compared to uninfected controls. A similar phenomenon was observed with structural proteins, which were represented in higher proportions in the TB groups than in the uninfected controls group. Cytoskeletal and structural proteins are important for cell movement and provide extracellular proteins which form structures thus providing strength and protection to cells and tissue (Fu *et al.*, 2012; Garrett and Grisham, 2005). Higher cytoskeletal and structural proteins in TB may be due to lung tissue remodelling that takes place during disease progression. It was also not surprising to find these proteins in abundance in all samples tested as they are constantly required to maintain their function in the presence or absence of the disease. Similarly, high cytoskeletal proteins were identified by Fu and colleagues (Fu *et al.*, 2012). However, they found that the cytoskeletal proteins were downregulated following TB infection except for ARP2 actin-related protein 2 homolog and tropomyosin isoform which were upregulated.

Defence and immunity proteins were higher in the TB groups compared to the uninfected controls group. However, the difference was not highly significant. The innate immunity is the first line of defence against invasion by *M.tb*. Cells of the innate immune response,

express pattern recognition receptors (PRRs), through which they engage the bacteria and secrete host defence factors such as cytokines and chemokines (Hazlett and Wu, 2011; Marakalala *et al.*, 2011); Therefore the results indicate that the defence proteins continuously fight off inhaled particles in an attempt to protect the lungs against infections.

Another class of proteins present in higher percentages are the hydrolase proteins. Increased hydrolases were noticed in the uninfected controls group compared to the TB groups. As part of the innate immunity response, macrophages are involved in the capture of *M.tb*. These macrophages reside in the alveolar surfactant film. Hydrolases are present in both the alveolar surfactant film and macrophages (Arcos *et al.*, 2011; Torrelles, 2012). However, hydrolases that are secreted into the surfactant film are different from lysosomal hydrolases, with the latter proteins known to degrade bacteria upon phagolysosome fusion. The hydrolases that were detected in the TB BAL group are likely to be from the alveolar surfactant film rather than the lysosomes within macrophages. Arcos *et al.* (2011) showed that hydrolases present in the alveolar lining fluid can modify the mycobacterial cell envelope resulting in altered intracellular trafficking. Moreover, exposure of *M.tb* to the hydrolases led to the induction of protective effects characterized by pro-inflammatory cytokine production and reduced bacterial survival within macrophages (Arcos *et al.*, 2011). Thus, surfactant hydrolases have potential in mediating host defence against TB progression.

Also found in the alveolar surfactant protein (SP) fraction are four surfactant apoproteins called SP-A, -B, -C, and –D (Torrelles, 2012). Interestingly, through PANTHER, the surfactant protein was assigned its own protein class. This group consisted of SP-A2. This protein is an isoform of the SP-A family. The SP-A is a lipoprotein synthesized and secreted by the type II epithelial cells of the lung and Clara cells of the terminal bronchioles (Hu *et al.*, 2012; Kishore *et al.*, 2006). This surfactant protein plays a role in the reduction of surface tension at the air-liquid interface in the lung during gas-exchange, maintaining the integrity of the alveoli, and in the modulation of inflammatory and immunological responses (Silveyra and Floros, 2013; Wang *et al.*, 2009). The surfactant protein A2 was found in both uninfected controls and TB BALs. The uninfected controls' samples were tracheal aspirates that were procured from patients with no respiratory infections and diseases. Hence, it was surprising

that SP-A2 was identified in the tracheal aspirates of healthy individuals and not in TB sputum. Sputum proteins are representative of alveolar cells (Nicholas *et al.*, 2006). The mechanism behind this alveolar surface protein in tracheal aspirates is not yet understood.

As part of the innate immunity, alveolar macrophages would express PRRs which would result in a cascade of immune responses including phagocytosis, signal transduction and the induction of T-cell mediated immunity (Marakalala *et al.*, 2011; Torrelles, 2012). *M.tb* has been shown to trigger host immune responses through specific molecules signaling downstream receptors such as Toll-like receptors (TLRs), nucleotide-binding oligomerization domain-like (NODs) receptors and C-type lectin-like receptors (CLRs) (Marakalala *et al.*, 2011). The results showed a higher percentage of proteins associated with signaling molecules in the TB group than uninfected controls. The higher signaling molecules in the TB group may be attributed to active signaling events induced upon the recognition of the bacteria.

A higher percentage of extracellular matrix (ECM) was observed in uninfected controls than in the TB group. The ECM is crucial in maintaining normal lung function, ventilation and gas exchange (Pelosi *et al.*, 2007). In order to maintain the physiological balance of the lung ECM, regulatory mechanisms such as the degradation of the ECM by matrix metalloproteinases (MMPs) are employed to maintain a balance between synthesis and degradation of the ECM. MMPs also play a role in tissue remodeling and cellular recruitment (Ong *et al.*, 2014). The decrease in ECM in the TB group may be attributed to tissue remodelling and possibly the destruction of the ECM due to the spread of the bacteria in the TB group. The proliferation of *M.tb* in the lungs may lead to TB-mediated necrosis and cavitation of granulomas as a result of hyper-inflammation (Elkington *et al.*, 2011; Ong *et al.*, 2014). A higher percentage of the ECM protein would be expected in uninfected controls as they would be maintaining the normal functioning of the lungs.

The proteomic analysis revealed other protein classes whose differential expression was interesting but their relationship to TB is poorly understood. For instance transfer/carrier proteins were two-fold higher in TB group than in the uninfected controls group. This association remains an explorable area of future research. Another example of poorly

understood proteins is a class of chaperones, which were higher in uninfected controlscompared to the TB BALs. These proteins can mediate a form of autophagy, in which some cytosolic proteins are targeted for degradation in the lysosomes (Kaushik and Cuervo, 2012). Autophagy is an important response in TB in that stimuli enabling cells that induce autophagy may kill intracellular *M.tb* (Bradfute *et al.*, 2013). Hence detailed understanding of its relationship with chaperones in the context of the disease will likely yield exciting outcomes.

The current study utilized a combination of proteomics and mass spectrometry to identify classes of proteins that can potentially be used as bio-signatures in TB. With a dire need for alternative diagnostics, expression trends of specific host proteins could be exploited into designing tools that can predict host susceptibility or protection against the disease.

CHAPTER 5 : ISOLATION AND PURIFICATION OF MUCINS BY WESTERN BLOTTING

5.1 Introduction

In order to study the mechanism and ultimately the structure of proteins, the proteins must be purified (Berg *et al.*, 2002; Garrett and Grisham, 2005). There is however no single universal method to isolate and purify all proteins as they vary in water solubility, size and charge. Mucins are high molecular weight glycoproteins that are large in size and mass. Additionally, mucins are polydisperse, extensively glycosylated, heterogeneous and have high viscosity in solution (Harding, 1989; Thornton *et al.*, 1997). These characteristics are a limiting factor in the analysis of mucins as the majority of mucin subunits range between 200 kDa and 10 MDa (Issa *et al.*, 2011). Holden et al., in 1971, reported that the tendency of mucins to form gels at moderate concentrations and their ability to adhere to supporting media suggests that they are held together by strong intermolecular forces (Holden *et al.*, 1971).

Over the past years considerable efforts have been made in developing techniques to separate and identify mucins in accordance with their large size and polydispersity. Sheehan *et al.* (1991) have shown that in order to study respiratory mucins, the integrity of the core protein must be maintained throughout the process of purification through the addition of denaturants and protease inhibitors to eliminate endogenous proteolytic activity. Therefore mucous gels are extracted in 6M guanidinium hydrochloride (GuHCl) containing EDTA to limit metalloproteinases and NEM to suppress degradation by thiol proteinases (Carlstedt and Sheehan, 1984).

(Creeth and Denborough, 1970) demonstrated the success of the use of a technique involving sedimentation equilibrium in a caesium chloride gradient when working with high molecular weight glycoproteins. Their findings were later supported by (Bhaskar and Reid, 1981) and (Woodward *et al.*, 1982). The success of this technique has been crucial in the isolation and purification of mucins. The purified mucins are then separated using electrophoresis.

A few reports appear in the literature on the investigation of mucins by SDS polyacrylamide gel electrophoresis (PAGE) (Mall *et al.*, 1999; Pearson *et al.*, 1981). However purified mucins do not penetrate the acrylamide gels because of their large size and extensive glycosylation. In 1971, Holden et al. reported the use of agarose to facilitate the entry and migration of mucins in the gel. Agarose gel electrophoresis followed by Western blotting has thus, in more recent times, become the standard technique to investigate purified mucins after they have been reduced (Sheehan *et al.*, 2004; Thornton *et al.*, 1996).

This chapter therefore aimed at evaluating the types of mucins secreted in TB and non-TB respiratory mucus. The specific objectives were to identify mucins by Western blotting firstly in crude material, namely tracheal aspirates from patients with non-lung disease, BALs with a variety of diseases, and TB sputa with the TB group HIV negative and positive and 2 cases of MDR-TB. The second approach was to identify mucins in the groups described after purification by CsCl density gradient ultracentrifugation. Mucins were subjected to Western blotting from individual fractions of the second density gradient ultra-centrifugation at a density of 1.39-1.40 g/ml.

5.2 Results

5.2.1 Identification of respiratory mucins from crude samples

Mucins were investigated in tracheal aspirates of patients undergoing surgery for non-respiratory conditions, BALs (for various diseases, see methods section 2.3.1) and sputa collected from the patients without and with a diagnosis of TB. Crude mucus was reduced, alkylated, dialysed against water and lyophilised and subjected to electrophoresis on agarose gel (See methods section 2.6). Following electrophoresis the gels were transferred to nitrocellulose membranes and probed with anti-secretory mucin antibodies, namely, anti (-MUC2, -MUC5AC, -MUC5B and -MUC7) antibodies (see methods section 2.7).

5.2.1.1 Identification of mucins in crude tracheal aspirates of patients undergoing surgery for non-lung diseases controls/normal?

Tracheal aspirates were collected by an anaesthetist from patients undergoing surgery for various reasons besides lung disease. These aspirates were designated uninfected controls. Mucins identified from tracheal aspirates from patients undergoing surgical procedures of non-lung diseases are illustrated in Figure 5.1 (lanes 1-4). Distinct MUC5AC bands with similar electrophoretic mobility and intensity were observed from the normal tracheal aspirates. The MUC5AC band in lane 4 was larger and brighter than the bands in lanes 1-3. MUC5B appeared as a smear with varying electrophoretic mobility. MUC5B had migrated further down the gel in comparison to MUC5AC. Single distinct bands of MUC2 with similar electrophoretic mobility were observed whilst MUC7 migrated further into the gel, with each sample varying in mobility.

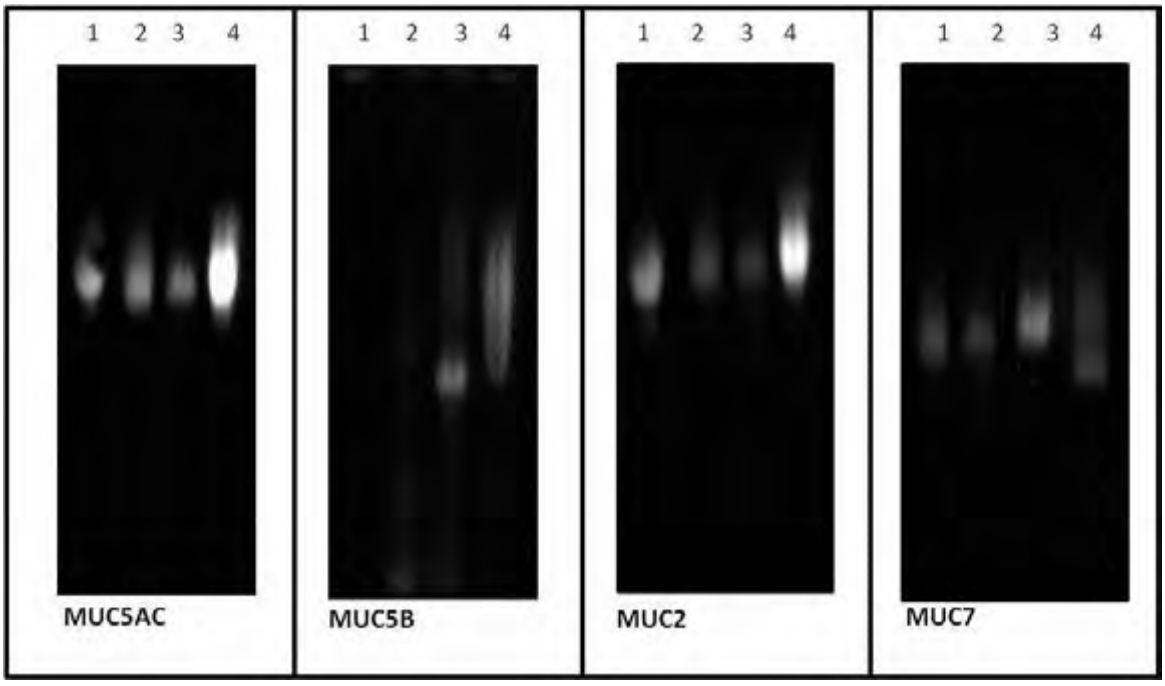

Figure 5.1: Agarose gel electrophoresis of reduced crude uninfected mucus from tracheal aspirates undergoing surgical procedures for non-lung diseases.

Reduced and alkylated crude tracheal aspirate mucus was electrophoresed on a 0.7% agarose gel and subsequently blotted onto nitrocellulose membrane. The blot was probed with anti (-MUC5AC, -MUC5B, -MUC2 and -MUC7) antibodies.

5.2.1.2 Identification of mucins in crude bronchoalveolar lavage (BALs) from patients with a variety of lung diseases.

Bronchoalveolar lavages were obtained from patients with suspected lung disease and underwent bronchoscopy. Notable differences were seen in the band intensities. Brighter MUC5AC bands were seen in samples from patients with and without TB indicating higher levels of MUC5AC in BALs (Figure 5.2). MUC5AC migrated to a similar position on the gel. Sarcoidosis comprised the largest group of the non-TB group. Despite similar electrophoretic mobility of MUC5AC within the sarcoidosis group, inter-individual variations were observed for equal loadings. One sarcoidosis patient had a very intense and widespread smear which suggested a wide range of charge for the MUC5AC population in this case (Figure 5.2). A similar observation was made for MUC5AC in alveolar proteinosis whilst pneumonia showed a clear single band. A single band of MUC5AC was seen in TB alone whilst the material from a patient with TB and HIV was a large bright smear, again suggesting the presence of more than one population of MUC5AC of varying charges.

MUC5B appeared as a smear over a large area (Figure 5.2). This suggested the presence of different populations of MUC5B suggesting a heterogeneous distribution of this mucin. When compared to MUC5AC, the MUC5B material was less intense with hardly a band for TB and TB with HIV. MUC2 bands appeared to have similar electrophoretic mobility to MUC5AC (Figure 5.3). When compared to MUC5AC, the MUC2 bands were fainter except one sarcoidosis patient. There is a more intense band for TB/HIV in MUC2 than in MUC5B. MUC7 was not detected in the BALs. The analysed BALs gave similar patterns in the migration of mucin bands for MUC5AC, MUC5B and MUC2 between the patients with and without TB. In all cases for MUC5AC, MUC5B and MUC2, the band was more visible for TB in HIV.

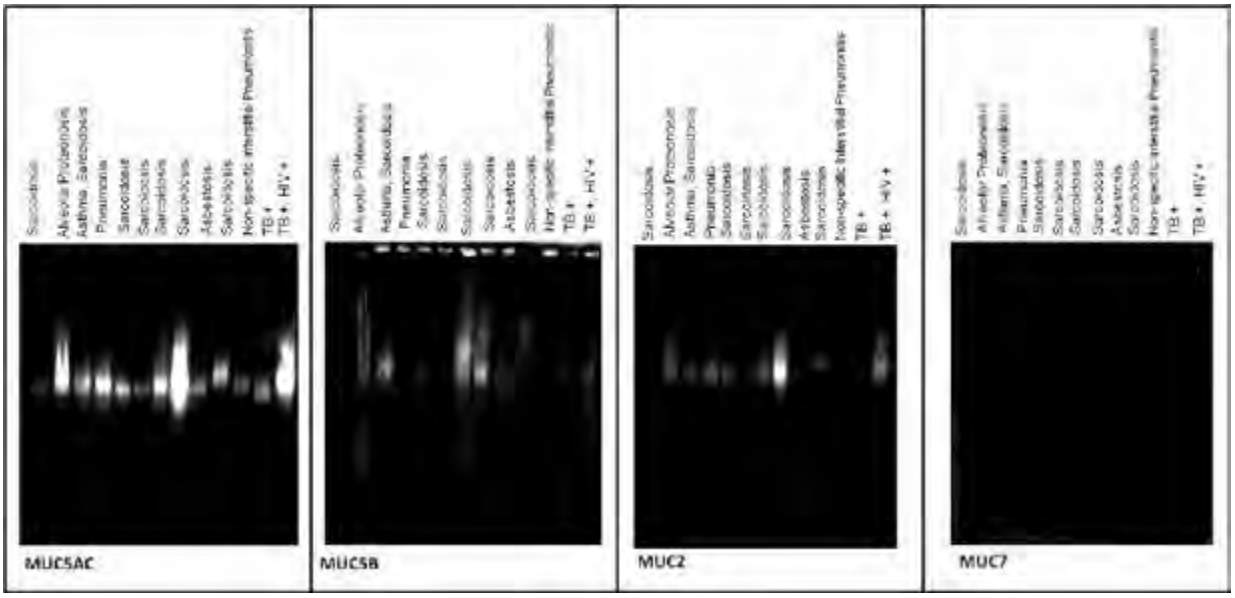

Figure 5.2: Identification of reduced crude non-TB and TB mucus from crude bronchoalveolar lavages.

Reduced and alkylated crude TB and non-TB BAL mucus was electrophoresed on a 0.7% agarose gel and subsequently blotted onto nitrocellulose membrane. The blot was probed with anti (-MUC5AC, -MUC5B and -MUC2) antibodies.

5.2.1.3 Identification of mucins in crude sputa

Sputa were obtained by expectoration from patients diagnosed with TB (see methods section 2.3.3). Varying populations of MUC5AC and MUC5B mucins were observed in TB sputa as compared to the BALs in Figure 5.2. These populations are illustrated in Figure 5.3 (lanes 1-17). MUC5AC presented largely as a single band with similar electrophoretic mobility appearing as a smear with inter-individual variation. In some cases, MUC5AC was barely visible (Figure 5.4 lanes 7 and 12). Figure 5.4 lane 15 had the brightest band with a much wider smear. Higher levels of MUC5AC were detected in TB sputa when compared to MUC5B.

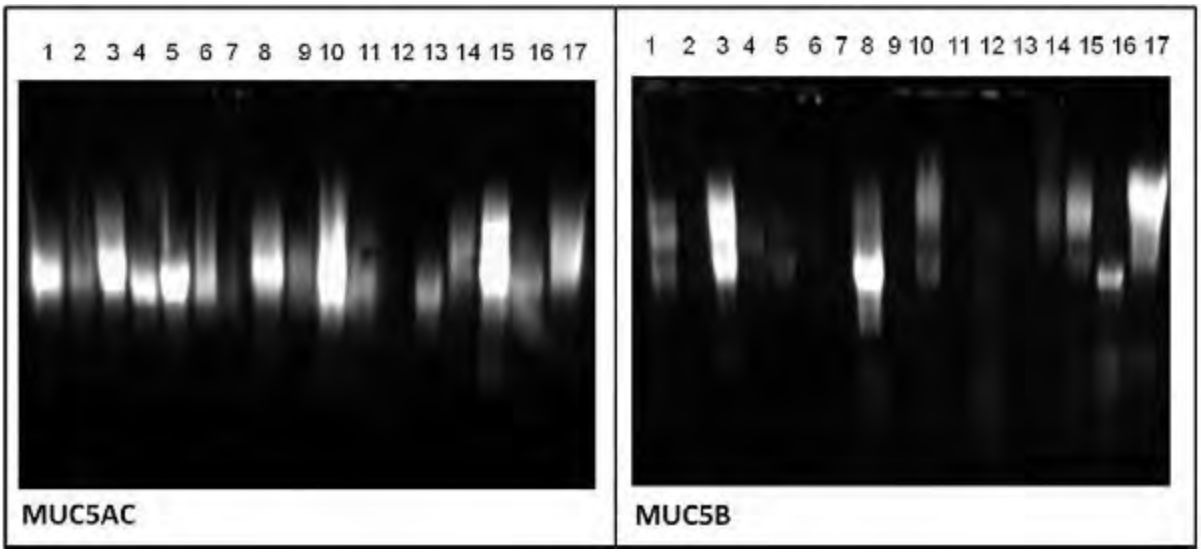

Figure 5.3: Identification of MUC5AC and MUC5B following agarose gel electrophoresis of reduced crude TB sputa.

Reduced and alkylated crude TB sputa were electrophoresed on a 0.7% agarose gel and subsequently blotted onto nitrocellulose membrane. The blot was probed with anti (-MUC5AC and -MUC5B) antibodies.

Interesting observations were made upon closer examination of the MUC5B from patients with TB. Two forms of MUC5B charges were observed from the samples loaded in lanes 8, 10, 15 and 17 (Figure 5.3). The migration of MUC5B on the gel was similar in the samples of patients in lanes 10 and 15. On the contrary, the migration of MUC5B in samples of the patient in lane 8 was lower on the gel compared to those in lanes 10 and 15. Three bands of MUC5B charges were observed from the samples in lanes 1 and 16 (Figure 5.3). The presence and appearance of the three MUC5B bands is a novel phenomenon in TB, of which the one with the highest mobility could be a protein (A Mall in personal communication with the late John Sheehan). Notable differences were seen in the migration of the three MUC5B bands on the gel from samples in lanes 1 and 16. The migration of MUC5B appeared higher in lane 1 indicative of high density population while a lower density population was observed in lane 16, lower on the gel.

No MUC2 was present in the TB sputa. MUC7 bands appeared as a smear over a large area suggesting the presence of different populations of MUC7 (Figure 5.4). The material in lanes 12 and 15 displayed the greatest heterogeneity. The MUC7 bands migrated further down the gel when compared to MUC5AC and MUC5B as depicted in Figure 5.3. There was much inter-individual variation for MUC7.

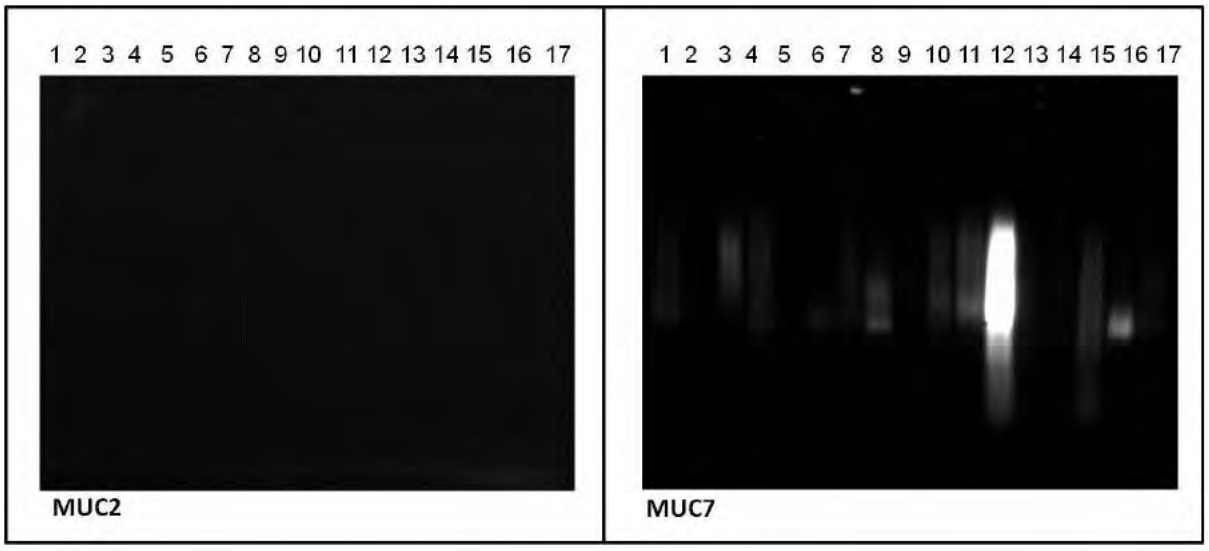

Figure 5.4: Identification of MUC2 and MUC7 following agarose gel electrophoresis of reduced crude TB sputa.

Reduced and alkylated crude TB sputa were electrophoresed on a 0.7% agarose gel and subsequently blotted onto nitrocellulose membrane. The blot was probed with anti (-MUC2 and -MUC7) antibodies.

In summary, in crude samples, all the mucins examined (MUC5AC, MUC5B, MUC2 and MUC7) were identified in uninfected controls. No MUC7 was found in BALs and no MUC2 was found in sputa.

5.2.1.4 The presence of mucins in TB patients co-infected with HIV

The reduced crude sputa were further assessed to determine whether there were differences between TB and TB co-infected with HIV. Tracheal aspirates from uninfected controls were compared to TB sputa. Very little variation in the intensities of the MUC5AC bands were observed between the samples from TB group and samples from the TB group co-infected with HIV (Figure 5.5). Slight variations in the migration of MUC5AC were observed between the TB group (TB group and TB group co-infected with HIV) and the uninfected controls. There was very little variation in MUC5B band intensities between the samples within the TB group. MUC5B bands appeared as a smear suggesting the presence of more than one population of the mucin with varying charges (Figure 5.5). Generally, MUC5AC was higher in the TB group than that in uninfected controls. No MUC2 was detected in the TB group whilst a single band with similar electrophoretic mobility was observed in uninfected controls.

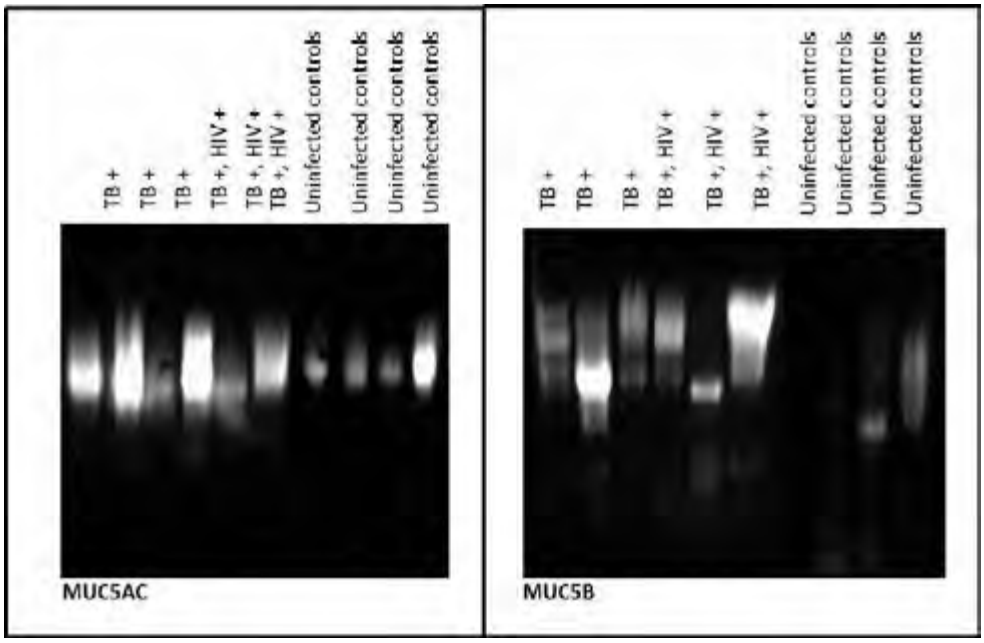

Figure 5.5: Comparison of MUC5AC and MUC5B in TB, TB/HIV and uninfected reduced crude respiratory mucus.

Reduced and alkylated mucus was electrophoresed on a 0.7% agarose gel and subsequently blotted onto nitrocellulose membrane. The blot was probed with anti (-MUC5AC and -MUC5B) antibodies.

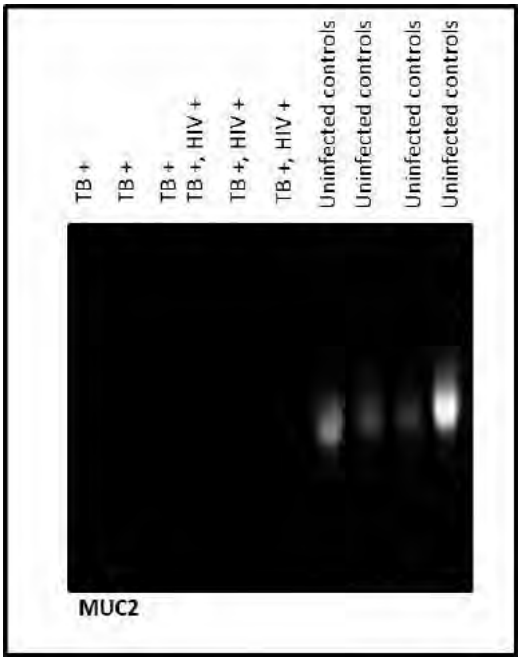

Figure 5.6: Comparison of MUC2 in TB, TB/HIV and uninfected reduced crude respiratory mucus.

Reduced and alkylated mucus was electrophoresed on a 0.7% agarose gel and subsequently blotted onto nitrocellulose membrane. The blot was probed with anti-MUC2 antibody.

5.2.1.5 Identification of respiratory mucins in Multi Drug Resistant (MDR)-TB

Of the 63 patients with TB only 2 cases presented with MDR-TB. Following western blotting, no mucins were identified in MDR patients compared to the TB patients. A dot blot was thus conducted to validate the Western blot results. No mucins were detected in one of the MDR-TB cases. The second case showed higher levels of MUC5AC. MUC7 mucins were secreted in the MDR patient whilst traces of MUC5B and MUC2 were observed in uninfected controls (Figure 5.7). The reduction and absence of secreted gel-forming mucins in MDR-TB prompted the investigation into determining whether reported membrane-bound mucins in the respiratory tract were present in this type of TB. A dot blot analysis of the membrane-bound mucins showed traces of MUC16 and the absence of MUC1 and MUC4 (Figure 5.8) in MDR-TB when compared to uninfected controls.

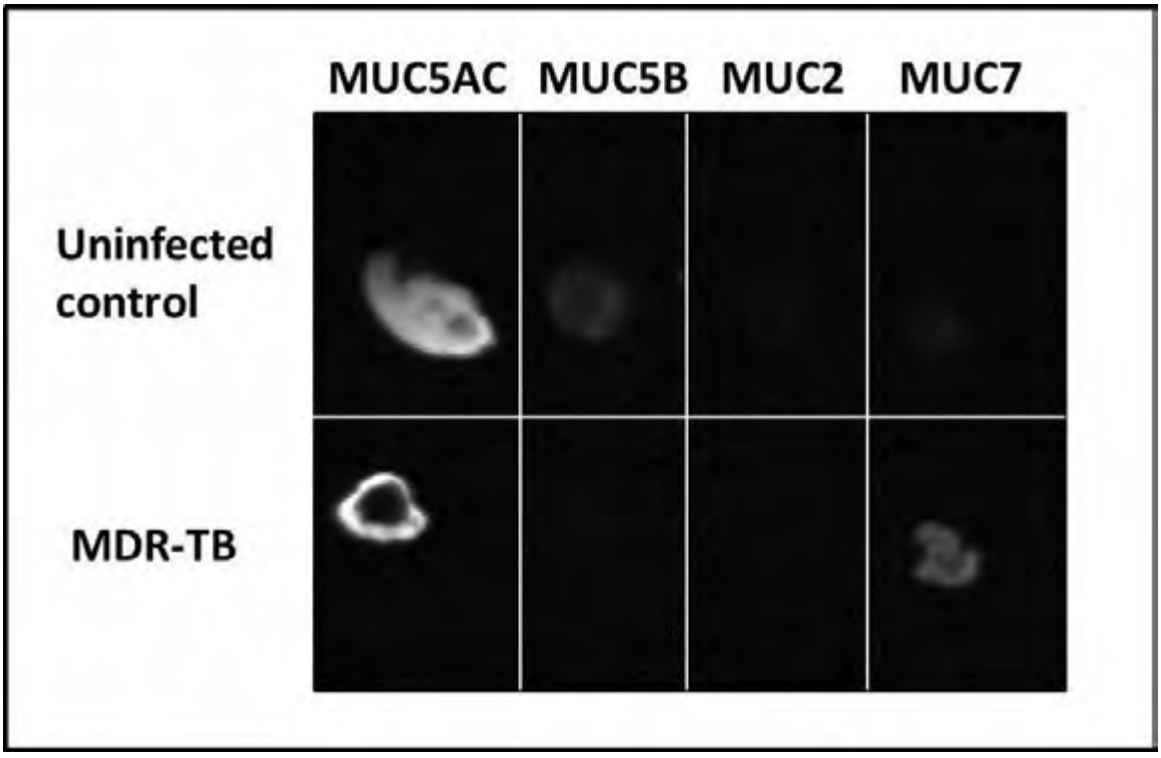

Figure 5.7:Dot blot analysis of secreted mucins of MDR-TB sputum in comparison to tracheal aspirate of an uninfected control.

Reduce and alkylated mucus from MDR-TB sputum and uninfected tracheal aspirate were dot blotted onto nitrocellulose membrane. The blots were probed with anti (-MUC5AC, -MUC5B, -MUC2 and -MUC7) antibodies.

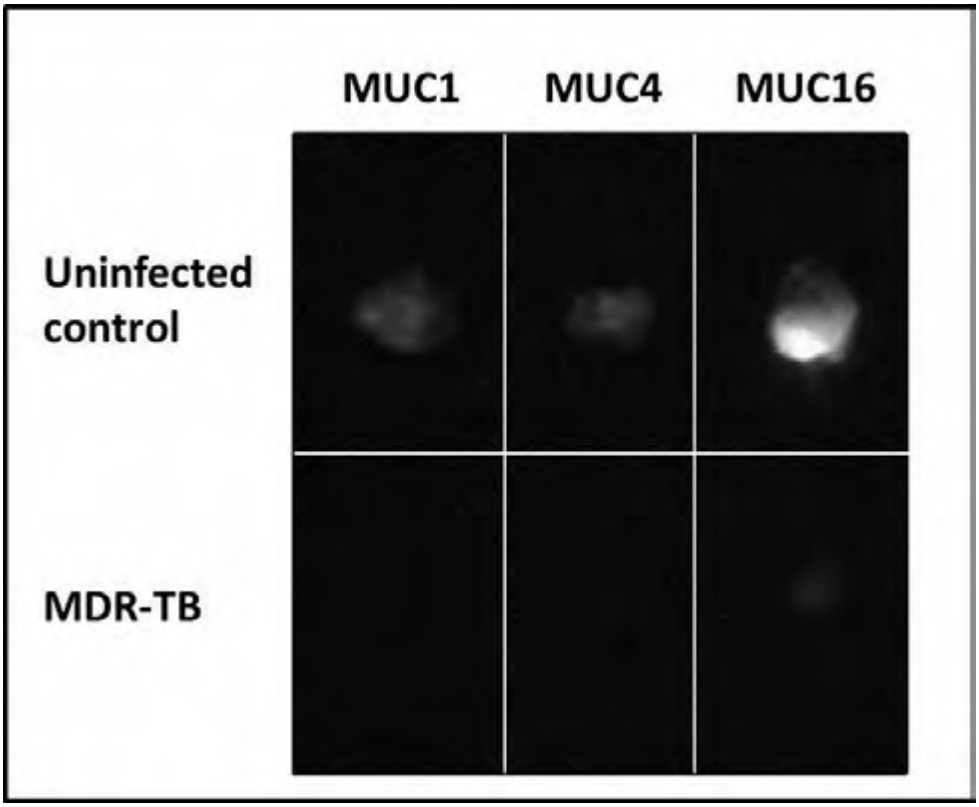

Figure 5.8: Dot blot analysis of membrane-bound mucins of MDR-TB sputum in comparison to tracheal aspirate of an uninfected control.

Reduced and alkylated mucus from MDR-TB sputum and uninfected tracheal aspirate were dot blotted onto nitrocellulose membrane. The blots were probed with anti (-MUC1, -MUC4 and -MUC16) antibodies.

5.2.2 Identification of respiratory mucins from purified samples

5.2.2.1 Caesium chloride density gradient ultracentrifugation

Mucus from patients with and without respiratory infections and diseases were collected in denaturing media (6M GuHCl and a cocktail of protease inhibitors; 10 mM EDTA, 5 mM NEM and 1 mM PMSF). The mucins were extracted by a two-step caesium chloride isopycnic density gradient ultra-centrifugation to remove protein and DNA contamination. Subsequently purified mucin fractions were desalted by dialysis, lyophilized and their masses determined and recorded.

Through this technique, a clear separation of protein and mucins of the TB and non-TB mucus occurs as shown in Figure 5.9. Mucins fractionated at a density between 1.39 and 1.40 g/ml generally in fractions 4-7 in the samples.

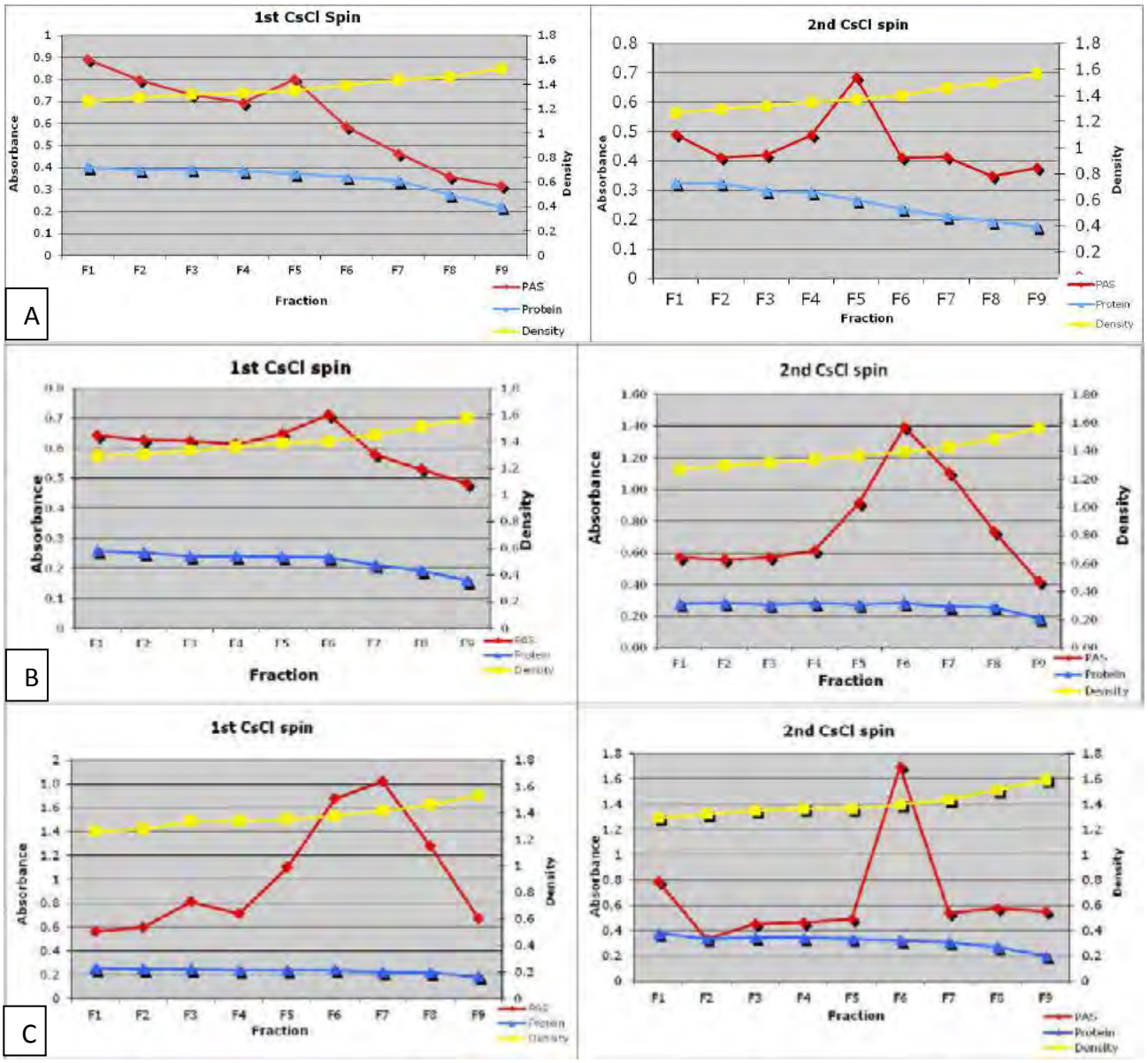

Figure 5.9: Caesium chloride density-gradient ultra-centrifugation profiles of respiratory mucins.

Freeze dried mucus was dissolved in 4M GuHCl containing protease inhibitors, and the density adjusted to 1.39 to 1.40g/ml with solid CsCl. Density-gradient ultra-centrifugation was performed in a Beckman L45 ultracentrifuge for 48h at 40 000 rpm (105 000 x g) at 4˚C, twice. Fractions from (A) sputa, (B) tracheal aspirates and (C) bronchoalveolar lavages were tested for PAS reactivity (absorbance at 540 nm) ( ), protein content using Bradford assay (absorbance at 595 nm) ( ) and the density of each fraction was determined ( ).

5.2.2.2 Identification of mucins from purified tracheal aspirates from uninfected controls

The presence of mucins was investigated in each fraction collected after the second CsCl spin. Figure 5.10 illustrates the CsCl density gradient profile following the second spin. The mucin-rich fractions were observed between fractions 5 and 7 with the mucin peak observed in fraction 6 (Figure 5.10). Figure 5.11 shows the different charge densities of MUC5AC and MUC5B following Western blotting. MUC5AC bands were observed in the middle of the gel. MUC5AC bands were observed in fraction 4 and traces were observed in fraction 8, which fell outside the mucin-rich fractions (fractions 5–7) as shown in Figure 5.11. The MUC5AC band in fraction 5 appeared as a smear in comparison to the other MUC5AC bands. MUC5AC bands appeared smaller than the MUC5B bands. MUC5B bands were observed in mucin-rich fractions and also in fractions 4 and 8. The bands appeared as large smears suggesting varying populations of MUC5B. MUC5B bands were observed higher on the gel in comparison to the MUC5AC bands. Furthermore, the size of the MUC5B smear appeared to increase with the density within the mucin-rich fractions (Figure 5.11).

Increased band intensities of MUC2 were observed from the mucin-rich fractions Figure 5.12 fractions 5-7). Traces of MUC2 were observed in Figure 5.12 fraction 4. The MUC5B band in fraction 5 appeared as a smear. MUC2 bands were observed lower on the gel compared to MUC5AC and MUC5B bands. No MUC7 mucins were detected from the purified mucin fractions. Varying levels of MUC5AC, MUC5B and MUC2 mucins were identified in the respiratory mucus of patients without TB. There were increased levels of MUC5B compared to the MUC5AC and MUC2.

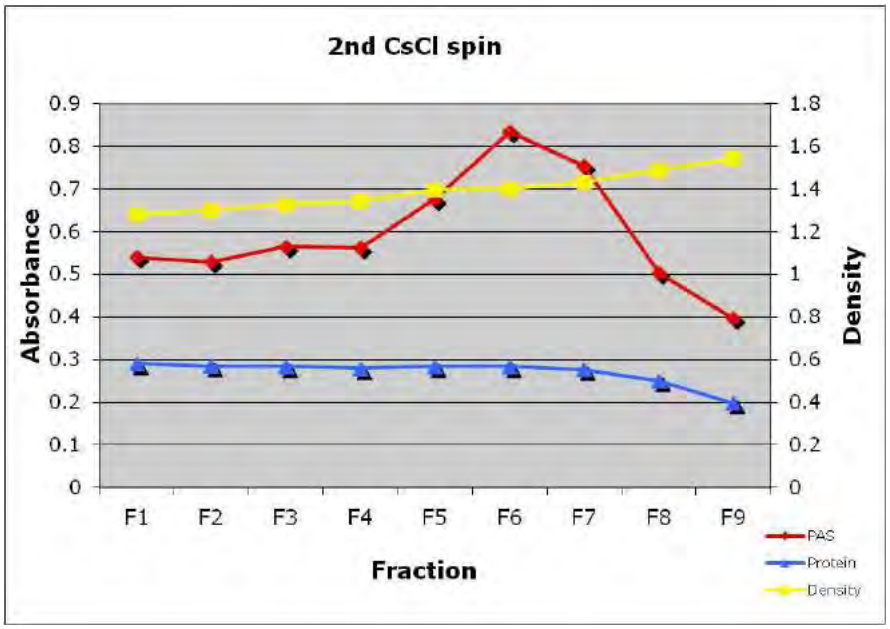

Figure 5.10: Caesium chloride density gradient ultra-centrifugation profile of purified tracheal aspirates of uninfected controls.

Reduced tracheal aspirates was dissolved in 4M GuHCl containing protease inhibitors, and the density adjusted to 1.39 to 1.40g/ml with solid CsCl. Density-gradient ultra-centrifugation was performed in a Beckman L45 ultracentrifuge for 48h at 40 000 rpm (105 000 x g) at 4˚C, twice. Each fraction was tested for PAS reactivity (absorbance at 540 nm) ( ), protein content using Bradford assay (absorbance at 595 nm) ( ) and the density of each fraction was determined ( ). Fractions rich in mucin were observed in fractions 5 – 7.

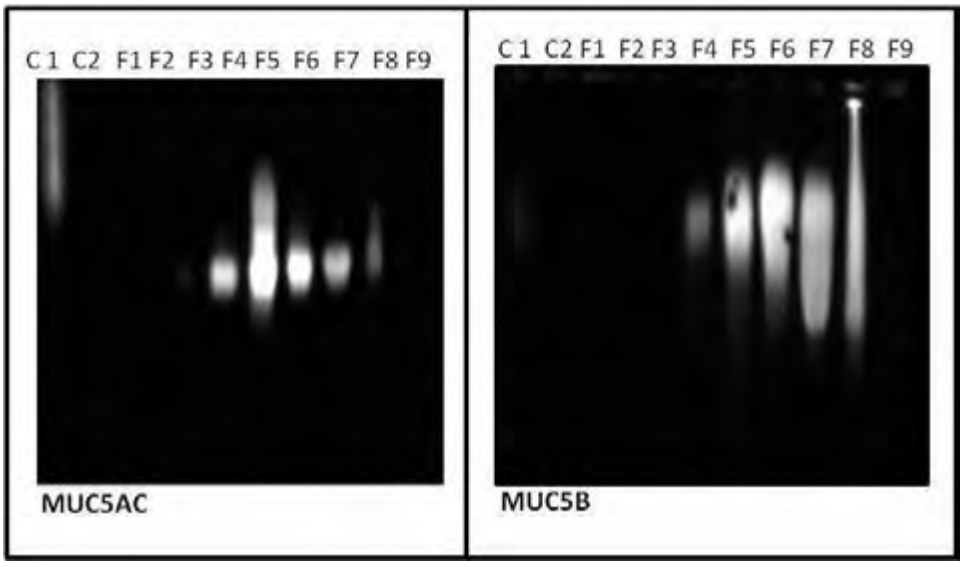

Figure 5.11: Identification of MUC5AC and MUC5B in purified fractions after second caesium gradient spin from tracheal aspirates of uninfected controls following agarose gel electrophoresis.

Reduced and alkylated purified non-TB tracheal aspirate fractions were electrophoresed on a 0.7% agarose gel and subsequently blotted onto a nitrocellulose membrane. The blot was probed with anti-(MUC5AC and MUC5B) antibodies. C1 denotes positive control and C2 negative control. For MUC5AC, C1 = gastric mucus (MUC5AC) and C2 = colon mucus (MUC2). For MUC5B, C1 = saliva (MUC5B) and C2 = colon mucus (MUC2).

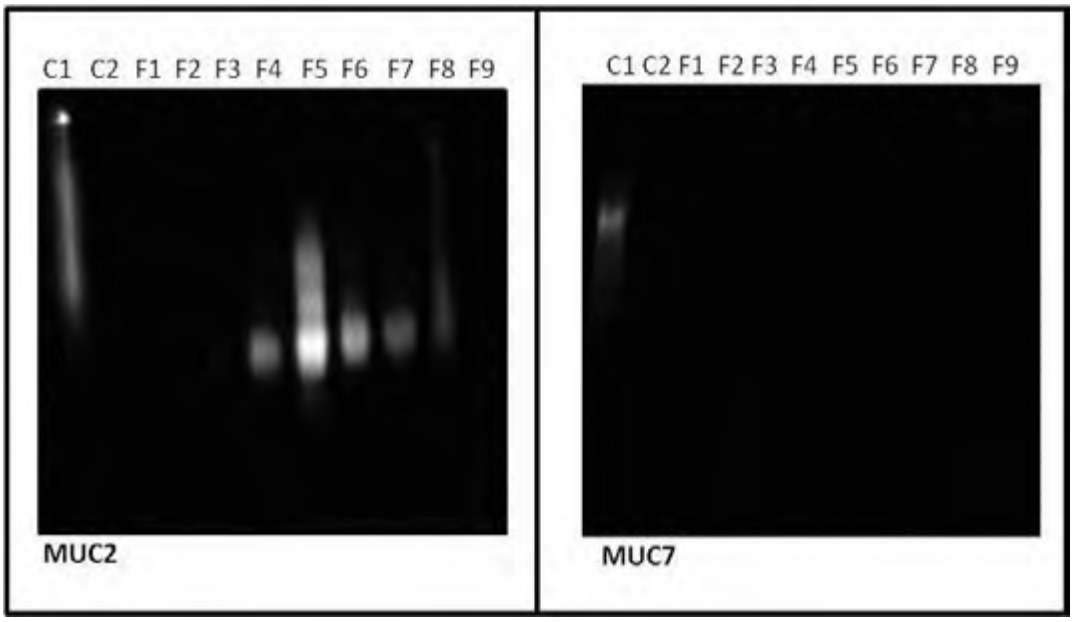

Figure 5.12: Identification of MUC2 and MUC7 in purified fractions after second caesium gradient spin from tracheal aspirates of uninfected controls following agarose gel electrophoresis.

Reduced and alkylated purified non-TB tracheal aspirate fractions after the second caesium gradient spin were electrophoresed on a 0.7% agarose gel and subsequently blotted onto a nitrocellulose membrane. The blot was probed with anti (-MUC2 and -MUC7) antibodies. C1 denotes positive control: and C2 negative control. For MUC2, C1 = colon mucus (MUC2) and C2 = gastric mucus (MUC5AC). For MUC7, C1 = saliva (MUC7) and C2 = gastric mucus (MUC5AC).

5.2.2.3 Identification of mucins from purified sputum from patients with TB

The presence of mucins in sputum from patients with TB was investigated in each fraction collected after the second CsCl density-gradient ultra-centrifugation. Figure 5.13 shows the CsCl density-gradient profile following the second spin. The mucin-rich fractions were observed between fractions 5 and 7 with the mucin peak observed in fraction 6 densities (Figure 5.13). Following Western blotting, a single MUC5AC band was observed in all fractions and showed similar electrophoretic mobility in the gel (Figure 5.14). Traces of MUC5AC were observed in fractions 1, 2 and 9. Brighter bands were observed between fractions 3 and 8. There seemed to be a greater charge variation of the mucins in fractions 4 and 6 than in other fractions as the bands appeared as large smears (Figure 5.14). MUC5B was mainly observed in the late fractions (fractions 6 – 9 in Figure 5.14) at higher densities. Traces of MUC5B were noticed in fraction 4. MUC5B had similar charge migration on the gel except for fraction 6 which migrated less than the other fractions (Figure 5.14).

MUC2 was observed in the late fractions (fractions 6 – 9). Differing electrophoretic mobility of MUC2 populations were observed in fractions 6 and 8 (Figure 5.15). A single band of MUC7 with low intensity was observed in fraction 6 within the mucin-rich fractions illustrated in figure 5.15. The MUC7 band had migrated further than the other mucin bands.

It was noteworthy that MUC5AC had brighter bands compared to MUC5B, MUC2 and MUC7 mucin fractions. This indicated that there were higher levels of MUC5AC compared to MUC5B, MUC2 and MUC7 in the TB samples. Interestingly, MUC5AC and MUC5B mucin subunits showed similar electrophoretic mobility indicative of similar charge densities between the two mucins.

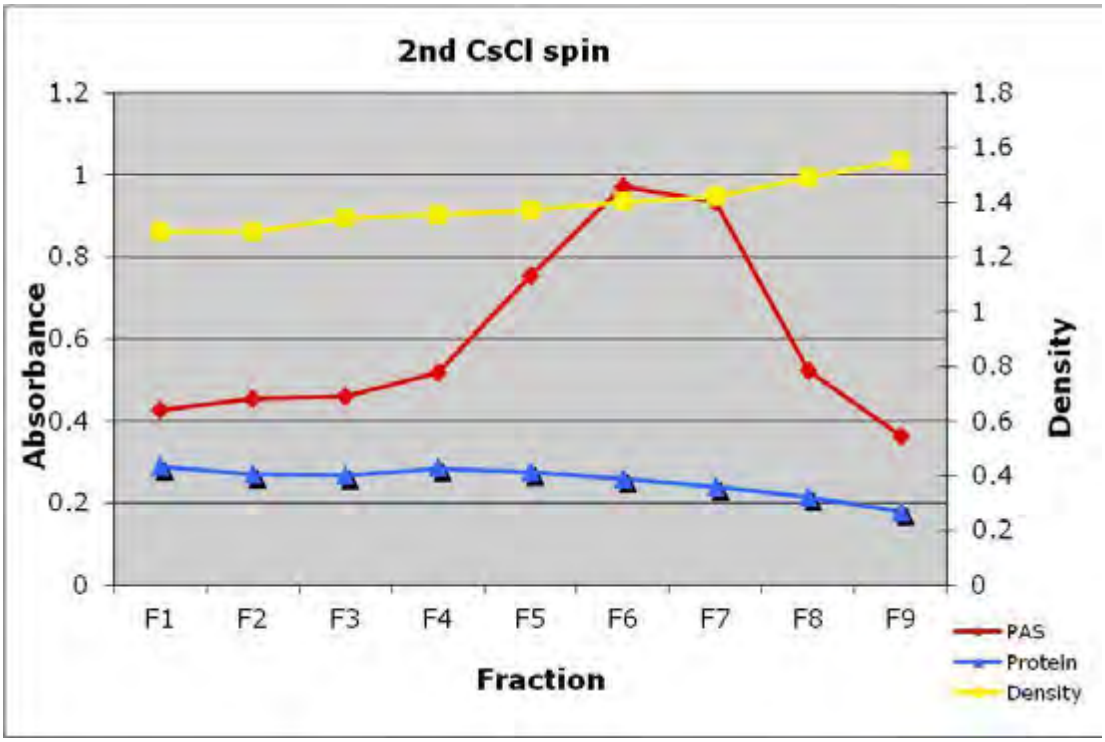

Figure 5.13: Caesium chloride density gradient ultra-centrifugation profile of TB samples.

Reduced sputum was dissolved in 4M GuHCl containing protease inhibitors and the density adjusted to 1.39 to 1.40g/ml with solid CsCl. Density-gradient ultra-centrifugation was performed in a Beckman L45 ultracentrifuge for 48h at 40 000 rpm (105 000 x g) at 4˚C, twice. Teach fraction was tested for PAS reactivity (absorbance at 540 nm) ( ), protein content using Bradford assay (absorbance at 595 nm) ( ) and the density of each fraction was determined ( ). Fractions rich in mucin were observed in fractions 5–7.

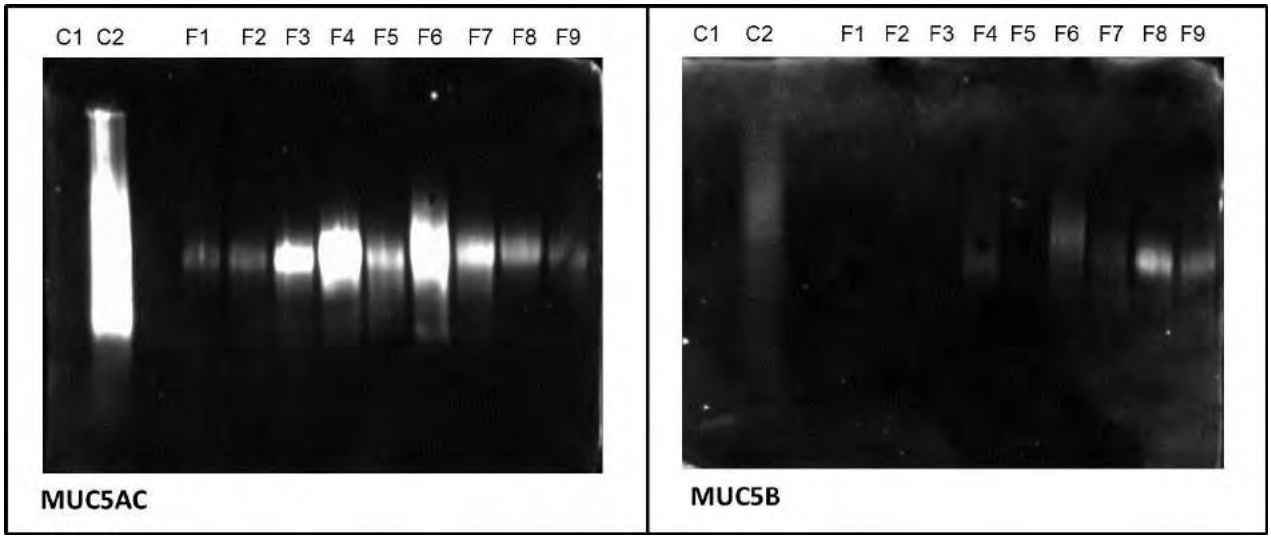

Figure 5.14: Agarose gel electrophoresis of purified and reduced TB mucin fractions.

Reduced and alkylated purified TB fractions were electrophoresed on a 0.7% agarose gel and subsequently blotted onto nitrocellulose membrane. The blot was probed with anti (-MUC5AC and MUC5B) antibodies.

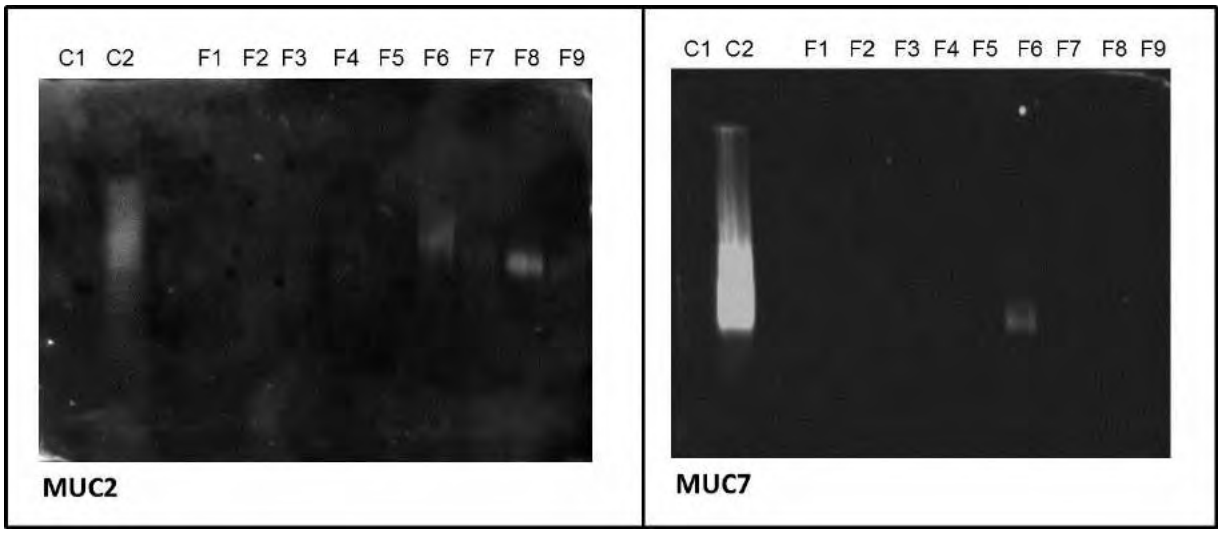

Figure 5.15: Agarose gel electrophoresis of purified and reduced TB mucins.

Reduced and alkylated purified TB fractions were electrophoresed on a 0.7% agarose gel and subsequently blotted onto nitrocellulose membrane. The blot was probed with anti-(MUC7 and MUC2) antibodies.

In summary, in purified samples, no MUC7 was identified in uninfected controls. In BALs, small yields of purified fractions were found following lyophilising. However, these small fractions were insufficient for Western blot analyses. In sputa, all the mucins examined (MUC5AC, MUC5B, MUC2 and MUC7) were identified in uninfected controls. Table 5.1 below summarises the secreted mucins in TB and non-TB.

Table 5.1: A summary of the secreted mucins in TB and non-TB mucus

Diagnosis	Number of patients recruited	MUC5AC	MUC5B	MUC2	MUC7
Uninfected controls	17	17	17	4	12
Definite TB - BALs	8	4	4	3	0
Sarcoidosis	53	47	47	12	0
Lung Cancer	4	4	3	1	0
Pulmonary Alveolar Proteinosis	4	3	3	0	0
Asthma	1	1	1	0	0
Bronchiectasis	6	4	4	0	0
Pneumonitis	5	5	5	2	0
COPD	1	1	1	0	0
Asbestosis	1	1	1	1	0
Silicosis	2	1	1	1	0
Interstitial Lung Disease	7	7	7	2	0
LIP	3	1	1	1	0
Definite TB - Sputa	56	53	53	2	18

5.3 Discussion

Initially, mucins were purified according to the CsCl density-gradient ultra-centrifugation as previously described by Creeth *et al.* (1977) and in later years by (Hovenberg *et al.*, 1996; Thornton *et al.*, 1996; Wickstrom *et al.*, 1998). Following CsCl density-gradient ultracentrifugation, effective separation of mucins was assessed by PAS assay, protein determination and measuring the density of fractions from the isolation process. However, using this technique, the yield of lyophilised material from each fraction was too small and in some cases resulted in loss of mucins. These losses and small yields of purified fractions hampered further analyses of the resulting mucin-rich fractions. It was thus decided to analyse crude reduced, alkylated and dialysed respiratory mucus as this resulted in higher yields of lyophilised material. Regardless of the small yield of mucins, purification by CsCl density-gradient was successful as it showed clear separation of mucins from the proteins. However it did not indicate the inter-individual variations.

In order to overcome the obstacle experienced by Thornton *et al.* (1995) where mucins did not readily enter the SDS PAGE, an agarose gel electrophoresis technique was employed according to (Tytgat *et al.*, 1995). This technique separated mucins according to their charge instead of size. Once the mucins were separated by agarose gel electrophoresis the gel was vacuum blotted onto a nitrocellulose membrane for Western Blot analysis.

Analysis by Western blot showed inter-individual variations in both the quantity (observed through intensities) and charge of the mucins in specimens from TB and uninfected controls. Upon examination, mucins were observed in non-mucin rich fractions (as seen in Figures 5.14 and 5.15) with varying densities in the purified samples. This indicated broad mucin populations in TB. Broad mucin populations have been previously observed in the sputum of a chronic-bronchitic patient (Wickstrom *et al.*, 1998). Mucins in both Figures 5.14 and 5.15 were examined in individual fractions following the second density gradient ultracentrifugation. This was carried out to examine the populations of mucins in each fraction. The use of this technique was inspired by Thornton *et al.* (1996) where they used the technique to analyse different populations of MUC5AC following separation by ion-exchange chromatography.

The overall electrophoretic mobility of MUC5AC on a gel is consistent in the TB and non-TB respiratory mucus from the tracheal aspirates, BALs and sputa. Therefore MUC5AC appears to be consistent with charge density. A phenomenon also observed by Thornton *et al.* (1996) that despite the variations in the level of MUC5AC mucin between respiratory samples, the electrophoretic mobility and charge density remains similar. In contrast, the electrophoretic mobility of MUC5B varied between individuals. This indicated the heterogeneous nature of MUC5B previously reported by (Wickstrom *et al.*, 1998). The previous separation of MUC5B by Mono-Q chromatography indicated 2 differently charged states of the mucin (Thornton and Sheehan, 2004). In this study 3 glycoforms of MUC5B were observed in TB, the one with the greatest mobility possibly a protein (A. Mall in conversation with the late John Sheehan).

In general, more MUC5AC than MUC5B was observed in both the TB and non-TB groups. Reports in literature have indicated that both MUC5AC and MUC5B are present in healthy individuals (Henke *et al.*, 2004; Kirkham *et al.*, 2002; Rose and Voynow, 2006). When comparing the TB group to the non-TB group higher levels of MUC5AC and MUC5B were observed in the TB group. These increased levels of MUC5AC and MUC5B might possibly indicate a defence mechanism employed in the fight against infection by *Mycobacterium tuberculosis*.

MUC2 was mainly present in uninfected controls with only 2 cases in the TB group. A preliminary study on mucins in TB in our laboratory indicated the presence of MUC2 in adults with TB (Govender, 2006)The Govender study further demonstrated a pronounced doublet of MUC2 in TB. However, this study only found a single band of MUC2. Reports on MUC2 mucin in the respiratory tract indicate the presence of MUC2 in nasal epithelial cells, in the case of allergic rhinitis and laryngeal cancer respectively (Voynow *et al.*, 1998). MUC2 was further reported by (Vinall *et al.*, 2000), to be associated with the protection of atopic individuals preventing them from developing asthma. The inconsistencies in the expression of MUC2 in this study might be as a result of the association of the MUC2 mucin with allergies (Takeuchi *et al.*, 1995).

No MUC7 mucins were detected from BALs. However, it was detected in sputa suggesting that sputa were contaminated with saliva. However, great care was taken when collecting the

respiratory mucus in order to limit contamination by salivary mucins. The rinsing of the mouth with water was encouraged before the expulsion of sputum.

Two patients were found to be infected with MDR-TB within the TB group. Western blot analysis was carried out to identify the secreted mucins in MDR-TB. However, the experiments yielded negative results. It was thus decided to analyse the mucus on dot blots as the concentration of the mucins can be increased without using more sample. The dot blot analysis showed no detection of mucins in one case, while the other case mainly showed mucin depletion and traces of MUC5AC, MUC7 and MUC16. Upon further examination of the latter case, the MDR-TB patient was found to have *Pseudomonasaeruginosa* infection with resistance to the antibiotics administered.

P. aeruginosa is an opportunistic pathogen. It is associated with both acute and chronic lung infections especially in people with Cystic Fibrosis (da Silva *et al.*, 2013; Landry *et al.*, 2006). A few reports on the interaction of *P. aeruginosa* and mucins have demonstrated that *P. aeruginosa* stimulated the production of MUC2 and MUC7 respectively (Li *et al.*, 2006). The depletion of mucins in MDR-TB mucus suggested that there was mucin degradation by *P. aeruginosa*. Work by Aristoteli and Willcox (2003), on microbial keratitis in corneal ulceration demonstrated that mucin-depleting *Pseudomonas* strains have a long-term growth advantage implying that mucins were used as nutrient source in the progression of the infection. The MDR-TB patient produced high viscosity mucus although the depletion of mucins was noticed from the patient. The production of the high quantity of mucus was probably as a result of the presence of *P. aeruginosa*.

This chapter of the study has demonstrated that both MUC5AC and MUC5B are the major secreted mucins in both TB and non-TB respiratory mucus. The secretion of MUC2 seems to be influenced by allergies. No MUC7 was found in BALs, indicating that mucins from the expectorated through the mouth are contaminated with salivary mucins.

CHAPTER 6 : AMINO ACID ANALYSIS OF THE PURIFIED MUCINS

6.1 Introduction

As mentioned in previous chapters, mucin apoproteins are rich in repetitive serine, threonine and proline amino acid residues often referred to as the STP-rich domain. As amino acids are the monomers of proteins, their analysis contributes towards the understanding of the structure of mucins and apomucins. Amino acid analysis is performed to estimate the quantitative amounts of amino acids present in a sample (Yan and Packer, 2000).

Once the respiratory mucins were isolated and purified as described in chapter 5, their amino acid composition was determined through amino acid analysis. Amino acid analysis is a valuable technique used to quantitatively estimate amino acids in a given sample (Yan and Packer, 2000). The technique involves the acid hydrolysis of amino acid peptide bonds, separation, derivatization and their detection (Dołowy and Pyka, 2014; Yan and Packer, 2000).

The aim of this chapter was to determine amino acid content of mucins by HPLC from polysaccharide-free polypeptide chains. Sixteen samples were analysed, four samples per group.

6.2 Results

The carbohydrate side chains were hydrolysed from the purified mucins to yield polysaccharide-free polypeptide chains. The amino acid composition of the purified mucins was determined by HPLC analysis employing a polystyrene-divinylbenzene cross-linked cation-exchange resin with post-column orthophthalaldehyde (OPA) fluorescence detection. In order to determine proline residues, a sodium hypochlorite reagent was allowed to react with proline on the column in order to convert it into an OPA-detectable derivative. The respiratory mucins were found to contain high amounts of threonine, serine and glutamic acid. Glutamic acid was the highest amino acid in TB and non-TB. A higher percentage of

glutamic acid was observed in patients co-infected with HIV. The identified amino acids are presented in Table 6.1. The threonine, serine and proline amino acids which are the distinguishing characteristic in mucins were 28.9% in non-TB, 28.7 % in non-TB/HIV, 26.7 % in TB and 28.0 % in TB/HIV.

Table 6.1: Amino acid composition of purified mucins in TB and non-TB

Amino acids	Non-TB (mol %)	Non-TB/HIV (mol %)	TB (mol %)	TB/HIV (mol %)
Aspartic acid	8.4	8.6	8.9	8.4
Threonine	10.1	10.8	10.3	10.3
Serine	9.9	10.2	8.8	9.0
Glutamic acid	10.4	10.8	10.3	11.0
Proline	8.9	7.7	7.6	8.7
Glycine	7.0	6.8	7.0	7.4
Alanine	6.9	6.6	7.5	7.9
Valine	7.0	7.6	8.1	7.0
Methionine	0.9	0.7	0.8	0.9
Isoleucine	3.3	2.8	3.0	3.2
Leucine	8.4	8.6	8.5	8.2
Tyrosine	3.6	4.6	4.2	3.1
Phenylalanine	3.7	3.8	4.0	3.8
Histidine	3.6	3.4	3.5	3.8
Lysine	3.6	3.4	3.6	3.2
Arginine	4.3	3.6	3.9	4.1
Total	100	100	100	100

6.3 Discussion

There were no significant differences in the amino acid composition between the TB and non-TB groups. No significant differences were observed in the percentage of the STP amino acid residue. Increased amounts were noted in glutamic acid, leucine, aspartic acid, valine, glycine and alanine amino acids. The significance in the increase of these amino acids is unknown. Following the analysis of amino acids, the mucus was further analysed to determine the oligosaccharides in order to give insight into the glycosylation of the mucins.

CHAPTER 7 : O-GLYCAN ANALYSIS OF RESPIRATORY MUCUS IN TB

7.1 Introduction

Mucins as glycoproteins form part of proteins that are post-translationally modified. The most common modifications widely described in proteins are glycosylation, hydroxylation, acetylation phosphorylation and ubiquitation (Karve and Cheema, 2011). Glycosylation influences protein conformation, flexibility, charge and hydrophobicity (Blixt and Westerlind, 2014; Takahashi *et al.*, 2009). Mucins are characterized by extensive stretches of O-glycosylation. O-glycosylation is the most abundant form of glycosylation that plays a role in cell adhesion (Fukuda, 2002). This most common type of glycosylation is characterised by the addition of N-acetylgalactosamine (GalNAc) to the hydroxyl group of either serine or threonine residues (Brockhausen *et al.*, 2009; Tian and Ten Hagen, 2009). This is the simplest O-glycan and it is called the Tn antigen. The Tn antigen can be extended to form eight different inner core structures; with core 1 through 4 being the most common O-glycan core structures (Brockhausen *et al.*, 2009; Cherian *et al.*, 2015). Furthermore the latter core structures have been shown to occur as extended, complex O-glycans that carry antigens for ABO blood group and Lewis type.

Short O-GalNAc glycans can be further elongated to form complex O-glycans that terminate in sialic acid, fucose, sulfate, antigens for ABO and Lewis blood group determinants. The function of the O-linked glycans includes protection against pathogens, i.e. reports on sialic acid have shown that it serves as a binding site for various pathogens and toxins (Schauer, 2009, 2004; Varki, 2008). Mucins play a pivotal role in the mucosal defence by binding bacteria through the adhesions on the bacterial membranes (Sonawane *et al.*, 2012; Widdicombe, 1995). However, the specificity is dependent on the types of sialic acid, modifications and linkages to the oligosaccharide side chains (3 or 6-linked sialic acid).

The aim of this chapter was to determine and describe the O-glycans found in respiratory mucus. The specific objectives were to identify oligosaccharides from proteins of the mucus separated by gel electrophoresis and then release the O-glycans by reductive alkaline β-

elimination. Crude mucus was reduced, alkylated, dialysed against water, lyophilised and then separated on a composite gel (AgPAGE) and 3-8% SDS-NuPAGE by electrophoresis. Separated proteins were then blotted on PVDF membrane and subsequently stained with Alcian Blue to visualise the glycoproteins bands. The mucin bands were excised and subjected to reductive β-elimination (Schulz *et al.*, 2002). Released O-glycans were analysed by LC-MS/MS in negative-ion mode as described previously (Schulz *et al.*, 2002). Three samples were analysed from the uninfected controls group, BALs group and Sputa group respectively; and only one MDR-TB sample was analysed.

7.2 Results

7.2.1. SDS PAGE analysis

Oligosaccharides were investigated in TB and non-TB. Non-TB mucus samples were collected from tracheal aspirates of patients undergoing surgery for non-respiratory conditions (see methods section 2.3.1). The samples are the uninfected controls. TB mucus samples were collected from bronchoalveolar lavages (BALs) and sputa. Three samples were analysed from each group.

In the uninfected controls, all glycoprotein bands were seen above 250 kDa. Two glycoprotein bands were observed from one uninfected control (sample 1). Only one glycoprotein band was observed from the remaining two samples (uninfected control 2 and 3) in the group (Figure 7.1). One glycoprotein band was also observed in all the BAL 1-3 samples (Figure 7.1). Again, the observed glycoprotein bands were above 250 kDa. In sputa, glycoproteins with varying molecular weights between the 150 kDa mark and above were observed in lanes 8 and 10 (Figure 7.1). The remaining sample only had one band above 250 kDa. The MDR sample showed a similar pattern to sputa of varying molecular weights between the 150 kDa mark and above. When comparing samples, the glycoprotein bands from the uninfected controls' samples, sputa samples and the MDR sample were brighter than the bands from the BAL samples. BAL 1-2 samples appeared fainter than the BAL 3 sample (Figure 7.1). It was noted that BAL 1-2 samples were co-infected with HIV.

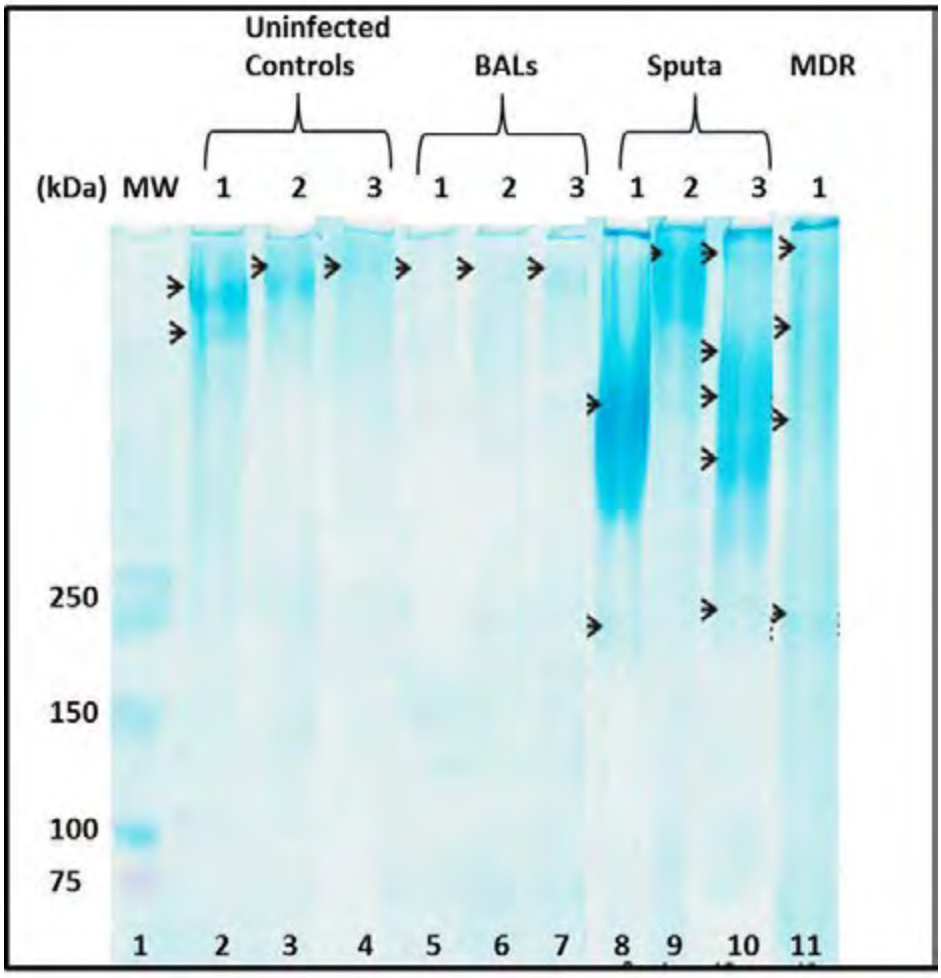

Figure 7.1: A 3-8% SDS-NuPAGE analysis of oligosaccharides in respiratory mucus from uninfected controls and in TB.

Respiratory mucus was reduced and alkylated, separated by 3-8% Tris-acetate NuPAGE, blotted onto polyvinylidene fluoride (PVDF) membrane and stained with Alcian Blue. Oligosaccharide bands (indicated with black arrows). MW is the molecular weight marker lane. Lanes 2-4: represent biological replicates of tracheal aspirates from uninfected controls. Lanes 5-7: biological replicates of bronchoalveolar lavages (BALs) from patients with TB. Lanes 8-10: biological replicates of sputa for patients with TB; Lanes 11: sputum from a patient with multi-drug resistant (MDR) TB.

7.2.2. LC-MS analysis of O-glycans

In order to analyse the O-glycans, the glycoprotein bands were excised from the blot generated in Figure 7.1. The O-glycans were then released from the blot by reductive alkaline β-elimination. The resulting glycans were then analysed by liquid chromatography

coupled to electrospray tandem mass spectrometry (LC-ESI-MS/MS) and their LC chromatograms are illustrated in Figure 7.2.

Five core types of O-glycans were detected, namely; core 1, core 2, core 3, core 4 and core 5. High amounts of cores 1, 2, 3 and 4 were detected in uninfected controls (Figure 7.1 and Table 7.1). Sialyl-Tn angtigens were also detected at lower amounts of an average of 5.2%. Small amounts of core 5 glycans (< 1%) were detected in uninfected controls.

High amounts of cores 1 and 2 glycans were detected in BALs. The BAL 1 and 2 were co-infected with HIV. No core 3 glycans were detected in sample 1, while 0.5% was detected in sample 2 and 35.8% detected in sample 3. No core 4 and core 5 glycans were detected in BAL 1 and 2. Compared to BAL 1 and 2, 35.8%, 7.4% and 1.3% of core 3, core 4 and core 5 glycans were detected in BAL 3 (Table 7.1).

A similar pattern observed in uninfected controls was noticed in sputa. High amounts of cores 1, 2, 3 and 4 were detected in sputa with Sialyl-Tn antigens detected in samples 2 and 3. High amounts of core 1 and core 2 were detected in the MDR sample. Lower amounts of core 3 and the Tn antigens were detected in MDR at 7.3% and 5.4% respectively.

More sulfation of the core 1 structures was observed when compared to sialylation and fucosylation in uninfected controls. Core 2 structures consisted mainly of fucosylated and α2,3-linked sialic acid as compared to sulfated glycans. Core 3 structures consisted of both α2,3-linked sialic acid and α2,6-linked sialic acid. However, more α2,6-linked sialic acid were observed from the structures. Fucosylation and sulphation of core 3 structures was also observed. However, more structures were sialylated and fucoslylated than sulfated. Core 4 structures were sialylated, fucosylated and sulfated. No significant differences were noticed with the distribution of the modifications among samples. More α2,3-linked sialic acids were noted.

In general, the majority of the O-glycans were sialylated. The majority of fucosylated O-glycans were associated to blood type and Lewis type. Sulphation of the glycans were found to be more prevalent in sputa than in uninfected controls and BALs.

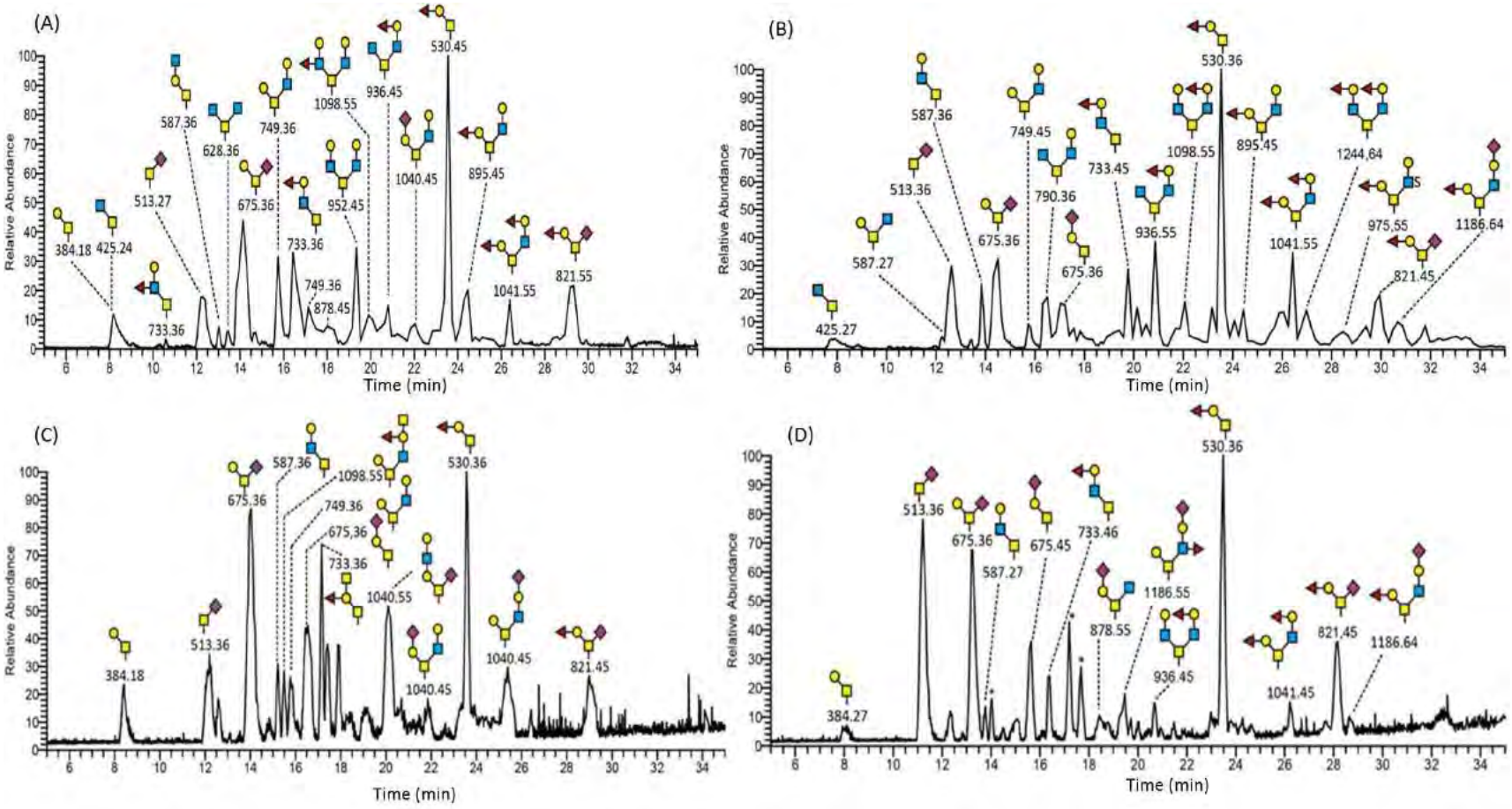

Figure 7.2: LC-MS chromatograms of respiratory mucus in uninfected controls and in TB.

Mass spectra from liquid chromatography-mass spectrometry (LC-MS) of O-glycans released from respiratory mucus separated by SDS-AgPAGE and blotted to PVDF. A: Tracheal aspirate from uninfected controls. B: Bronchoalveolar lavage (BAL) from patient with TB. C: Sputum from patient with TB. D: Sputum from patient with multi-drug resistant (MDR) TB.

Table 7.1: Percentages of the relative amounts of the different putative O-glycan structures detected using LC-MS

						Uninfected controls			BALs			Sputa			MDR
Name	**Composition**	**Putative structure**	**Core**	**Blood type**	**Lewis type**	**1**	**2**	**3**	**1**	**2**	**3**	**1**	**2**	**3**	**MDR**
384	Hex1HexNAc1	Galβ1-3GalNAcol	1	–	–	4.7	6.1	2.8	6.9	2.9	1.8	0.6	1.6	2.5	3.3
425	HexNAc2	GlcNAcβ1-3GalNAcol	3	–	–	–	–	1.2	–	–	1.2	0.2	1.8	0.8	–
464	Hex1HexNAc1Sul1	S-Galβ1-3GalNAcol	1	–	–	–	–	–	–	–	–	–	–	1.1	–
513	NeuAc1HexNAc1	NeuAcα2-6GalNAcol	0	–	–	1.9	5.2	3.2	6.5	3.8	2.9	–	3.9	3.0	5.4
530	Hex1HexNAc1dHex1	Fucα1-2Galβ1-3GalNAcol	1	H	–	–	4.9	3.5	8.4	3.2	2.6	5.4	5.2	2.3	3.2
587-1	Hex1HexNAc2	Galβ1-3**(GlcNAcβ1-6)**GalNAcol	2	–	–	0.7	1.0	0.7	–	–	–	0.2	0.8	1.1	–
587-2	Hex1HexNAc2	GlcNAcβ1-3Galβ1-3GalNAcol	1	–	–	–	1.0	0.8	–	–	–	–	–	–	–
587-3	Hex1HexNAc2	Galβ1-4GlcNAcβ1-3GalNAcol	3	–	–	0.4	0.9	1.0	–	0.5	1.9	2.1	2.1	1.3	1.4
587-4	Hex1HexNAc2	Galβ1-3GlcNAcβ1-3GalNAcol	3	–	–	2.5	2.3	1.1	–	–	–	3.5	0.2	1.5	–
628	HexNAc3	GlcNAcβ1-3**(GlcNAcβ1-6)**GalNAcol	4	–	–	–	–	0.4	–	–	–	–	0.7	0.4	–
667-1	Hex1HexNAc2Sul1	Galβ1-3**(6SGlcNAcβ1-6)**GalNAcol	2	–	–	–	–	–	–	–	–	0.4	–	0.3	–
667-2	Hex1HexNAc2Sul1	Gal-(S)GlcNAcβ1-3GalNAcol	3	–	–	–	–	–	–	–	–	–	–	0.6	–
667-3	Hex1HexNAc2Sul1	Gal-(S)GlcNAcβ1-3GalNAcol	3	–	–	0.9	–	0.2	–	–	0.4	–	–	0.5	–
675-1	NeuAc1Hex1HexNAc1	Galβ1-3(NeuAcα2-6)GalNAcol	1	–	–	2.0	7.4	3.5	6.6	5.9	3.7	3.3	3.8	4.2	4.9
675-2	NeuAc1Hex1HexNAc1	NeuAcαα2-3Galβ1-3GalNAcol	1	–	–	1.7	3.8	1.4	3.6	3.7	2.1	1.2	1.9	2.0	2.1
716-1	NeuAc1HexNAc2	GlcNAcβ1-3**(NeuAcα2-6)**GalNAcol	3	–	–	1.0	1.3	0.9	–	–	4.3	1.4	1.2	0.9	1.2
716-2	NeuAc1HexNAc2	GalNAcα1-3**(NeuAcα2-6)**GalNAcol	5	–	–	–	0.7	0.4	–	–	0.6	0.6	0.6	0.6	1.3
733-1	Hex1HexNAc2dHex1	Galβ1-3(Fucα1-4)GlcNAcβ1-3GalNAcol	3	–	a/x	1.3	–	0.6	–	–	1.0	–	0.6	–	–
733-2	Hex1HexNAc2dHex1	Galβ1-4(Fucα1-3)GlcNAcβ1-3GalNAcol	3	–	a/x	0.2	–	–	–	–	–	–	–	–	–
733-3	Hex1HexNAc2dHex1	Fucα1-2Galβ1-3GlcNAcβ1-3GalNAcol	3	H	–	–	–	1.5	–	–	0.5	–	1.2	1.9	1.4
733-4	Hex1HexNAc2dHex1	Fucα1-2(GalNAcα1-3)Galβ1-3GalNAcol	1	A	–	–	–	–	–	2.6	–	–	–	–	–
733-5	Hex1HexNAc2dHex1	Fucα1-2Galβ1-4GlcNAcβ1-3GalNAcol	3	H	–	–	–	0.3	–	–	0.4	–	1.6	0.5	1.0
733-6	Hex1HexNAc2dHex1	Fucα1-2Galβ1-3**(GlcNAcβ1-6)**GalNAcol	2	H	–	–	–	0.4	–	–	–	–	0.3	0.2	1.1
749-1	Hex2HexNAc2	Galβ1-3**(Galβ1-4GlcNAcβ1-6)**GalNAcol	2	–	–	1.7	3.8	3.3	4.6	2.1	0.9	3.3	1.5	3.1	0.5
749-2	Hex2HexNAc2	Galβ1-4GlcNAcβ1-3Galβ1-3GalNAcol	1	–	–	–	1.5	0.9	–	0.9	0.3	–	0.3	0.3	0.5

Name	Composition	Putative structure	Core	Blood type	Lewis type	1	2	3	1	2	3	1	2	3	MDR
790-1	Hex1HexNAc3	GlcNAcβ1-3**(Galβ1-4GlcNAcβ1-6)**GalNAcol	4	–	–	0.6	–	0.9	–	–	–	1.2	1.0	0.5	0.3
790-2	Hex1HexNAc3	Galβ1-4GlcNAcβ1-3**(GlcNAcβ1-6)**GalNAcol	4	–	–	0.1	–	0.4	–	–	–	–	–	0.1	–
813-1	Hex1HexNAc2dHex1Sul1	Gal(Fuc)(6S)GlcNAcβ1-3GalNAcol	3	–	–	1.9	–	–	–	–	–	–	–	–	–
813-2	Hex1HexNAc2dHex1Sul1	Fucα1-2Gal-(S)GlcNAcβ1-3GalNAcol	3	H	–	0.0	–	–	–	–	0.2	–	0.1	0.3	–
813-3	Hex1HexNAc2dHex1Sul1	S-Gal(Fuc)GlcNAcβ1-3GalNAcol	3	–	a/x	1.8	–	–	–	–	–	–	–	–	–
813-4	Hex1HexNAc2dHex1Sul1	Fucα1-2Gal-(S)GlcNAcβ1-3GalNAcol	3	H	–	–	–	–	–	–	–	–	0.2	0.2	–
813-5	Hex1HexNAc2dHex1Sul1	Fucα1-2Galβ1,3**(6S-GlcNAcβ1,6)**GalNAcol	2	H	–	–	–	–	3.6	–	–	–	0.3	0.4	–
821	NeuAc1Hex1HexNAc1dHex1	Fucα1-2Galβ1-3**(NeuAcα2-6)**GalNAcol	1	H	–	–	7.5	3.5	5.0	4.7	0.4	–	2.8	0.8	3.2
829-1	Hex2HexNAc2Sul1	Galβ1-3**[Galβ1-4(6S)GlcNAcβ1-6]**GalNAcol	2	–	–	–	–	0.2	–	–	–	0.5	0.0	0.6	–
829-2	Hex2HexNAc2Sul1	Gal(S)GlcNAc-Galβ1-3GalNAcol	1	–	–	–	–	0.3	–	–	–	–	–	–	–
829-3	Hex2HexNAc2Sul1	Gal-GlcNAc-(S)Galβ1-3GalNAcol	1	–	–	1.2	5.5	0.9	–	2.3	0.4	2.4	0.4	3.1	–
829-4	Hex2HexNAc2Sul1	Gal-GlcNAc-(S)Galβ1-3GalNAcol	1	–	–	–	–	0.8	–	–	–	–	0.4	–	–
870	Hex1HexNAc3Sul1	S+GlcNAcβ1-3**(Gal-GlcNAcβ1-6)**GalNAcol	4	–	–	–	–	–	–	–	–	–		0.7	–
878-1	NeuAc1Hex1HexNAc2	Gal-GlcNAcβ1-3**(NeuAcα2-6)**GalNAcol	3	–	–	0.5	6.2	0.8	–	–	2.7	0.9	1.0	1.1	–
878-2	NeuAc1Hex1HexNAc2	GlcNAcβ1-4Galβ1-3**(NeuAcα2-6)**GalNAcol	1	–	–	3.9	2.8	0.8	–	–	–	2.7	–	0.3	–
878-3	NeuAc1Hex1HexNAc2	NeuAcα2-6Galβ1-4GlcNAcβ1-3GalNAcol	3	–	–	–	–	–	–	–	0.5	–	–	–	–
878-4	NeuAc1Hex1HexNAc2	NeuAcα2-3Galβ1-3**(GlcNAcβ1-6)**GalNAcol	1	–	–	–	–	0.4	–	–	–	0.3	0.3	0.3	1.2
878-5	NeuAc1Hex1HexNAc2	NeuAcα2-3Galβ1-4GlcNAcβ1-3GalNAcol	3	–	–	–	–	0.2	–	–	6.7	2.8	1.3	0.5	–
879	Hex1HexNAc2dHex2	Fucα1-2Gal(Fuc)GlcNAcβ1-3GalNAcol	3	H	b/y	–	–	–	–	–	–	–	–	–	0.7
895-1	Hex2HexNAc2dHex1	Galβ1-3[Gal(Fuc)GlcNAcβ1-6]GalNAcol	2	–	a/x	1.7	1.4	0.9	–	–	0.9	–	0.6	1.3	–
895-2	Hex2HexNAc2dHex1	Galβ1-3[Gal(Fuc)GlcNAcβ1-6]GalNAcol	2	–	a/x	0.3	–	–	–	–	–	–	–	–	–
895-3	Hex2HexNAc2dHex1	Gal(Fuc)GlcNAc-Galβ1-3GalNAcol	1	–	a/x	–	1.5	0.4	–	–	–	–	–	0.2	0.7
895-4	Hex2HexNAc2dHex1	Gal(Fuc)GlcNAc-Galβ1-3GalNAcol	1	–	a/x	–	1.7	0.7	–	–	–	–	–	0.1	0.0
895-5	Hex2HexNAc2dHex1	Galβ1-3**(Fucα1-2Galβ1-4GlcNAcβ1-6)**GalNAcol	2	H	–	–	0.8	0.6	5.2	–	–	–	1.0	0.9	1.9
895-6	Hex2HexNAc2dHex1	Fucα1-2Galβ1-3**(Galβ1-4GlcNAcβ1-6)**GalNAcol	2	H	–	–	6.0	1.8	6.8	1.4	0.2	–	1.0	1.2	1.5
936-1	Hex1HexNAc3dHex1	Fucα1-2Gal-GlcNAcβ1-3**(GlcNAcβ1-6)**GalNAcol	4	H	–	–	–	0.2	–	–	–	–	–	–	–
936-2	Hex1HexNAc3dHex1	GlcNAcβ1-3**(Fucα1-2Galβ1-4GlcNAcβ1-6)**GalNAcol	4	H	–	–	–	0.8	–	–	–	–	2.9	0.6	1.7
952	Hex2HexNAc3	Galβ1-4GlcNAcβ1-3**(Galβ1-4GlcNAcβ1-6)**GalNAcol	4	–	–	1.5	3.4	1.9	–	–	0.2	2.6	0.7	1.1	0.7

Name	Composition	Putative structure	Core	Blood type	Lewis type	1	2	3	1	2	3	1	2	3	MDR
959	Hex1HexNAc2dHex2Sul1	Fucα1-2Gal-(Fuc)(S)GlcNAcβ1-3GalNAcol	3	H	b/y	–	–	–	–	–	–	–	0.6	–	–
966	NeuAc2Hex1HexNAc1	NeuAcα2-3Galβ1-3**(NeuAcα2-6)**GalNAcol	1	–	–	–	–	1.0	1.9	10.8	1.5		1.6	0.7	4.2
975-1	Hex2HexNAc2dHex1Sul1	Gal(Fuc)(6S)GlcNAc-Galβ1-3GalNAcol	1	–	a/x	3.0	–	1.4	–	–	–	0.7	0.2	0.2	–
975-2	Hex2HexNAc2dHex1Sul1	Gal(Fuc)(6S)GlcNAc-Galβ1-3GalNAcol	1	–	a/x	–	–	–	–	–	–	1.6	–	0.7	–
975-3	Hex2HexNAc2dHex1Sul1	S+Galβ1-3(Fucα1-2Galβ1-4GlcNAcβ1-6)GalNAcol	2	H	–	–	–	–	–	–	–	–	–	0.5	–
975-4	Hex2HexNAc2dHex1Sul1	Galβ1-3**[Gal(Fuc)(S)GlcNAcβ1-6]**GalNAcol	2	–	a/x	–	–	0.3	–	–	–	–	–	–	–
975-5	Hex2HexNAc2dHex1Sul1	Fucα1-2Galβ1-3**[Galβ1-4(6S)GlcNAcβ1-6]**GalNAcol	2	H	–	–	–	1.0	7.0	–	0.5	–	1.1	3.6	–
1024-1	NeuAc1Hex1HexNAc2dHex1	Fuc(Gal)GlcNAcβ1-3(NeuAcα2-6)GalNAcol	3	–	a/x	2.6	–	1.2	–	–	2.4	–	–	–	–
1024-2	NeuAc1Hex1HexNAc2dHex1	Fuc(Gal)GlcNAcβ1-3(NeuAcα2-6)GalNAcol	3	–	a/x	0.9	–	–	–	–	–	–	–	–	–
1024-3	NeuAc1Hex1HexNAc2dHex1	NeuAcα2-3Gal(Fuc)GlcNAcβ1-3GalNAcol	3	–	a/x	–	–	–	–	–	2.8	0.4	0.3	0.3	–
1024-4	NeuAc1Hex1HexNAc2dHex1	Fucα1-2Galβ-GlcNAcβ1-3**(NeuAcα2-6)**GalNAcol	3	H	–	–	–	0.5	–	–	–	–		0.6	–
1024-5	NeuAc1Hex1HexNAc2dHex1	Fucα1-2Galβ-GlcNAcβ1-3**(NeuAcα2-6)**GalNAcol	3	H	–	–	–	0.4	–	–	0.4	–	1.0	0.5	–
1032-1	Hex2HexNAc3Sul1	S + GlcNAcβ1-3Galβ1-3Gal**(Galβ1-4GlcNAcβ1-6)**GalNAcol	2	–	–	0.6	–	0.5	–	–	–	0.5	–	0.4	–
1032-2	Hex2HexNAc3Sul1	Gal-GlcNAcβ1--3**[Gal-(S)GlcNAcβ1-6]**GalNAcol	4	–	–	1.0	–	1.1	–	–	–	2.3	–	1.8	–
1040-1	NeuAc1Hex2HexNAc2	Galβ1-4GlcNAcβ1-3Galβ1-3**(NeuAcα2-6)**GalNAcol	1	–	–	–	8.7	1.8	4.0	4.1	2.0	0.8	1.1	0.9	2.3
1040-2	NeuAc1Hex2HexNAc2	NeuAcα2-3Galβ1-3**(Galβ1-4GlcNAcβ1-6)**GalNAcol	2	–	–	0.8	7.9	1.1	6.3	4.1	0.3	1.4	0.8	0.8	2.1
1040-3	NeuAc1Hex2HexNAc2	Galβ1-3**(NeuAcα2-3Galβ1-4GlcNAcβ1-6)**GalNAcol	2	–	–	1.0	6.8	0.5	5.3	5.1	3.6	4.4	3.5	3.0	0.7
1041-1	Hex2HexNAc2dHex2	Fucα1-2Gal(Fuc)GlcNAcβ1-3Galβ1-3GalNAcol	1	H	b/y	–	–	–	–	–	–	–	0.4	–	1.5
1041-2	Hex2HexNAc2dHex2	Gal(Fuc)GlcNAc-(Fuc)Galβ1-3GalNAcol	1		a/x	–	–	0.2	–	–	–	–	0.3	–	–
1041-3	Hex2HexNAc2dHex2	Fucα1-2Gal(Fuc)GlcNAcβ1-3Galβ1-3GalNAcol	1	H	b/y	–	–	0.4	–	–	–	–	0.2	–	–
1041-4	Hex2HexNAc2dHex2	Fucα1-2Galβ1-3**(Fucα1-2Galβ1-4GlcNAcβ1-6)**GalNAcol	2	H	–	–	–	1.1	5.4	–	–	–	3.2	–	1.0
1081	NeuAc1Hex1HexNAc3	GlcNAcβ1-3**(NeuAcα2-3Galβ1-4GlcNAcβ1-6)**GalNAcol	4	–	–	–	–	0.9	–	–	1.1	2.9	2.8	1.2	3.3
1098-1	Hex2HexNAc3dHex1	Galβ1-3**[Fucα1-2(GalNAcα1-3)Galβ1-4GlcNAcβ1-6]**GalNAcol	2	A	–	–	–	1.0	–	2.5	–	–	–	–	–
1098-2	Hex2HexNAc3dHex1	Gal(Fuc)GlcNAc-Galβ1-3**(GlcNAcβ1-6)**GalNAcol	2	–	a/x	–	–	0.4	–	–	–	–	–	–	–
1098-3	Hex2HexNAc3dHex1	Gal(Fuc)GlcNAcβ1-3**(Galβ1-4GlcNAcβ1-6)**GalNAcol	4	–	a/x	–	–	1.0	–	–	–	–	0.6	0.5	0.9
1098-4	Hex2HexNAc3dHex1	Galβ1-4GlcNAcβ1-3**(Fucα1-2Galβ1-4GlcNAcβ1-6)**GalNAcol	4	H	–	–	–	0.7	–	–	–	–	1.4	0.6	2.0

Name	Composition	Putative structure	Core	Blood type	Lewis type	1	2	3	1	2	3	1	2	3	MDR
1098-5	Hex2HexNAc3dHex1	Fucα1-2Galβ1-4GlcNAcβ1-3**(Galβ1-4GlcNAcβ1-6)**GalNAcol	4	H	–	–	–	0.4	–	–	–	–	0.7	0.4	–
1104-1	NeuAc1Hex1HexNAc2dHex1Sul1	NeuAcα2-3(S)Gal(Fuc)GlcNAcβ1-3GalNAcol	3	–	a/x	2.0	–	–	–	–	–	–	–	–	–
1104-2	NeuAc1Hex1HexNAc2dHex1Sul1	NeuAcα2-3Gal(Fuc)(6S)GlcNAcβ1-3GalNAcol	3	–	a/x	2.3	–	–	–	–	–	–	–	–	–
1112	Hex2HexNAc3Sul2	2S+Gal-GlcNAcβ1-3**(GalGlcNAcβ1-6)**GalNAcol	4	–	–	–	–	–	–	–	–	–	–	–	–
1114-1	Hex3HexNAc3	Gal-GlcNAcb1-3Galb1-3**(Galb1-4GlcNAcb1-6)**GalNAcol	2	–	–	0.7	–	0.7	–	–	–	0.6	–	–	–
1114-2	Hex3HexNAc3	Galβ1-3**(Galβ1-4GlcNAcβ1-3Galβ1-4GlcNAcβ1-6)**GalNAcol	2	–	–	–	–	0.1	–	–	–	–	–	–	–
1120	NeuAc1Hex2HexNAc2Sul1	S + Galβ1-4GlcNAcβ1-3Galβ1-3**(NeuAcα2-6)**GalNAcol	1	–	–	–	–	3.3	–	–	–	–	–	0.4	–
1121-1	Hex2HexNAc2dHex2Sul1	Fucα1-2Galβ1-3**[Fucα1-2Gal(S)GlcNAcβ1-6]**GalNAcol	2	–	–	–	–	–	–	–	–	–	0.8	1.5	–
1121-2	Hex2HexNAc2dHex2Sul1	Fucα1-2Galβ1-3**[Fucα1-2Galβ1-4(6S)GlcNAcβ1-6]**GalNAcol	2	–	–	–	–	1.0	–	–	0.9	–	0.8	1.5	–
1169	NeuAc2Hex1HexNAc2	NeuAcα2-3Galβ1-4GlcNAcβ1-3**(NeuAcα2-6)**GalNAcol	3	–	–	–	–		–	–	4.6	–	–	–	–
1170	NeuAc1Hex1HexNAc2dHex2	Fucα1-2Gal(Fuc)GlcNAcβ1-3**(NeuAcα2-6)**GalNAcol	3	–	b/y	–	–	0.4	–	–	1.1	–	0.6	–	1.5
1178-1	Hex2HexNAc3dHex1Sul1	Gal-GlcNAcβ1-3**[Gal(Fuc)(6S)GlcNAcβ1-6]**GalNAcol	4	–	a/x	0.8	–	–	–	–	–	–	–	–	–
1178-2	Hex2HexNAc3dHex1Sul1	Gal-GlcNAc-(Fuc)Gal-(S)GlcNAcβ1-3GalNAcol	3	–	–	3.4	–	1.1	–	–	–	1.0	–	0.1	–
1178-3	Hex2HexNAc3dHex1Sul1	Fucα1-2Gal-GlcNAcβ1-3**(S-Gal-GlcNAcβ1-6)**GalNAcol	4	H	–	–	–		–	–	–	–	–	0.4	–
1178-4	Hex2HexNAc3dHex1Sul1	Fucα1-2Gal-GlcNAcβ1-3**(S-Gal-GlcNAcβ1-6)**GalNAcol	4	H	–	–	–	0.6	–	–	0.8	–	1.0	3.6	–
1178-5	Hex2HexNAc3dHex1Sul1	Fucα1-2Gal-GlcNAcβ1-3**(S-Gal-GlcNAcβ1-6)**GalNAcol	4	H	–	–	–	–	–	–	–	–	0.7	0.8	–
1186-1	NeuAc1Hex2HexNAc2dHex1	Gal(Fuc)GlcNAc-Galβ1-3**(NeuAcα2-6)**GalNAcol	1	–	a/x	–	–	0.1	–	–	–	–	–	–	–
1186-2	NeuAc1Hex2HexNAc2dHex1	Galβ1-3**[NeuAcα2-3Galβ1-4(Fucα1-3)GlcNAcβ1-6]**GalNAcol	2	–	a/x	1.4	–	0.9		1.4	2.3	1.5	0.7	0.8	1.3
1186-3	NeuAc1Hex2HexNAc2dHex1	Galβ1-3**[NeuAcα2-3Galβ1-3(Fucα1-4)GlcNAcβ1-6]**GalNAcol	2	–	a/x	1.5	–	–	–	–	–	0.8	–	–	–
1186-4	NeuAc1Hex2HexNAc2dHex1	NeuAcα2-3Galβ1-3**(Fucα1-2Galβ1-4GlcNAcβ1-6)**GalNAcol	2	H	–	–	–	0.6	–	–	–	–	1.2	0.6	1.8
1186-5	NeuAc1Hex2HexNAc2dHex1	NeuAcα2-3Galβ1-3**[Gal(Fuc)GlcNAcβ1-6]**GalNAcol	2	–	a/x	–	–	0.5	–	–	0.7	–	0.6	–	–
1186-6	NeuAc1Hex2HexNAc2dHex1	Fucα1-2Galβ1-3**(NeuAcα2-3Galβ1-4GlcNAcβ1-6)**GalNAcol	2	H		–	–	1.5	4.1	–	2.1	–	2.6	1.4	3.3
1187	Hex2HexNAc2dHex3	Fucα1-2Galβ1-3**[Fucα1-2Gal(Fuc)GlcNAcβ1-6]**GalNAcol	2	H	b/y	–	–	0.8	–	–	–	–	–	–	1.0
1194-1	Hex3HexNAc3Sul1	S + Galβ1-3**(Galβ1-4GlcNAcβ1-3Galβ1-4GlcNAcβ1-6)**GalNAcol	2	–	–	–	–	0.5	–	–	–	–	–	0.7	–

Name	Composition	Putative structure	Core	Blood type	Lewis type	1	2	3	1	2	3	1	2	3	MDR
1194-2	Hex3HexNAc3Sul1	S + Gal-GlcNAc-Gal-GlcNAc-Galβ1-3GalNAcol	1	–	–	–	–	0.5	–	–	–	–	–	–	–
1227	NeuAc1Hex1HexNAc3dHex1	GlcNAcβ1-3**[NeuAcα2-3Gal(Fuc)GlcNAcβ1-6]**GalNAcol	4	–	a/x	–	–	–	–	–	0.7	0.6	–	–	–
1243-1	NeuAc1Hex2HexNAc3	NeuAcα2-6Galβ1-4GlcNAcβ1-3**(Galβ1-4GlcNAcβ1-6)**GalNAcol	4	–	–	6.6	–	1.4	–	–	0.8	7.1	1.7	0.7	–
1243-2	NeuAc1Hex2HexNAc3	NeuAcα2-3Galβ1-4GlcNAcβ1-3Galβ1-4GlcNAcβ1-3GalNAcol	3	–	–	–	–	–	–	–	0.6	–	–	–	–
1244-1	Hex2HexNAc3dHex2	Gal(Fuc)GlcNAcβ1-3**[Gal(Fuc)GlcNAcβ1-6]**GalNAcol	4	–	a/x	–	–	0.2	–	–	–	–	–	–	–
1244-2	Hex2HexNAc3dHex2	Fucα1-2Galβ1-4GlcNAcβ1-3**(Fucα1-2Galβ1-3GlcNAcβ1-6)**GalNAcol	4	H	–	–	–	0.9	–	–	–	–	1.4	0.7	1.6
1244-3	Hex2HexNAc3dHex2	Fucα1-2Galβ1-4GlcNAcβ1-3**(Fucα1-2Galβ1-4GlcNAcβ1-6)**GalNAcol	4	H	–	–	–	0.4	–	–	–	–	2.0	0.4	2.5
1258	Hex2HexNAc3dHex1Sul2	S-Gal-GlcNAcβ1-3**[Gal(Fuc)(6S)GlcNAcβ1-6]**GalNAcol	4	–	a/x	4.0	–		–	–	–	–	–	0.9	–
1266-1	NeuAc1Hex2HexNAc2dHex1Sul1	S + NeuAcα2-3Galβ1-3**[Gal(Fuc)GlcNAcβ1-6]**GalNAcol	2	–	a/x	–	–	0.9	–	–	–	–	–	–	–
1266-2	NeuAc1Hex2HexNAc2dHex1Sul1	NeuAc+Fuc+Galβ1-3**[Galβ1-4(6S)GlcNAcβ1-6]**GalNAcol	2	–	–	–	–	1.8	–	–	–	–	–	–	–
1266-3	NeuAc1Hex2HexNAc2dHex1Sul1	NeuAc+Fuc+Galβ1-3**[Galβ1-4(6S)GlcNAcβ1-6]**GalNAcol	2	–	–	–	–	–	–	–	–	–	–	0.9	–
1267	Hex2HexNAc2dHex3Sul1	Fucα1-2Galβ1-3**[Fucα1-2Gal(Fuc)(S)GlcNAcβ1-6]**GalNAcol	2	H	a/x	–	–	–	–	–	–	–	–		–
1274	Hex3HexNAc3Sul2	2S + Galβ1-3**(Galβ1-4GlcNAcβ1-3Galβ1-4GlcNAcβ1-6)**GalNAcol	2	–	–	–	–	3.7	–	–	–	–	–	2.7	–
1301	Hex2HexNAc4dHex1	GalNAcα1-3(Fucα1-2)Galβ1-4GlcNAcβ1-3**(Galβ1-4GlcNAcβ1-6)**GalNAcol	4	A	–	–	–	–	–	–	–	–	–	–	–
1315	NeuAc2Hex1HexNAc2dHex1	NeuAcα2-3Gal(Fuc)GlcNAcβ1-3**(NeuAcα2-6**)GalNAcol	3	–	a/x	–	–	–	–	–	3.3	–	–	–	–
1324-1	Hex2HexNAc3dHex2Sul1	S-Gal(Fuc)GlcNAc-Gal(Fuc)GlcNAcβ1-3GalNAcol	3	–	a/x	–	–	–	–	–	–	–	–	–	–
1324-2	Hex2HexNAc3dHex2Sul1	Fucα1-2Gal-GlcNAc-(Fuc)Gal-(S)GlcNAcβ1-3GalNAcol	3	H	–	–	–	0.5	–	–	0.3	–	0.4	–	–
1324-3	Hex2HexNAc3dHex2Sul1	S+Fucα1-2Gal-GlcNAcβ1-3**(Fucα1-2Gal-GlcNAcβ1-6)**GalNAcol	4	H	–	–	–	–	–	–	–	–	0.4	1.1	–
1324-4	Hex2HexNAc3dHex2Sul1	S+Fucα1-2Gal-GlcNAcβ1-3**(Fucα1-2Gal-GlcNAcβ1-6)**GalNAcol	4	H	–	–	–	–	–	–	–	–	0.3	0.1	–
1331-1	NeuAc2Hex2HexNAc2	NeuAcα2-3Galβ1-3**(NeuAcα2-6Galβ1-4GlcNAcβ1-6)**GalNAcol	2	–	–	–	–	–	–	12.1	2.0		1.6	0.3	9.1
1331-2	NeuAc2Hex2HexNAc2	NeuAcα2-3Galβ1-3**(NeuAcα2-3Galβ1-4GlcNAcβ1-6)**GalNAcol	2	–	–	–	–	–	1.6	26.3	5.7	5.4	5.7	1.5	10.0
1332-1	NeuAc1Hex2HexNAc2dHex2	Fucα1-2Gal(Fuc)GlcNAc-Galβ1-3**(NeuAcα2-6)**GalNAcol	1	–	b/y	–	–	0.3	–	–	–	–	–	–	–

Name	Composition	Putative structure	Core	Blood type	Lewis type	1	2	3	1	2	3	1	2	3	MDR
1332-2	NeuAc1Hex2HexNAc2dHex2	Fucα1-2Galβ1-3**[NeuAcα2-3Gal(Fuc)GlcNAcβ1-6]**GalNAcol	2	H	a/x	–	–	0.5	–	–	–	–	–	–	2.5
1332-3	NeuAc1Hex2HexNAc2dHex2	NeuAcα2-3Gaβ1-3**[Fucα1-2Gal(Fuc)GlcNAcβ1-6]**GalNAcol	2	H	a/x	–	–	0.8	–	–	–	–	–	0.3	–
1332-4	NeuAc1Hex2HexNAc2dHex2	Fucα1-2Galβ1-3**[NeuAcα2-3Gal(Fuc)GlcNAcβ1-6]**GalNAcol	2	H	a/x	–	–	0.6	–	–	–	–	–	0.4	–
1340-1	Hex3HexNAc3dHex1Sul1	S+Gal(Fuc)GlcNAc-Gal-GlcNAc-Galβ1-3GalNAcol	1	–	a/x	–	–	–	–	–	–	–	–	0.1	–
1340-2	Hex3HexNAc3dHex1Sul1	S+Gal(Fuc)GlcNAc-Gal-GlcNAc-Galβ1-3GalNAcol	1	–	a/x	–	–	–	–	–	–	–	–	0.2	–
1389-1	NeuAc1Hex2HexNAc3dHex1	NeuAcα2-3Galβ1-4GlcNAcβ1-3**(Fucα1-2Galβ1-4GlcNAcβ1-6)**GalNAcol	4	H	–	3.0	–	–	–	–	–	2.3	–	–	–
1389-2	NeuAc1Hex2HexNAc3dHex1	NeuAcα2-3Gal(Fuc)GlcNAcβ1-3**(GalGlcNAcβ1-6)**GalNAcol	4	–	a/x	–	–	–	–	–	0.3	–	–	–	–
1389-3	NeuAc1Hex2HexNAc3dHex1	Fucα1-2Galβ1-4GlcNAcβ1-3**(NeuAcα2-3Galβ1-4GlcNAcβ1-6)**GalNAcol	4	H	–	–	–	1.6	–	–	–	–	2.8	0.9	3.7
1389-4	NeuAc1Hex2HexNAc3dHex1	NeuAcα2-3Gal(Fuc)GlcNAcβ1-3**(Gal-GlcNAcβ1-6)**GalNAcol	4	–	a/x	–	–	–	–	–	–	–	1.6	0.5	–
1390-1	Hex2HexNAc3dHex3	Fucα1-2Gal-GlcNAcβ1-3**[Fucα1-2Gal(Fuc)GlcNAcβ1-6]**GalNAcol	4	H	b/y	–	–	0.6	–	–	–	–	0.3	–	–
1390-2	Hex2HexNAc3dHex3	Fucα1-2Gal-(Fuc)GlcNAcβ1-3**(Fucα1-2Gal-GlcNAcβ1-6)**GalNAcol	4	H	b/y	–	–	–	–	–	–	–	0.5	–	–
1404-1	Hex2HexNAc3dHex2Sul2	2S + Fucα1-2Galβ1-4GlcNAcβ1-3**[Gal(Fuc)GlcNAcβ1-6]**GalNAcol	4	H	a/x	–	–	–	–	–	–	–	–	–	–
1404-2	Hex2HexNAc3dHex2Sul2	2S + Fucα1-2Galβ1-4GlcNAcβ1-3**(Fucα1-2Galβ1-4GlcNAcβ1-6)**GalNAcol	4	H	–	1.5	–	0.3	–	–	–	–	–	–	–
1405	NeuAc1Hex3HexNAc3	NeuAc+Galβ1-3**(Galβ1-4GlcNAcβ1-3Galβ1-4GlcNAcβ1-6)**GalNAcol	2	–	–	–	–	–	–	–	–	–	–	–	–
1406	Hex3HexNAc3dHex2	Fucα1-2Gal-GlcNAc(Fucα1-2)Galβ1-3**(Galβ1-4GlcNAcβ1-6)**GalNAcol	2	H	b/y	–	–	0.4	–	–	–	–	–	–	–
1411	NeuAc2Hex2HexNAc2Sul1	NeuAcα2-3Galβ1-3**[NeuAcα2-3Galβ1-3(6S)GlcNAcβ1-6]**GalNAcol	2	–	–	–	–		–	–	–	–	1.2	–	–
1420-1	Hex3HexNAc3dHex1Sul2	2S + Fucα1-2Galβ1-3**(Gal-GlcNAc-Gal-GlcNAcβ1-6)**GalNAcol	2	H	–	7.2		1.7	–	–	–	1.5	–	0.6	–
1420-2	Hex3HexNAc3dHex1Sul2	2S+Gal(Fuc)GlcNAc-Gal-GlcNAc-Galβ1-3GalNAcol	1	–	a/x	–	–	–	–	–	–	–	–	0.9	–
1420-3	Hex3HexNAc3dHex1Sul2	2S+Gal(Fuc)GlcNAc-Gal-GlcNAc-Galβ1-3GalNAcol	1	–	a/x	–	–	–	–	–	–	–	–	1.1	–
1463	Hex3HexNAc4dHex1	Galβ1-3**[GalNAcα1-3(Fucα1-2)Galβ1-4GlcNAcβ1-3Galβ1-4GlcNAcβ1-6]**GalNAcol	2	A	–	–	–	–	–	–	–	–	–	–	–
1469	NeuAc1Hex2HexNAc3dHex1Sul1	NeuAc+Fuc+S+Galβ1-4GlcNAcβ1-3**(Galβ1-4GlcNAcβ1-6)**GalNAcol	4	–	–	–	–	–	–	–	–	–	–	–	–
1477-1	NeuAc2Hex2HexNAc2dHex1	NeuAcα2-3Galβ1-3**[NeuAcα2-3Gal(Fuc)GlcNAcβ1-6]**GalNAcol	2	–	a/x	–	–	–	–	–	1.2	–	–	–	4.6

Name	Composition	Putative structure	Core	Blood type	Lewis type	1	2	3	1	2	3	1	2	3	MDR
1477-2	NeuAc2Hex2HexNAc2dHex1	NeuAcα2-3Galβ1-3**[NeuAcα2-3Gal(Fuc)GlcNAcβ1-6]**GalNAcol	2	–	a/x	1.2	–	–	–	–	1.6	1.2		1.3	–
1479	Hex4HexNAc4	Galβ1-4GlcNAcβ1-3Galβ1-3**(Galβ1-4GlcNAcβ1-3Galβ1-4GlcNAcβ1-6)**GalNAcol	2	–	–	–	–	0.1	–	–	–	–	–	–	–
1485	NeuAc1Hex3HexNAc3Sul1	NeuAc+S+Galβ1-3**(Galβ1-4GlcNAcβ1-3Galβ1-4GlcNAcβ1-6)**GalNAcol	2	–	–	–	–	–	–	–	–	–	–	–	–
1486	Hex3HexNAc3dHex2Sul1	Galβ1-3**[Fucα1-2Gal-GlcNAc(S)Gal(Fuc)GlcNAcβ1-6]**GalNAcol	2	H	–	–	–	–	–	–	–	–	–	–	–
1527	Hex2HexNAc4dHex2Sul1	GalNAcα1-3(Fucα1-2)Galβ1-3**[GalNAcα1-3(Fucα1-2)Gal-(S)GlcNAcβ1-6]**GalNAcol	2	A	–	–	–	–	–	–	–	–	–	–	–
1534-1	NeuAc2Hex2HexNAc3	NeuAcα-3Gal-GlcNAcβ1-3**(NeuAcα2-3Gal-GlcNAcβ1-6)**GalNAcol	4	–	–	–	–	–	–	–	–	1.0	–	–	–
1534-1	NeuAc2Hex2HexNAc3	NeuAcα-3Gal-GlcNAcβ1-3**(NeuAcα2-3Gal-GlcNAcβ1-6)**GalNAcol	4	–	–	–	–	–	–	–	–	–	–	–	–
1535-1	NeuAc1Hex2HexNAc3dHex2	NeuAcα2-3Gal(Fuc)GlcNAc-Gal(Fuc)GlcNAcβ1-3GalNAcol	3	–	a/x	–	–	–	–	–	0.3	–	–	–	–
1535-2	NeuAc1Hex2HexNAc3dHex2	NeuAcα2-3Galβ1-3**[GalNAcα1-3(Fucα1-2)Gal(Fuc)GlcNAcβ1-6]**GalNAcol	2	A	a/x	–	–	–	–	–	–	–	–	–	–
1535-3	NeuAc1Hex2HexNAc3dHex2	NeuAcα2-3Gal-GlcNAcβ1-3**[Fucα1-2Gal(Fuc)GlcNAcβ1-6]**GalNAcol	4	H	b/y	–	–	0.6	–	–	–	–	0.2	1.0	–
1535-4	NeuAc1Hex2HexNAc3dHex2	Fucα1-2Gal(Fuc)GlcNAcβ1-3**[NeuAcα2-3Gal-GlcNAcβ1-6]**GalNAcol	4	H	b/y	–	–	–	–	–	–	–	0.7	0.3	–
1551	NeuAc1Hex3HexNAc3dHex1	Galβ1-3**[NeuAcα2-3Galβ1-4GlcNAcβ1-3Galβ1-4(Fuc)GlcNAcβ1-6]**GalNAcol	2	–	a/x	–	–	–	–	–	–	0.5	–	–	–
1557	NeuAc2Hex2HexNAc2dHex1Sul1	NeuAcα2-3Galβ1-3**[NeuAcα2-3Galβ1-4(Fucα1-3)(6S)GlcNAcβ1-6]**GalNAcol	2	–	a/x	–	–	–	–	–	–	–	–	–	–
1566-1	Hex3HexNAc3dHex2Sul2	2S + Fuc + Fucα1-2Galβ1-3**(Gal-GlcNAc-Gal-GlcNAcβ1-6)**GalNAcol	2	H	a/x	6.2	–	0.9	–	–	–	2.2	–	–	–
1566-2	Hex3HexNAc3dHex2Sul2	2S+Gal(Fuc)GlcNAc-Galβ1-3**[Gal(Fuc)GalNAcβ1-6]**GalNAcol	2	–	a/x	–	–	–	–	–	–	–	–	0.3	–
1592	NeuAc1Hex2HexNAc4dHex1	GalNAcα1-3(Fucα1-2)Gal-GlcNAcβ1-3**(NeuAcα2-3Gal-GlcNAcβ1-6)**GalNAcol	4	A	–	–	–	–	–	–	–	–	–	–	–
1609	Hex3HexNAc4dHex2	Gal-GlcNAcβ1-3**[Fucα1-2Gal(Fuc)GlcNAc-Gal-GlcNAcβ1-6]**GalNAcol	4	H	b/y	–	–	0.3	–	–	–	–	–	–	–
1614	NeuAc2Hex2HexNAc3Sul1	S+NeuAcα-3Gal-GlcNAcβ1-3**(NeuAcα2-3Gal-GlcNAcβ1-6)**GalNAcol	4	–	–	–	–	–	–	–	–	–	–	–	–
1615-1	NeuAc1Hex2HexNAc3dHex2Sul1	Gal(Fuc)(S)GlcNAc-Gal(Fuc)GlcNAcβ1-3**(NeuAcα2-6)**GalNAcol	3	–	a/x	3.2	–	–	–	–	–	–	–	–	–
1615-2	NeuAc1Hex2HexNAc3dHex2Sul1	NeuAcα-3Gal-(Fuc)GlcNAcβ1-3**[Gal-(Fuc)(6S)GlcNAcβ1-6]**GalNAcol	4	–	a/x	–	–	–	–	–	–	–	–	–	–
1623	Hex3HexNAc4dHex1Sul2	2S+Gal(Fuc)GlcNAc-Galβ1-3**[Gal(Fuc)GalNAcβ1-6]**GalNAcol	2	–	a/x	–	–	–	–	–	–	–	–	2.2	–

Name	Composition	Putative structure	Core	Blood type	Lewis type	1	2	3	1	2	3	1	2	3	MDR
1625	Hex4HexNAc4dHex1	Gal-GlcNAc-Galβ1-3**[Gal(Fuc)GlcNAc-Gal-GlcNAcβ1-6]**GalNAcol	2	–	a/x	–	–	–	–	–	–	0.2	–	–	–
1631-1	NeuAc1Hex3HexNAc3dHex1Sul1	Galβ1-3**[NeuAcα2-6Gal-GlcNAc(S)Gal(Fuc)GlcNAcβ1-6]**GalNAcol	2	–	a/x	–	–	–	–	–	–	–	–	–	–
1631-2	NeuAc1Hex3HexNAc3dHex1Sul1	Fucα1-2Galβ1-3**[NeuAc-Gal-GlcNAc-Galβ1-4(6S)GlcNAcβ1-6]**GalNAcol	2	H	–	–	–	–	–	–	–	–	–	0.3	–
1631-3	NeuAc1Hex3HexNAc3dHex1Sul1	Fucα1-2Galβ1-3**[NeuAc-Gal-GlcNAc-Galβ1-4(6S)GlcNAcβ1-6]**GalNAcol	2	H	–	–	–	–	–	–	–	1.8	0.5	–	–
1631-4	NeuAc1Hex3HexNAc3dHex1Sul1	NeuAcα2-3Galβ1-3**[Gal(Fuc)(6S)GlcNAcGal(6S)GlcNAcβ1-6]**GalNAcol	2	–	a/x	–	–	–	–	–	–	–	–	–	–
1650	Hex2HexNAc5dHex2	GalNAcα1-3(Fucα1-2)Gal-GlcNAcβ1-3**[GalNAcα1-3(Fucα1-2)Gal-GlcNAcβ1-6]**GalNAcol	4	A	–	–	–	–	–	–	–	–	–	–	–
1680-1	NeuAc2Hex2HexNAc3dHex1	Fuc + NeuAcα2-3Gal-GlcNAcβ1-3**(NeuAcα2-3Gal-GlcNAcβ1-6)**GalNAcol	4	–	–	–	–	–	–	–	–	0.9	–	–	–
1680-2	NeuAc2Hex2HexNAc3dHex1	Fuc + NeuAcα2-3Gal-GlcNAcβ1-3**(NeuAcα2-3Gal-GlcNAcβ1-6)**GalNAcol	4	–	–	–	–	–	–	–	–	1.3	2.3	0.8	–	–
1689	Hex3HexNAc3dHex2Sul1	Galβ1-4GlcNAcβ1-3**[Gal(Fuc)(6S)GlcNAcGal(Fuc)GlcNAcβ1-6]**GalNAcol	4	–	a/x	–	–	–	–	–	–	–	–	–	–
1696-1	NeuAc2Hex3HexNAc3	NeuAcα2-3Galβ1-3**(NeuAcα2-6Galβ1-4GlcNAcβ1-3Galβ1-4GlcNAcβ1-6)**GalNAcol	2	–	–	–	–	–	–	–	–	1.1	–	–	–	–
1696-2	NeuAc2Hex3HexNAc3	NeuAcα2-3Galβ1-3**(NeuAcα2-3Galβ1-4GlcNAcβ1-3Galβ1-4GlcNAcβ1-6)**GalNAcol	2	–	–	–	–	–	–	–	–	8.8	–	3.4	–	–
1697-1	NeuAc1Hex3HexNAc3dHex2	NeuAcα2-3Galβ1-4(Fuc)GlcNAcβ1-3**[Gal(Fuc)GlcNAcβ1-6]**GalNAcol	2	–	a/x	–	–	–	–	–	–	0.8	–	–	–
1697-2	NeuAc1Hex3HexNAc3dHex2	Fucα1-2Gal(Fuc)GlcNAc-Galβ1-3**(NeuAcα2-3Galβ1-4GlcNAcβ1-6)**GalNAcol	2	–	b/y	–	–	–	–	–	–	–		–	–
1697-3	NeuAc1Hex3HexNAc3dHex2	NeuAcα2-3Galβ1-3**[Fucα1-2Galβ1-4GlcNAcβ1-3(Fucα1-2)Galβ1-4GlcNAcβ1-6]**GalNAcol	2	H	–	–	–	–	–	–	–	–	0.4	–	–
1697-4	NeuAc1Hex3HexNAc3dHex2	Fucα1-2Gal-GlcNAc(Fucα1-2)Galβ1-3**[NeuAcα2-3Gal-GlcNAcβ1-6]**GalNAcol	2	H	b/y	–	–	–	–	–	–	–	–	–	–
1712	Hex3HexNAc3dHex3Sul2	Fucα1-2Galβ1-3**[Gal(Fuc)(S)GlcNAc-Gal(Fuc)(S)GlcNAcβ1-6]**GalNAcol	2	H	a/x	–	–	–	–	–	–	–	–	1.1	0.0
1754	NeuAc1Hex3HexNAc4dHex1	GalNAcα1-3(Fucα1-2)Galβ1-3**[NeuAcα2-3Galβ1-4GlcNAcβ1-3Galβ1-4GlcNAcβ1-6]**GalNAcol	2	A	–	–	–	–	–	–	–	–	–	–	–
1760	NeuAc2Hex2HexNAc3dHex1Sul1	S+Fuc + NeuAcα2-3Gal-GlcNAcβ1-3**(NeuAcα2-3Gal-GlcNAcβ1-6)**GalNAcol	4	–	–	–	–	–	–	–	–	–	–	–	–
1769-1	Hex3HexNAc4dHex2Sul2	Gal(Fuc)(6S)GlcNAc-Gal-GlcNAcβ1-3**[Gal(Fuc)(6S)GlcNAcβ1-6]**GalNAcol	4	–	a/x	–	–	–	–	–	–	–	–	–	–
1769-2	Hex3HexNAc4dHex2Sul2	Gal(Fuc)(6S)GlcNAc-Gal-GlcNAcβ1-3**[Gal(Fuc)(6S)GlcNAcβ1-6]**GalNAcol	4	–	a/x	6.5	–	–	–	–	–	1.6		1.3	–

Name	Composition	Putative structure	Core	Blood type	Lewis type	1	2	3	1	2	3	1	2	3	MDR
1770	NeuAc1Hex4HexNAc4	Galβ1-3**(NeuAcα2-3Galβ1-4GlcNAcβ1-3Galβ1-4GlcNAcβ1-3Galβ1-4GlcNAcβ1-6)**GalNAcol	2	–	–	–	–	–	–	–	–	0.9	–	–	–
1771-1	Hex4HexNAc4dHex2	Gal(Fuc)GlcNAc-Galβ1-3**[Gal(Fuc)GlcNAc-GalGlcNAcβ1-6]**GalNAcol	2		a/x	1.3	–	–	–	–	–	–	–	–	–
1771-2	Hex4HexNAc4dHex2	Fucα1-2Galβ1-4GlcNAcβ1-3(Fucα1-2)Galβ1-3**(Galβ1-4GlcNAcβ1-3Galβ1-4GlcNAcβ1-6)**GalNAcol	2	H	–	–	–	0.2	–	–	–	–	–	–	–
1771-3	Hex4HexNAc4dHex2	Fucα1-2Galβ1-4GlcNAcβ1-3Galβ1-3**(Fucα1-2Galβ1-4GlcNAcβ1-3Galβ1-4GlcNAcβ1-6)**GalNAcol	2	H	–	–	–	0.2	–	–	–	–	–	–	–
1777	NeuAc1Hex3HexNAc3dHex2Sul1	NeuAc+Galβ1-3**[Gal(Fuc)GlcNAc(S)Gal(Fuc)GlcNAcβ1-6]**GalNAcol	2	–	a/x	–	–	–	–	–	–	1.2	–	–	–
1785-1	Hex4HexNAc4dHex1Sul2	Fuc+ 2S +Galβ1-4GlcNAcβ1-3Galβ1-3**(Galβ1-4GlcNAcβ1-3Galβ1-4GlcNAcβ1-6)**GalNAcol	2	–	–	–	–	3.9	–	–	–	–	–	1.3	–
1785-2	Hex4HexNAc4dHex1Sul2	Fuc+ 2S +Galβ1-4GlcNAcβ1-3Galβ1-3**(Galβ1-4GlcNAcβ1-3Galβ1-4GlcNAcβ1-6)**GalNAcol	2	–	–	–	–	–	–	–	–	–	–	2.0	–
1796	Hex2HexNAc4dHex3	GalNAcα1-3(Fucα1-2)Gal-GlcNAcβ1-3**[GalNAcα1-3(Fucα1-2)Gal-(Fuc)GlcNAcβ1-6]**GalNAcol	4	A	a/x	–	–	–	–	–	–	–	–	–	–
1812	Hex3HexNAc5dHex2	GalNAcα1-3(Fucα1-2)Galβ1-3**[GalNAcα1-3(Fucα1-2)Galβ1-4GlcNAcβ1-3Galβ1-4GlcNAcβ1-6]**GalNAcol	2	A	–	–	–	–	–	–	–	–	–	–	–
1826-1	NeuAc2Hex2HexNAc3dHex2	NeuAcα2-3Gal(Fuc)GlcNAcβ1-3**[NeuAcα2-3Gal(Fuc)GlcNAcβ1-6]**GalNAcol	4	–	a/x	–	–	–	–	–	0.7	–	–	–	–
1826-2	NeuAc2Hex2HexNAc3dHex2	NeuAcα2-3Gal(Fuc)GlcNAcβ1-3**[NeuAcα2-3Gal(Fuc)GlcNAcβ1-6]**GalNAcol	4	–	a/x	–	–	–	–	–	0.6	–	–	–	–
1826-3	NeuAc2Hex2HexNAc3dHex2	NeuAcα2-3Gal(Fuc)GlcNAcβ1-3**[NeuAcα2-3Gal(Fuc)GlcNAcβ1-6]**GalNAcol	4	–	a/x	–	–	–	–	–	–	–	–	–	–
1834-1	NeuAc1Hex3HexNAc4dHex1Sul1	NeuAc+2(Hex-HexNAc)+Galβ1-3**[Gal(Fuc)(S)GlcNAcβ1-6]**GalNAcol	2	–	a/x	–	–	–	–	–	–	–	–	–	–
1834-2	NeuAc1Hex3HexNAc4dHex1Sul1	NeuAc+2(Hex-HexNAc)+Galβ1-3**[Gal(Fuc)(S)GlcNAcβ1-6]**GalNAcol	2	–	a/x	–	–	–	–	–	–	0.7	–	–	–
1842-1	NeuAc2Hex3HexNAc3dHex1	NeuAcα2-3Gal-GlcNAc-Galβ1-3**[NeuAcα2-3Gal(Fuc)GlcNAcβ1-6]**GalNAcol	2	–	a/x	–	–	–	–	–	–	–	–	–	–
1842-2	NeuAc2Hex3HexNAc3dHex1	Fuc + NeuAcα2-3Galβ1-3**(NeuAcα2-3Galβ1-4GlcNAcβ1-3Galβ1-4GlcNAcβ1-6)**GalNAcol	2	–	–	–	–	–	–	–	–	5.3	5.3	0.7	–	–
1857	NeuAc1Hex3HexNAc3dHex2Sul2	NeuAc+S+Galβ1-3**[Gal(Fuc)GlcNAc(S)Gal(Fuc)GlcNAcβ1-6]**GalNAcol	2	–	a/x	–	–	–	–	–	–	–	–	–	–
1915	Hex3HexNAc4dHex3Sul2	Gal(Fuc)(6S)GlcNAc-Gal-(Fuc)GlcNAcβ1-3**[Gal(Fuc)(6S)GlcNAcβ1-6]**GalNAcol	4	–	a/x	–	–	–	–	–	–	0.9	–	1.2	–
1917	Hex4HexNAc4dHex3	Fucα1-2Galβ1-4GlcNAcβ1-3**(Fucα1-2Galβ1-4GlcNAcβ1-6)**Galβ1-3**[Fucα1-2Galβ1-4GlcNAcβ1-6]**GalNAcol	2	H	–	–	–	–	–	–	–	–	0.3	–	–
1922	NeuAc2Hex3HexNAc3dHex1Sul1	S+NeuAcα2-3Gal-GlcNAc-Galβ1-3**[NeuAcα2-3Gal(Fuc)GlcNAcβ1-6]**GalNAcol	2	–	a/x	–	–	–	–	–	–	–	–	–	–

Name	Composition	Putative structure	Core	Blood type	Lewis type	1	2	3	1	2	3	1	2	3	MDR
1931	Hex4HexNAc4dHex2Sul2	2Fuc+ 2S +Galβ1-4GlcNAcβ1-3Galβ1-3**(Galβ1-4GlcNAcβ1-3Galβ1-4GlcNAcβ1-6)**GalNAcol	2	–	–	–	–	2.3	–	–	–	–	–	0.8	–
1988	NeuAc2Hex3HexNAc3dHex2	2Fuc + NeuAcα2-3Galβ1-3**(NeuAcα2-3Galβ1-4GlcNAcβ1-3Galβ1-4GlcNAcβ1-6)**GalNAcol	2	–	–	–	–	–	–	–	0.7	1.0	–	–	–
2002	NeuAc2Hex3HexNAc3dHex1Sul2	2S+NeuAcα2-3Gal-GlcNAc-Galβ1-3**[NeuAcα2-3Gal(Fuc)GlcNAcβ1-6]**GalNAcol	2	–	a/x	–	–	–	–	–	–	–	–	–	–
2061	NeuAc2Hex4HexNAc4	NeuAcα2-3Galβ1-3**(NeuAcα2-3Galβ1-4GlcNAcβ1-3Galβ1-4GlcNAcβ1-3Galβ1-4GlcNAcβ1-6)**GalNAcol	2	–	–	–	–	–	–	–	–	5.1	–	–	–
2063	Hex4HexNAc4dHex4	Fuc + Fucα1-2Galβ1-4GlcNAcβ1-3**(Fucα1-2Galβ1-4GlcNAcβ1-6)**Galβ1-3**[Fucα1-2Galβ1-4GlcNAcβ1-6]**GalNAcol	2	H	–	–	–	–	–	–	–	–	0.5	–	–
2068-1	NeuAc2Hex3HexNAc3dHex2Sul1	_S + 2Fuc + NeuAcα2-3Galβ1-3**(NeuAcα2-3Galβ1-4GlcNAcβ1-3Galβ1-4GlcNAcβ1-6)**GalNAcol	2	–	–	–	–	–	–	–	–	–	0.5	–	–
2068-2	NeuAc2Hex3HexNAc3dHex2Sul1	2S+Fuc+NeuAcα2-3Gal-GlcNAc-Galβ1-3[NeuAcα2-3Gal(Fuc)GlcNAcβ1-6]GalNAcol	2	–	a/x	–	–	–	–	–	–	–		–	–
						100	**100**	**100**	**100**	**100**	**100**	**100**	**100**	**100**	**100**

7.3 Discussion

Initially, this part of the study was aimed at identifying specific secreted mucin oligosaccharides following Western blotting. However, followingthe release of O-glycans by β-elimination, a white salt residue (BH4) was visible at the bottom of the tube of the eluted glycans. Several attempts to remove these salt residues failed. This was an enormous challenge as the eluted glycans could not be identified using the LC mass spectrometry. Drs. Niclas Karlsson and Chunsheng Jin offered their experience and assistance with determining the putative structures of the O-glycans from respiratory mucus.

Higher amounts of core 1–4 O-glycan structures were found in uninfected controls and sputa than in BALs. It is hypothesised that the mucus samples from uninfected controls (tracheal aspirates) and sputa might have been contaminated with salivary mucins. Furthermore, core 3 and core 4 structures diminished in BALs in the presence of HIV. Mucins with core 5 structures have been reported in human meconium and intestinal carcinoma tissue (Brockhausen *et al.*, 2009). However, this study found small amounts of core 5 O-glycan structures in the respiratory mucus (tracheal aspirates, BALs and sputa). Some core structures contained sialic acids, fucoses and sulfates respectively and as mixtures.

Sialic acids are negatively charged and hydrophobic (Varki, 2008). These properties are important in structural and modulatory roles. The O-glycan profiles showed more sialylated O-glycans. Specifically α2,3-linked terminal sialic acid and α2,6-linked terminal sialic acid. It has been reported that α2,3-linked terminal sialic acids and α2,6-linked terminal sialic acids play a crucial role in the initial process of infection; an observation that was demonstrated in a study where sialic acids from influenza viruses bound to airway epithelium (Varki, 2008). Additionally, α2,3-linked terminal sialic acids are present in the lower airways. Sialylation has also been described in inflammation in acute phase reaction (Varki, 2008). However, its role in altering the immune response remains unknown. Therefore, the presence of sialylation might also indicate inflammation as a result of TB. Sialylation has also been found to be responsible for colonization of airways by *Pseudomonas* species (Varki, 2008). This is

important to note as this opportunistic pathogen can use mucins as a nutrient source in the progression of an infection (Aristoteli and Willcox, 2003).

Another modification that is negatively charged sulfations. Sulfated glycans are known to confer ion exchange and viscosity (Lo-Guidice et al., 2007). Sulfated glycans have also been associated with cell adhesion and recognition on microbes.

Reports have indicated that fucosylation has been widely found in ABO blood groups and that it is important in blood transfusion (Becker and Lowe, 2003). The study found blood type H antigens from blood group O with terminal Fucα1-2Gal-, and A antigens from blood group A with terminal Fucα1-2(GalNAcα1-3)Gal-. Fucosylation has also been seen in microbe interaction. The best known interaction in the intestinal tract is with *Helicobacter pylori* where the microbe attached through Lewis b antigen (Becker and Lowe, 2003; Sonawane *et al.*, 2012). The majority of fucosylated O-glycans detected were associated to blood type and Lewis type (a/b/x/y). The significance of this in TB is not yet known. However, fucosylation has been extensively studied in cancer and has led tor sialyl Lewis A antigen as a biomarker in pancreatic cancer (Wantanabe *et al.*, 2016).

This chapter shows preliminary data in studying respiratory mucus in TB. It was found that core 3 and 4 diminish in the presence of HIV. The link between sialylation and sulfate is not known.

CHAPTER 8 : IMMUNOHISTOCHEMICAL ANALYSIS OF RESPIRATORY MUCINS IN LUNG TISSUE FROM TB INFECTED LUNGS

8.1 Introduction

Mucins are complex glycoproteins that are high in carbohydrate content. They are divided into neutral and acidic forms. Immunohistochemistry is a very valuable tool widely used in the localisation of proteins in tissue sections. Thornton and colleagues have reported that tissue distribution of mucins was determined through reactivity to the carbohydrates using classical and special histological stains for glycoproteins (Thornton *et al.*, 1997)).

Classical histological stains such as Haematoxylin and Eosin (H & E) are normally employed to determine histological diagnoses (Ali *et al.*, 2012). Special stains are used to determine the localisation and types of mucins expressed in tissue. The Periodic-Acid Schiff (PAS) and Alcian Blue (AB) stain combination is used to differentiate between neutral and acidic mucins in tissue sections. The PAS technique not only differentiates the mucins but also widely identifies glycoproteins and carbohydrates. Additionally, the AB stain is used to stain the mucopolysaccharides found in the goblet cells (Ali *et al.*, 2012). The acidic mucins are further subdivided into sulfated mucins (sulfomucins) and sialylated mucins (sialomucins). Histochemically, the usage of High Iron Diamine (HID)/AB stain in tissue separates sulfomucins and sialomucins (Ali *et al.*, 2012; Thornton *et al.*, 1997).

The aims of this chapter were to confirm the expressed mucins identified in the previous chapter using Western blotting and to describe the expression and location of respiratory mucins in TB lung tissue. The specialised stains, PAS/AB and HID/AB together with anti (-MUC2, -MUC5AC, -MUC5B, -MUC7 and -MUC16) antibodies were used to determine the mucins expressed in TB and to locate where the mucins are expressed.

Serial sections (2 µm) were cut from formalin fixed paraffin wax embedded lung tissue blocks prepared from tissue obtained at post mortem from fifteen TB infected lungs. In addition, 2 µm serial sections were cut from other tissues to serve as experimental controls. Colon tissue served as a control for MUC2, gastric tissue served as control for MUC5AC,

salivary gland tissue served as control for both MUC5B and MUC7, and ovarian teratoma tissue was a control for MUC16.

8.2 Results

8.2.1 PAS/AB

All tissue blocks selected for the study were prepared from post mortem lung specimens with a known TB diagnosis. Black pigment was observed in the bronchi of two patients. This black pigment is normally associated with environmental carbon. However the increased black pigmentation in these patients suggested that they were smokers.

The PAS/AB blue stain located the mucins in the lung tissue. Out of 15 tissue samples, 7 cases showed PAS/AB positivity. The PAS stain, which locates neutral mucins was considered positive when the cells stained magenta and the AB which stains acidic mucins was considered positive when cells stained blue. Lung tissues with both neutral and acidic mucins stained purple. Neutral mucins were observed in the bronchial epithelium, in the bronchial mucus glands and in the lumen of the bronchi. Acidic mucins were observed in the small bronchial glands and in the cartilage. Figure 8.1 illustrates the expression of mucins in the epithelium of the bronchus and the bronchial glands. Non-specific staining was seen in necrotic areas.

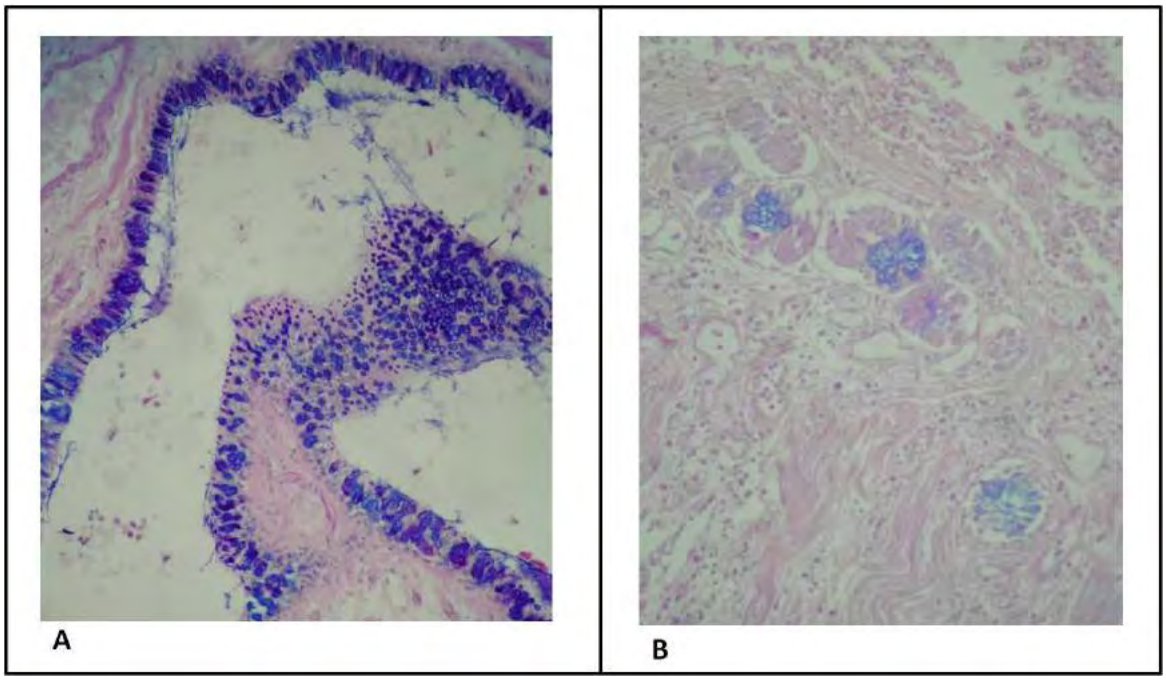

Figure 8.1: Identification of mucin glycoproteins in lung tissue PAS/AB.

(A) The goblet cells of the bronchus epithelium expressing mainly acidic mucins (blue) and some neutral mucins (pink) (X40). (B) The bronchial glands expressing acidic mucins (X40).

8.2.2 HID/AB

The acidic mucins were further analysed using the HID/AB stain to differentiate the sulfomucins and sialomucins. Sulfomucins stained black and sialomucins were observed as a blue colour. The sulfomucins and sialomucins were mainly observed in the goblet cells of the bronchi as depicted in Figure 8.2. Some goblet cells were exclusively sialomucins, some goblet cells were exclusively sulfated and other goblet cells contained a mixture of sulfomucins and sialomucins. Exclusive sialomucins and exclusive sulfomucins were also observed in the bronchial glands. Luminal mucins identified were mainly sialomucins.

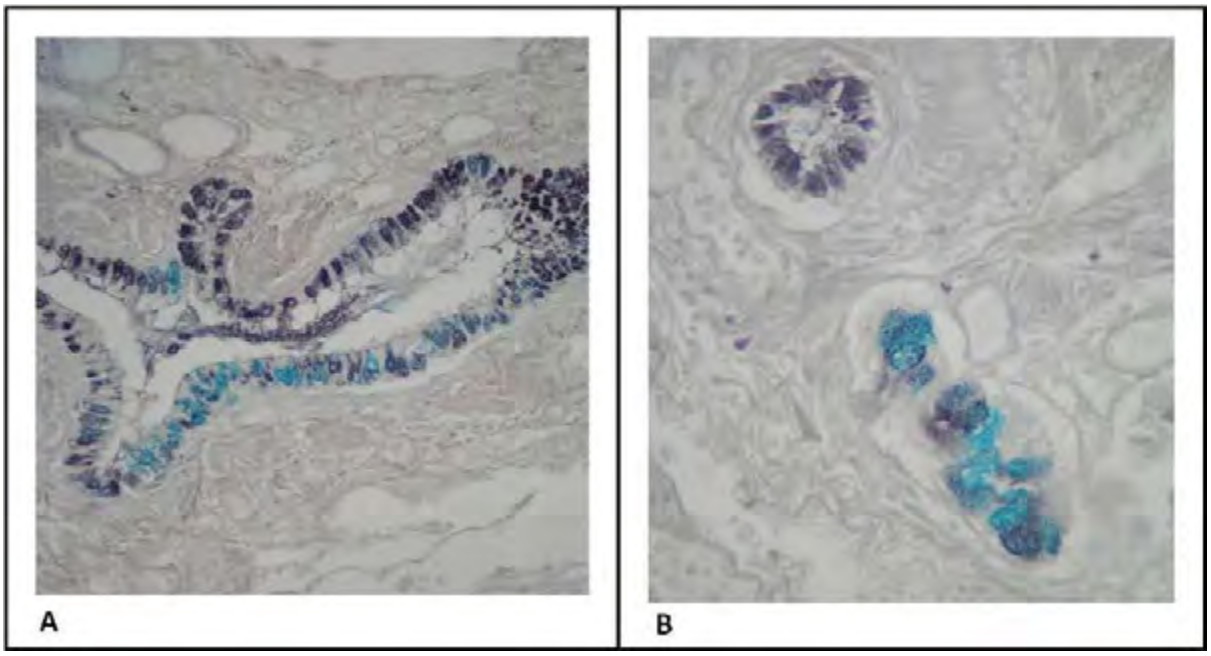

Figure 8.2: Expression of sulfomucins and sialomucins in lung tissue.

(A) Expression of sulfomucins (black) and sialomucins (blue) in the goblet cells of the bronchus epithelium (X80). (B) Expression of sulfomucins and sialomucins in the bronchial glands (X80).

8.2.3 Mucins in the lung tissue

The proportions of positively stained cells were graded as follows: 1+ (5-25 %); 2+ (26-50%); 3+ (51-75%) and 4+ (>75%).

8.2.3.1 MUC2

None of the lung tissue examined was positive for MUC2.

8.2.3.2 MUC5AC

MUC5AC expression was confined to the epithelium of the bronchi of 4 cases out of the 15 cases (Figure 8.3). However, MUC5AC was not expressed in all the goblet cells of all the patients. The proportion of positive staining was less than 50% in 3 cases. These were classified as 2+. One case was classified as 3+.

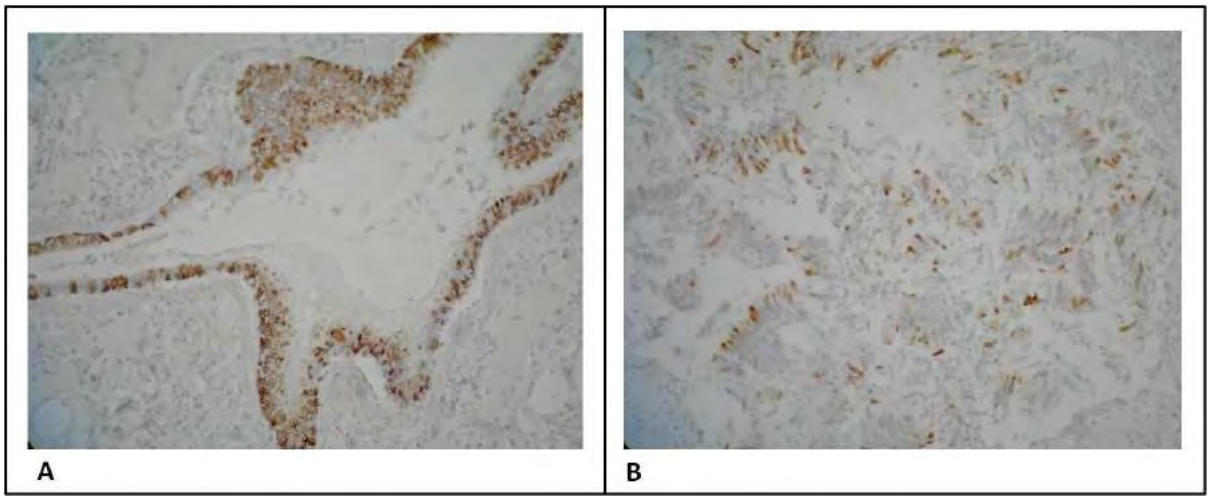

Figure 8.3: Immunohistochemical expression of the MUC5AC mucins in lung tissue.

(A) MUC5AC expression in the goblet cells of the bronchus (X40). (B) Expression of MUC5AC in the goblet cells of a disrupted epithelium at a magnification of X40.

8.2.3.3 MUC5B

Nine cases out of 15 were positive for MUC5B. Four cases were assigned a 4+ score with more than 75% of goblet cells of the bronchi and bronchial luminal mucin staining positive. The expression of MUC5B in the bronchi is demonstrated in Figure 8.4. Inconsistent focal luminal mucin staining was observed in 2 of the cases where less than 5% of the cells were positive for MUC5B. MUC5B was also expressed in the bronchial glands as shown in Figure 8.5. An allocation of 3+ was assigned to 3 cases, of which Type II pneumocytes were positive with 2+ in 2 of the cases. Focal staining in the necrotic area was observed in 7 of the cases as illustrated in Figure 8.5. MUC5B positive staining was also observed on the periphery of the cytoplasm of giant cells. The giant cells within the tuberculous granuloma are shown in Figure 8.6.

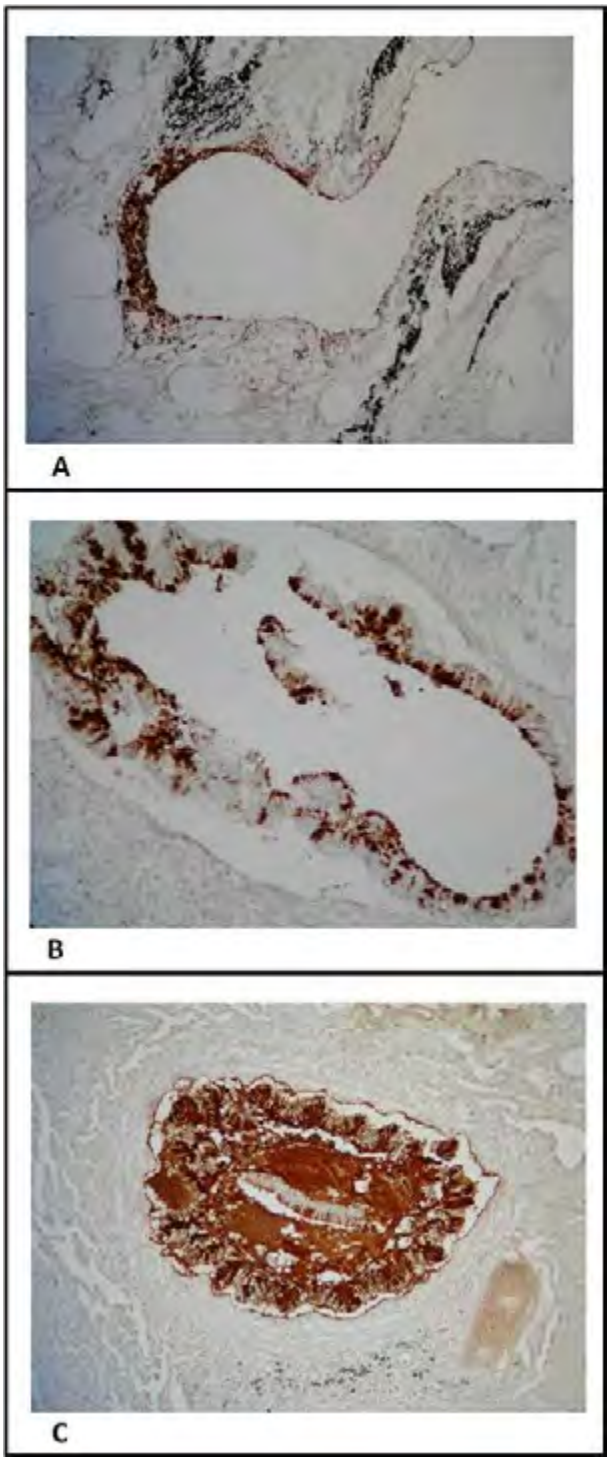

Figure 8.4: Immunohistochemical expression of the MUC5B mucins in bronchi.

(A) Expression of MUC5B in the goblet cells of the epithelium with a dark pigment from environmental carbon outside the bronchus (X40). (B) MUC5B expression in the goblet cells of the lining of the bronchus (x80). (C) Expression of the MUC5B luminal mucin in the bronchus (X40).

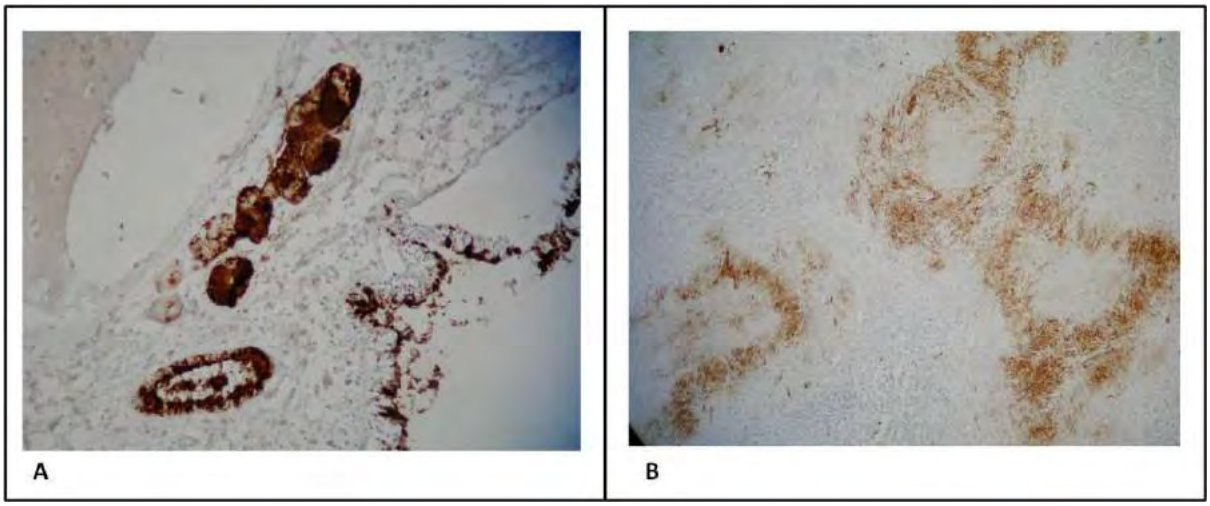

Figure 8.5: Immunohistochemical expression of the MUC5B mucins in lung tissue.

(A) MUC5B expression in the bronchial glands and the goblet cells of the bronchi (X80). (B) The expression of MUC5B in the necrotic areas in the TB lung, at magnification of X80.

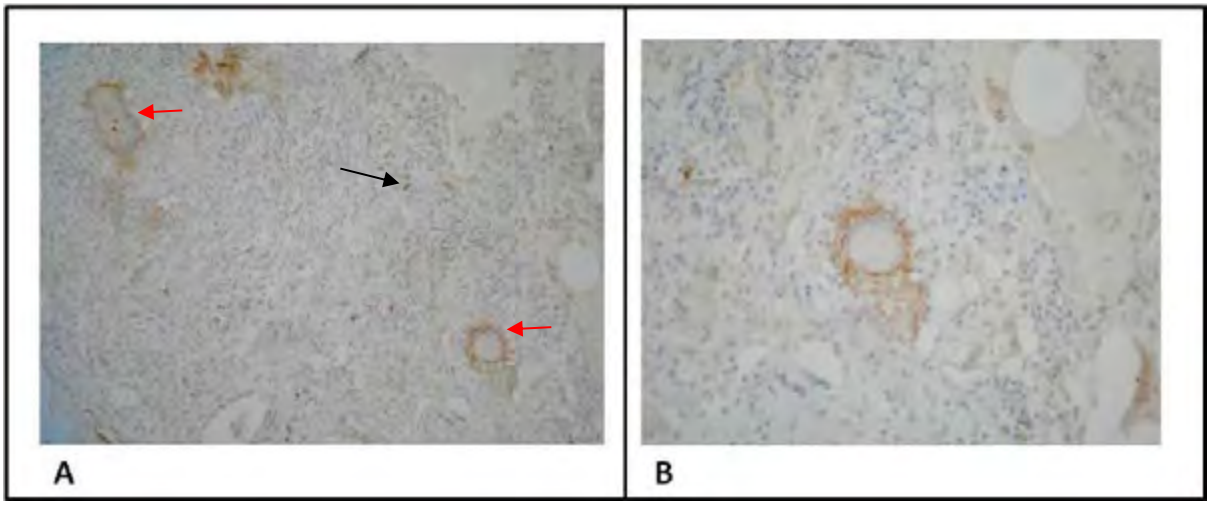

Figure 8.6: Expression of the MUC5B mucins in the tuberculous granuloma.

(A) Positive MUC5B staining on the periphery of the cytoplasm of the giant cells (red arrow heads) and in some of the epithelioid histiocytes of the granuloma (black arrow) (X80). (B) A magnified giant cell showing immunoreactivity of MUC5B on the periphery of the cytoplasm (X160).

8.2.3.4 MUC7

The expression of MUC7 was observed in all cases. One case showed the expression of MUC7 in the epithelia of the bronchi. In 2 cases, MUC7 was positive in the serous cells of the bronchial glands. Figure 8.7 illustrates the expression of MUC7 in the epithelia of the bronchi and the bronchial glands. Interestingly, in all 15 cases, focal staining of MUC7 was noted in the endothelial cells, giant cells in the granulomas, the epithelioid histiocytes of the granulomas and alveolar macrophages (histiocytes). MUC7 was observed in approximately 5% of the histiocytes in all the 15 cases. Figure 8.8 shows the expression of MUC7 in the granulomas. The MUC7 staining of giant cells was prominent in the centre of the cytoplasm. Sporadic staining was also observed in the alveolar space, and in one of the cases MUC7 was positive in caseous necrosis.

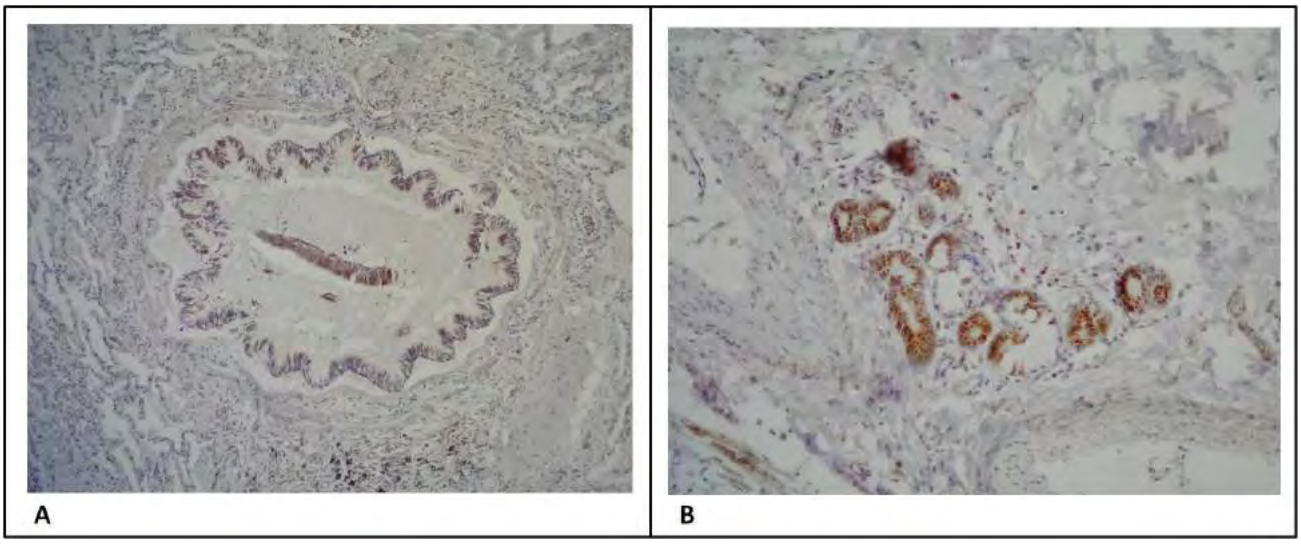

Figure 8.7: Expression of the MUC7 mucins in the epithelium of bronchus and bronchial glands.

(A) The epithelium of a bronchus expressing MUC7 mucins (X40). (B) Positive MUC7 staining in the serous cells of the bronchial glands (X80).

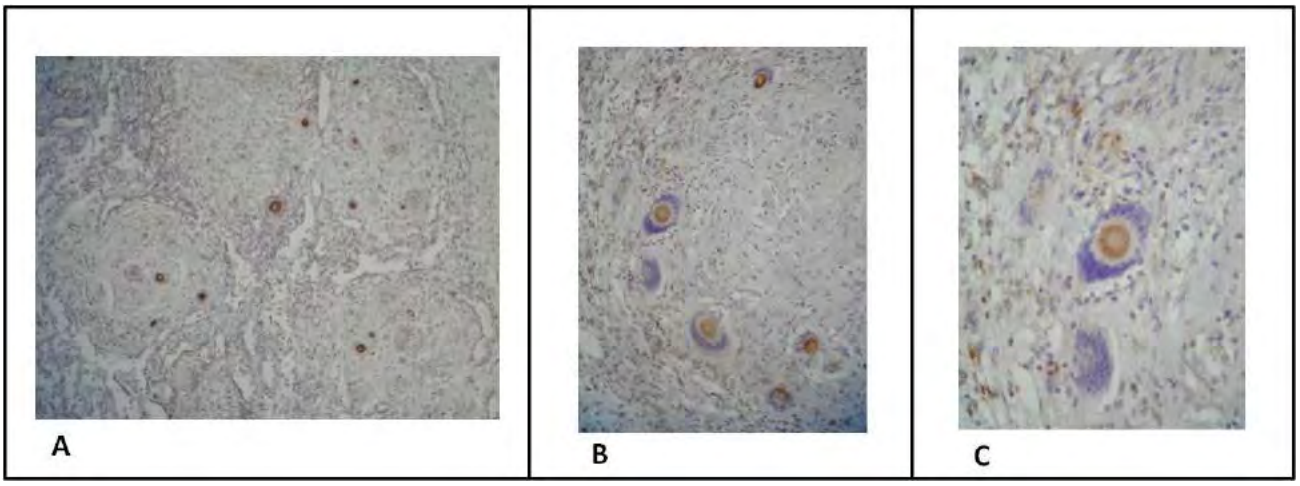

Figure 8.8: Expression of the MUC7 mucins in the tuberculous granulomas.

(A) Positive MUC7 staining in the granulomas (X40). (B) A magnified granuloma showing MUC7 staining of the central cytoplasm of the giant cells (X80). (C) A magnified giant cell showing staining of the central cytoplasm (X160).

8.2.3.5 MUC16

MUC16 positive staining was observed in 6 cases out of 15. MUC16 was expressed mainly in the goblet cells of the epithelia. Two cases were graded 4+, 1 case was graded 2+ and 3 cases were graded 1+. The expression of MUC16 was also observed in the bronchial glands, staining more than 75% of the cells in the glands. The expression of MUC16 in the bronchial epithelia and in the bronchial glands is depicted in Figure 8.9.

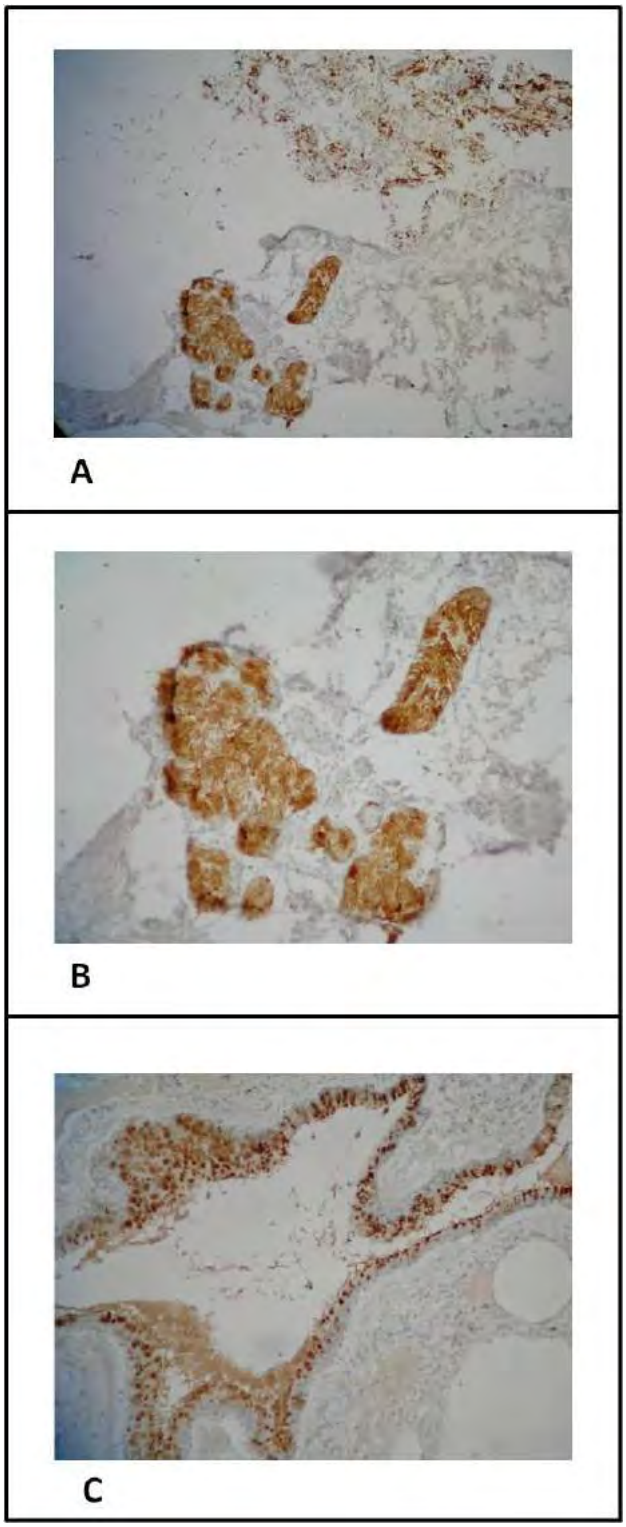

Figure 8.9: Expression of MUC16 mucins in the bronchial glands and in the epithelium of bronchus.

(A) Expression of MUC16 in the bronchial glands and the disrupted epithelium of the bronchus (X80). (B) Expression of MUC16 in the bronchial glands at a magnification of X160. (C) Goblet cells of the bronchial epithelium expressing MUC16 (X40).

8.3 Discussion

In normal tissue, mucin expression is regulated in a relatively organ- and cell-specific manner (Andrianifahanana *et al.*, 2006). However, distinct expression patterns are observed under pathologic conditions. MUC5AC mucins are expressed in the goblet cells of the epithelium and MUC5B mucins are expressed in the submucosal glands. However, MUC5B mucins have also been shown to be expressed in the surface epithelium.

The results in this study confirmed previous reports on the localisation of the expression of MUC5AC in the goblet cells of the respiratory epithelia in the lungs, the trachea and the bronchi (Lopez-Ferrer *et al.*, 2001). This study demonstrated that MUC5AC was expressed by bronchial cells and some goblet cells but not in all PAS positive epithelial cells. Work by Buisine and colleagues have shown the expression of MUC5AC from the developmental phase (Buisine *et al.*, 1999).

In this chapter, MUC5B was observed in both the bronchial epithelium and the bronchial glands. In addition, MUC5B was expressed in the granulomas. The reactivity of giant cells and histiocytes of the granuloma to both MUC5B and MUC7 respectively was an interesting finding in TB. The presence of *M.tb* in the lungs initiates an inflammatory immune response resulting in the recruitment of macrophages and neutrophils (Fallahi-Sichani *et al.*, 2013).

In TB, mature macrophages undergo transformation to form epithelioid histiocytes in the granuloma (that are characteristic of necrosis) and multinucleated giant cells (Ramakrishnan, 2012). Granulomas are described as aggregates of epithelioid histiocytes which form in an attempt to deal with bacteria that evade the immune system (Lugo-Villarino *et al.*, 2013; Mukhopadhyay and Gal, 2010).However, granulomas can dissociate as a result of increased necrosis and the accumulation of caseum in the center, ultimately forming cavities that disseminate and release the pathogen into the airways. The high expression of MUC5B and MUC7 in the giant cells of the granulomas suggests that these mucins are associated with solid granulomas that contain the infection through their intact cellular organization).

The giant cells are surrounded by lymphocytes that are primarily restricted to peripheral regions of granulomas, forming the lymphocytic cuff that keeps granulomas in an intact balanced state. This is the solid form of these pathological structures that is believed to control disease progression by containing or confining bacteria within the center of an intact granuloma.

MUC5B and MUC7 were found at different positions on the giant cells of the granulomas. MUC5B stained the periphery of the cytoplasm while MUC7 stained the centre (cytoplasm) of the giant cells. The significance of the differential staining is not yet known. In addition to its identification in the granulomas, MUC7 was detected in the serous cells in the bronchial glands of the lung tissue. The expression pattern mimicked the expression noticed in the salivary glands. This finding was consistent with that seen in studies investigating the expression of MUC7 in the respiratory tract (Li *et al.*, 2006; Sharma *et al.*, 1998). Moreover this study demonstrated the expression of MUC7 in the respiratory epithelium of the bronchi. The expression of MUC7 has never been previously reported in the epithelium of the human lung tissue. However, a study by (Li *et al.*, 2006) has shown the expression of MUC7 in the respiratory epithelium of the bronchioles of transgenic mice. They attributed this finding to the fact that their study examined MUC7 expression in transgenic mice lung tissue and not human lung tissue. They further found elevated MUC7 expression upon stimulation by the lipopolysaccharide of *P. aeruginosa*.

MUC7 is mainly secreted in the saliva and is also reported to be expressed in the respiratory tract. Most of the studies on the role of MUC7 have extensively focussed on the saliva. However, the role of MUC7 in respiratory diseases is not fully understood. Investigations on the interaction between MUC7 and oral bacteria such as *Streptococci* and *Staphylococcus aureus* have indicated that MUC7 provides a protective role in the oral cavity. Other studies have also been conducted to elucidate the role of MUC7 in the respiratory tract. Genetic studies have shown MUC7 to play a role in the protection of the respiratory tract of asthmatic individuals (Kirkbride *et al.*, 2001; Watson *et al.*, 2003). A study by (Fan and Bobek, 2010) has outlined the lack of understanding of MUC7 regulation in different stages of the different respiratory diseases. Their study however concluded that the elevation of MUC7 may facilitate the mucociliary clearance thereby playing a protective role in the

respiratory tract.

This chapter of the study has demonstrated that MUC5B together with MUC7 may provide a protective role in TB. Both MUC5B and MUC7 were expressed in the giant cells in the granulomas and the epithelioid histiocytes of the granulomas. Granulomas are considered to be the most common abnormality in pulmonary pathology (Mukhopadhyay and Gal, 2010). Furthermore they are reported to pose diagnostic challenges. Granulomas form in an attempt to contain infection by *M.tb*. Hence the expression of MUC5B and MUC7 in the granulomas might be in response to *M.tb* in an attempt to protect the lung against the bacteria.

CHAPTER 9 : GENERAL DISCUSSION AND CONCLUSION

Pathogens can enter the human body through several portals of entry. Most pathogens employ mechanisms such as evasion of the host defence, penetration of the host and adherence to host tissue. Many bacteria gain entry into the body by penetrating the mucous membranes and *Mycobaterium tuberculosis* (*M.tb*), the causative agent of tuberculosis (TB) is no exception (Neutra and Kozlowski, 2006). TB disease is among the top three leading causes of the death in the world (Cifuentes *et al.*, 2010). The aim of the study was to isolate and characterise mucus glycoproteins (mucins) in order to elucidate the role of the dominant secreted mucins in patients with TB.

Previous biochemical analyses of bronchial secretions have demonstrated that MUC5AC and MUC5B mucins are responsible for mucus gel formation. This study further confirmed that MUC5AC and MUC5B mucins are the major mucins secreted in TB. The Western blot analysis showed high levels of MUC5AC as compared to MUC5B in tracheal aspirates from uninfected controls, BALs and sputa from patients with TB. In contrast, the immunohistochemical analysis showed the expression of higher levels of the MUC5B mucin at lung tissue level. From these results, it is clear that MUC5B is highly expressed in the lung however lower levels are detected in the mucus. We therefore hypothesise that MUC5B is more tenacious and not easily expelled as compared to MUC5AC.

This study has also shown that MUC5AC mucin has similar charge densities in tracheal aspirates, BALs and sputa. A phenomenon supported by Thornton *et al.* (1996) that even though the level of MUC5AC mucin varies between respiratory samples, the electrophoretic mobility and charge density remains similar. This study further demonstrated MUC5AC and MUC5B mucins in BALs had similar charge densities in respiratory secretions. However the mobility of MUC5B varied between individuals indicative of the heterogeneous nature of MUC5B. MUC5B glycoforms were observed in tracheal aspirates and sputa. The existence of the MUC5B glycoforms in tracheal aspirates and sputa raised questions as to whether there are differences in the composition of MUC5B mucin in the lung, trachea and the mouth or saliva. Furthermore, whether saccharides are added to the MUC5B mucin produced in the lung during expectoration.

Immunohistochemisty has shown that granulomatous response in TB is characterized by MUC5B staining of the periphery of the giant cells and MUC7 staining in the cytoplasm of giant cells. The study has thus shown that mucus plays an important role in the recruitment of inflammatory responses and that both MUC5B and MUC7 seem to play a protective role in the granulomas. This could be a way of providing protection in the lung against *M.tb*.

In MDR-TB, mucins could not be detected from Western blot analysis. However, traces or no mucin was detected following dot blotting. This indicated depletion of mucins in MDR-TB. Further analysis of the patient indicated the presence of *Pseudomonas aeruginosa*. A study by (Aristoteli and Willcox, 2003) demonstrated that mucins were used as nutrient source in the progression of the infection. Therefore, the depletion of mucins in MDR-TB mucus suggested that there was mucin degradation by *P. aeruginosa*. Sialylation has also been found to be responsible for colonization of airways by *Pseudomonas* species (Varki, 2008). The O-glycan analysis showed high amounts of sialic acid in MDR-TB.

Protein studies have been undertaken to map and identify protein expression in healthy and diseased states. (Issa *et al.*, 2011) attempted to influence the migration of high molecular weight proteins during electrophoresis through the addition of urea to composite gels. However, they found that the addition of urea was beneficial in simplifying the gel casting procedure. In this study protein expression profiles were determined using 2D SDS PAGE. The 2D SDS PAGE together with AgPAGE and NuPAGE are systems used to analyse proteins. The different PAGES provide different stability of both protein and gel matrix and offer different resolutions. The study looked at tracheal aspirates from uninfected controls and BALs and sputa from patients with TB, in order to provide information about changes in protein composition in the airways in response to infection by *M.tb*. Cytoskeletal proteins, defence and immune proteins were higher in TB than in uninfected controls. These high cytoskeletal and structural proteins in TB may be due to lung tissue remodelling that takes place during disease progression. In addition, defence proteins might be higher in TB as they continuously fight off inhaled particles in an attempt to protect the lungs against infections

Glycosylation is one of the widely described post translational modifications. It provides many roles such as cell-cell interactions, protein stabilization to structural support and aiding in protein folding (Brockhausen *et al.*, 2009; Schauer, 2004). Core 3 and 4 O-glycan structures diminished in the presence of HIV.Core 5 structures were also detected using LC-MS. However, Core 5 structures are very rare. As this part of the work provided preliminary data, more investigations are required to confirm the presence of core 5 O-glycan structures and their differences.

Higher amounts of sialic acids which have been associated with inflammation in acute phase reaction and cell signaling events through cell-cell interaction were observed (Schauer, 2004; Varki, 2008). Protein analysis of respiratory secretions showed higher amounts of signaling molecules in TB. It is suggested that the higher signaling molecules found in TB may be attributed to active signaling events induced upon the recognition of the bacteria. Therefore, these increased signaling molecules could be related to the presence of increased sialic acids.

Limitations of the study

Sample procurement

- Individuals without respiratory diseases did not produce mucus even after sputum induction.
- Individuals without respiratory diseases do not undergo bronchoscopy as it is an invasive procedure.
- With the complication of HIV, some definite TB positive patients were sputum-scarce as they did not have a productive cough.
- All tissue blocks selected for the study were prepared from post mortem lung specimens with a known TB diagnosis. Lung tissue (from biopsies) could not be obtained from TB patients as the size of tissue obtained from biopsies is small for analysis.

Future work

- To expand the study on O-glycan structures as only three samples were examined in uninfected controls and TB. This expanded study should also investigate O-glycans from specific mucins excised following Western blotting. In addition, the presence of core 5 structures needs to be investigated further.
- The three bands of MUC5B found in TB samples following Western blotting need to be investigated further to confirm the bands identified.
- To design a cell culture (in vitro) model to establish the presence of MUC5B and MUC7; and to determine the pathways leading to the presence of MUC5B and MUC7 in the giant cells. An understanding of the pathophysiology of granulomas is critical for the design of new drugs and therapies.

Conclusion

This study has provided some information in understanding the behaviour of mucins in TB. Mucus was however weakened by opportunistic bacteria such as *P. aeruginosa* in MDR-TB. Co-infection of HIV in TB alters the structure of the O-glycans.

CHAPTER 10 : REFERENCES

Ali, M. E. S., Pearson, J. P. (2015). More Than One Disease Process in Chronic Sinusitis Based on Mucin Fragmentation Patterns and Amino Acid Analysis. *International Journal of Otolaryngology, 2015*, 8.

Ali, M. S., Pearson, J. P. (2007). Upper Airway Mucin Gene Expression: A Review. *The Laryngoscope, 117*(5), 932-938.

Ali, U., Nagi, A., Naseem, N., Ullah, E. (2012). Mucin Histochemistry in Tumours of Colon, Ovaries and Lung. *Journal of Cytology & Histology, 2012*.

Almutairi, F. M., Cifre, J. G. H., Adams, G. G., Kok, M. S., Mackie, A. R., de la Torre, J. G., Harding, S. E. (2016). Application of recent advances in hydrodynamic methods for characterising mucins in solution. *European Biophysics Journal, 45*(1), 45-54.

Andersch-Bjorkman, Y., Thomsson, K. A., Larsson, J. M. H. n., Ekerhovd, E., Hansson, G. C. (2007). Large scale identification of proteins, mucins, and their O-glycosylation in the endocervical mucus during the menstrual cycle. *Molecular & Cellular Proteomics, 6*(4), 708-716.

Andrianifahanana, M., Moniaux, N., Batra, S. (2006). Regulation of mucin expression: mechanistic aspects and implications for cancer and inflammatory diseases. *Biochemica et Biophysica Acta, 1765*(2), 189-222.

Arcos, J. s., Sasindran, S. J., Fujiwara, N., Turner, J., Schlesinger, L. S., Torrelles, J. B. (2011). Human Lung Hydrolases Delineate Mycobacterium tuberculosis “Macrophage Interactions and the Capacity To Control Infection. *The Journal of Immunology, 187*(1), 372-381.

Aristoteli, L. P., Willcox, M. D. (2003). Mucin degradation mechanisms by distinct Pseudomonas aeruginosa isolates in vitro. *Infection and immunity, 71*(10), 5565-5575.

Backstrom, M., Ambort, D., Thomsson, E., Johansson, M. E., Hansson, G. C. (2013). Increased understanding of the biochemistry and biosynthesis of MUC2 and other gel-forming mucins through the recombinant expression of their protein domains. *Molecular Biotechnology, 54*(2), 250-256.

Bajaj, D., Batra, J. K. (2012). *Heat Shock Proteins in Mycobacterium tuberculosis: Involvement in Survival and Virulence of the Pathogen*: INTECH Open Access Publisher.

Bansil, R., Turner, B. S. (2006). Mucin structure, aggregation, physiological functions and biomedical applications. *Current Opinion in Colloid & Interface Science, 11*(2–3), 164-170.

Becker, D., Lowe, J. (2003). Fucose: biosynthesis and biological function in mammals. *Glycobiology, 3*(7), 41R-53R.

Berg, J. M., Tymoczko, J. L., Stryer, L. (2002). Protein structure and function.

Bergeron, C. l., Boulet, L.-P. (2006). Structural changes in airway diseases*: Characteristics, mechanisms, consequences, and pharmacologic modulation. *CHEST Journal, 129*(4), 1068-1087.

Bhaskar, K., Reid, L. (1981). Application of density fraddient methods fot he study of mucus glycoprotein and other macromolecular components of the sol and gel phases of asthmatic sputa. *Journal of Biological Chemistry, 256*(14), 7583-7589.

Blixt, O., Westerlind, U. (2014). Arraying the post-translational glycoproteome (PTG). *Current opinion in chemical biology, 18*, 62-69.

Bradfute, S. B., Castillo, E. F., Arko-Mensah, J., Chauhan, S., Jiang, S., Mandell, M., Deretic, V. (2013). Autophagy as an immune effector against tuberculosis. *Current Opinion in Microbiology, 16*(3), 355-365.

Brashier, B. B., Kodgule, R. (2012). Risk factors and pathophysiology of chronic obstructive pulmonary disease (COPD). *J Assoc Physicians India, 60*, 17-21.

Brockhausen, I., Schachter, H., Stanley, P. (2009). O-GalNAc Glycans. In A. Varki, R. Cummings J. Esko (Eds.), *Essentials of glycobiology* (2nd ed.). Cold Spring Harbor NY: Cold Spring Harbor Press.

Buisine, M.-P., Devisme, L., Copin, M.-C., Durand-Reville, M., Gosselin, B., Aubert, J.-P., Porchet, N. (1999). Developmental mucin gene expression in the human respiratory tract. *American Journal of Respiratory Cell and Molecular Biology, 20*(2), 209-218.

Carlstedt, I., Lindgren, H., Sheehan, J. K. (1983). The macromolecular structure of human cervical-mucus glycoproteins. Studies on fragments obtained after reduction of disulphide bridges and after subsequent trypsin digestion. *Biochem J, 213*(2), 427-435.

Carlstedt, I., Sheehan, J. K. (1984). Macromolecular properties and polymeric structure of mucus glycoproteins. *Ciba Found Symp, 109*, 157-172.

Cherian, R. M., Jin, C., Liu, J., Karlsson, N. G., Holgersson, J. (2015). A Panel of Recombinant Mucins Carrying a Repertoire of Sialylated O-Glycans Based on Different Core Chains for Studies of Glycan Binding Proteins. *Biomolecules, 5*(3), 1810-1831.

Cifuentes, D. P., Ocampo, M., Curtidor, H., Vanegas, M., Forero, M., Patarroyo, M. E., Patarroyo, M. A. (2010). Mycobacterium tuberculosis Rv0679c protein sequences involved in host-cell infection: Potential TB vaccine candidate antigen. *BMC Microbiology, 10*(1), 1-12.

Colby, T., Leslie, K., Yousem, S. (2007). Lungs. In *Histology for pathologiists* (3rd ed., pp. 473-483). Philadelphia: Lippincottot Williams and Wilkins.

Corfield, A. P. (2015). Mucins: A biologically relevant glycan barrier in mucosal protection. *Biochimica et Biophysica Acta (BBA) - General Subjects, 1850*(1), 236-252.

Creeth, J., Bhaskar, K., Horton, J., Das, I., Lopez-Vidriero, M., Reid, L. (1977). The separation and characterization of bronchial glycoproteins by density-gradient methods. *Biochem Journal, 167*(3), 557-569.

Creeth, J., Denborough, M. (1970). The use of equilibrium-density-gradient methods for the preparation and characterization of blood-group-specific glycoproteins. *Biochem J, 117*, 879-891.

Curran, D. R., Cohn, L. (2010). Advances in Mucous Cell Metaplasia. *American Journal of Respiratory Cell and Molecular Biology, 42*(3), 268-275.

da Silva, L., Ferreira, F., Reis, F., de Britto, M., Levy, C., Clark, O., Ribeiro, J. (2013). Pseudomonas aeruginosa infection in patients with cystic fibrosis: scientific evidence regarding clinical impact, diagnosis, and treatment. *J Bras Pneumol, 39*(4), 495-512.

Davies, J. R., Herrmann, A., Russell, W., Svitacheva, N., Wickstrom, C., Carlstedt, I. (2002). Respiratory tract mucins: structure and expression patterns. *Mucus Hypersecretion in Respiratory Disease*, 76-88.

Davies, J. R., Kirkham, S., Svitacheva, N., Thornton, D. J., Carlstedt, I. (2007). MUC16 is produced in tracheal surface epithelium and submucosal glands and is present in secretions from normal human airway and cultured bronchial epithelial cells. *The International Journal of Biochemistry & Cell Biology, 39*(10), 1943-1954.

Davies, J. R., Svitacheva, N., Lannefors, L., Kornfalt, R., Carlstedt, I. (1999). Identification of MUC5B, MUC5AC and small amounts of MUC2 mucins in cystic fibrosis airway secretions. *Biochemical Journal, 344*(Pt 2), 321-330.

Dolowy, M., Pyka, A. (2014). Application of TLC, HPLC and GC methods to the study of amino acid and peptide enantiomers: a review. *Biomedical Chromatography, 28*(1), 84-101.

Elkington, P. T., Da Armiento, J. M., Friedland, J. S. (2011). Tuberculosis Immunopathology: The Neglected Role of Extracellular Matrix Destruction. *Science Translational Medicine, 3*(71), 71ps76-71ps76.

Evans, C. M., Kim, K., Tuvim, M. J., Dickey, B. F. (2009). Mucus hypersecretion in asthma: causes and effects. *Curr Opin Pulm Med, 15*(1), 4-11.

Fahy, J. V., Dickey, B. F. (2010). Airway Mucus Function and Dysfunction. *New England Journal of Medicine, 363*(23), 2233-2247.

Fallahi-Sichani, M., Marino, S., Flynn, J., Linderman, J., Kirschner, D. (2013). A system biology approach for understanding granuloma formation and function in tuberculosis. In *Systems Biology of Tuberculosis* (pp. 127-155). Springer New York.

Fan, H., Bobek, L. (2010). Regulation of human MUC7 mucin gene expression by cigarette smoke extract or cigarette smoke and Pseudomonas seruginosa lipopolysaccharide in human airway epithelial cells and in MUC7 transgenic mice. *The Open Respiratory Medicine Journal, 4*(1).

Fu, Y., Yi, Z., Guan, S., Zhang, S., Li, M. (2012). Proteomic analysis of sputum in patients with active pulmonary tuberculosis. *Clinical Microbiology and Infection, 18*(12), 1241-1247.

Fukuda, M. (2002). Roles of mucin-type O-glycans in cell adhesion. *Biochimica et Biophysica Acta (BBA) - General Subjects, 1573*(3), 394-405.

Garrett, R., Grisham, C. (2005). Biochemistry, Thomson Learning. *Inc., Stamford, Conn*.

Gorg, A., Bobermaier, C., Boguth, G., Scheibe, B., Wildgruber, R., Weiss, W. (2000). The current state of two-dimensional electrophoresis with immobilized pH gradients. *Electrophoresis, 21*(6), 1037-1053.

Govender, U. (2006). *The biochemical and molecular characterisation of respiratory mucins in TB.* University of Cape Town.

Groneberg, D. A., Eynott, P. R., Lim, S., Oates, T., Wu, R., Carlstedt, I., Roberts, P., McCann, B., Nicholson, A. G., Harrison, B. D., Chung, K. F. (2002). Expression of respiratory mucins in fatal status asthmaticus and mild asthma. *Histopathology, 40*(4), 367-373.

Guirado, E., Schlesinger, L. S. (2013). Modeling the Mycobacterium tuberculosis granuloma “the critical battlefield in host immunity and. *Frontiers in immunology, 4*(98), 2.

Gupta, A., Kaul, A., Tsolaki, A. G., Kishore, U., Bhakta, S. (2012). Mycobacterium tuberculosis: Immune evasion, latency and reactivation. *Immunobiology, 217*(3), 363-374.

Haenena, S., Clynenc, E., Nemeryb, B., Hoet, P., Vanoirbeekb, J. (2014). Biomarker discovery in asthma and COPD: Application of proteomics techniques in human and mice. *EuPA Open Proteomics, 4*, 101-112.

Harding, S. E. (1989). The macrostructure of mucus glycoproteins in solution. *Adv Carbohydr Chem Biochem, 47*, 345-381.

Hattrup, C. L., Gendler, S. J. (2008). Structure and function of the cell surface (tethered) mucins. *Annu. Rev. Physiol., 70*, 431-457.

Hauber, H., Foley, S., Hamid, Q. (2006a). Mucin overproduction in chronic inflammatory lung disease. *Canadian Respiratory Journal, 13*(6), 327 - 335.

Hauber, H.-P., Foley, S. C., Hamid, Q. (2006b). Mucin overproduction in chronic inflammatory lung disease. *Canadian Respiratory Journal : Journal of the Canadian Thoracic Society, 13*(6), 327-335.

Hazlett, L., Wu, M. (2011). Defensins in innate immunity. *Cell and tissue research, 343*(1), 175-188.

Henke, M. O., Renner, A., Huber, R. M., Seeds, M. C., Rubin, B. K. (2004). MUC5AC and MUC5B Mucins Are Decreased in Cystic Fibrosis Airway Secretions. *American Journal of Respiratory Cell and Molecular Biology, 31*(1), 86-91.

Holden, G., N., Y., Griggs, L., Weisbac, J. (1971). Gel electrophoresis of mucous glycoproteins.II. Effects of physical deaggregation and disulfide bond cleavage. *Biochem 10*, 3110-3113.

Hovenberg, H. W., Davies, J. R., Herrmann, A., Linden, C. J., Carlstedt, I. (1996). MUC5AC, but not MUC2, is a prominent mucin in respiratory secretions. *Glycoconj J, 13*(5), 839-847.

Hu, F., Liang, W., Ren, Z., Wang, G., Ding, G. (2012). Surfactant protein D inhibits lipopolysaccharide-induced monocyte chemoattractant protein-1expression in human renal tubular epithelial cells: implication for tubuloinstestitial fibrosis. *Clinical Experimental Immunology, 167*(3), 514-522.

Innes, A. L., Carrington, S. D., Thornton, D. J., Kirkham, S., Rousseau, K., Dougherty, R. H., Raymond, W. W., Caughey, G. H., Muller, S. J., Fahy, J. V. (2009). Ex vivo sputum analysis reveals impairment of protease-dependent mucus degradation by plasma proteins in acute asthma. *American journal of respiratory and critical care medicine, 180*(3), 203-210.

Issa, S. M. A., Schulz, B. L., Packer, N. H., Karlsson, N. G. (2011). Analysis of mucosal mucins separated by SDS-urea agarose polyacrylamide composite gel electrophoresis. *ELECTROPHORESIS, 32*(24), 3554-3563.

Jordan, T. S., Spencer, E. M., Davies, P. (2010). Tuberculosis, bronchiectasis and chronic airflow obstruction. *Respirology, 15*(4), 623-628.

Karim, S. S. A., Churchyard, G. J., Karim, Q. A., Lawn, S. D. (2009). HIV infection and tuberculosis in South Africa: an urgent need to escalate the public health response. *The Lancet, 374*(9693), 921-933.

Karve, T. M., Cheema, A. K. (2011). Small Changes Huge Impact: The Role of Protein Posttranslational Modifications in Cellular Homeostasis and Disease. *Journal of Amino Acids, 2011*.

Kato, K., Wang, S., Lin, Y., Kim, K. C. (2015). Role of Mucins In Respiratory Tract Inflammation *Recent Advances in Rhinosinusitis and Nasal Polyposis*, 103.

Kaushik, S., Cuervo, A. M. (2012). Chaperone-mediated autophagy: a unique way to enter the lysosome world. *Trends in Cell Biology, 22*(8), 407-417.

Kesimer, M., Kirkham, S., Pickles, R. J., Henderson, A. G., Alexis, N. E., DeMaria, G., Knight, D., Thornton, D. J., Sheehan, J. K. (2009). Tracheobronchial air-liquid interface cell culture: a model for innate mucosal defense of the upper airways? *American Journal of Physiology - Lung Cellular and Molecular Physiology, 296*(1), L92-L100.

Kesimer, M., Sheehan, J. (2012). Mass Spectrometric Analysis of Mucin Core Proteins. In M. A. McGuckin D. J. Thornton (Eds.), *Mucins* (Vol. 842, pp. 67-79): Humana Press.

Khan, A., Packer, N. H. (2006). Simple urinary sample preparation for proteomic analysis. *Journal of Preotione Research, 5*, 2824-2838.

Kim, K., McCracken, K., Lee, B., Shin, C., Jo, M., Lee, C., Ko, K. (1997). Airway goblet cell mucin: its structure and regulation of secretion. *European Respiratory Journal, 10*(11), 2644-2649.

Kim, W. (1997). Lung mucus: a clinician's view. *European Respiratory Journal, 10*(8), 1914-1917.

Kirkbride, H. J., Bolscher, J. G., Nazmi, K., Vinall, L. E., Nash, M. W., Moss, F. M., Mitchell, D. M., Swallow, D. M. (2001). Genetic polymorphism of MUC7: allele frequencies and association with asthma. *European Journal of Human Genetics, 9*(5), 347-354.

Kirkham, S., Sheehan, J., Knight, D., Richardson, P., Thornton, D. (2002a). Heterogeneity of airways mucus: variations in the amounts and glycoforms of the major oligomeric mucins MUC5AC and MUC5B. *Biochemical Journal, 361*(3), 537-546.

Kirkham, S., Sheehan, J. K., Knight, D., Richardson, P. S., Thornton, D. J. (2002b). Heterogeneity of airways mucus: variations in the amounts and glycoforms of the major oligomeric mucins MUC5AC and MUC5B. *Biochemical Journal, 361*(3), 537-546.

Kishore, U., Greenhough, T., Waters, P., Shrive, A., Ghai, R., Kamran, M., Beernal, A., Reid, K., Madan, T., Chakraborty, T. (2006). Surfactant proteins SP-A and SP-D: Structure, function and receptors. *Molecular Immunology, 43*(9), 1293-1315.

Kreda, S. M., Davis, C. W., Rose, M. C. (2012). CFTR, mucins, and mucus obstruction in cystic fibrosis. *Cold Spring Harb Perspect Med, 2*(9), a009589.

Kriegova, E., Melle, C., Kolek, V., Hutyrova, B., Mrazek, F., Bleul, A., du Bois, R. M., von Eggeling, F., Petrek, M. (2006). Protein Profiles of Bronchoalveolar Lavage Fluid from Patients with Pulmonary Sarcoidosis. *American journal of respiratory and critical care medicine, 173*(10), 1145-1154.

Kruh, N. A., Troudt, J., Izzo, A., Prenni, J., Dobos, K. M. (2010). Portrait of a pathogen: the Mycobacterium tuberculosis proteome in vivo. *PLoS One, 5*(11), e13938.

Lai, S. K., Wang, Y.-Y., Wirtz, D., Hanes, J. (2009). Micro- and macrorheology of mucus. *Advanced Drug Delivery Reviews, 61*(2), 86-100.

Landry, R., An, D., Hupp, J., Singh, P., Parsek, M. (2006). Mucin-Pseudomonas aeruginosa interactions promote biofilm formation and antibiotic resistance. *Molecular Microbiology, 59*(1), 142-151.

Lawn, S. D., Bekker, L.-G., Middelkoop, K., Myer, L., Wood, R. (2006). Impact of HIV Infection on the Epidemiology of Tuberculosis in a Peri-Urban Community in South Africa: The Need for Age-Specific Interventions. *Clinical Infectious Diseases, 42*(7), 1040-1047.

Li, Q. K., Shah, P., Li, Y., Aiyetan, P. O., Chen, J., Yung, R., Molena, D., Gabrielson, E., Askin, F., Chan, D. W., Zhang, H. (2013). Glycoproteomic Analysis of Bronchoalveolar Lavage (BAL) Fluid Identifies Tumor-Associated Glycoproteins from Lung Adenocarcinoma. *Journal of Proteome Research, 12*(8), 3689-3696.

Li, S., Intini, G., Bobek, L. A. (2006). Modulation of MUC7 Mucin Expression by Exogenous Factors in Airway Cells In Vitro and In Vivo. *American Journal of Respiratory Cell and Molecular Biology, 35*(1), 95-102.

Lindahl, M., Ståhlbom, B., Tagesson, C. (2001). Identification of a new potential airway irritation marker, palate lung nasal epithelial clone protein, in human nasal lavage fluid with two-dimensional electrophoresis and matrix-assisted laser desorption/ionization-time of flight. *ELECTROPHORESIS, 22*(9), 1795-1800.

Linden, S. K., Sutton, P., Karlsson, N. G., Korolik, V., McGuckin, M. A. (2008). Mucins in the mucosal barrier to infection. *Mucosal Immunol, 1*(3), 183-197.

Lopez-Ferrer, A., Curull, V., Barranco, C., Garrido, M., Lloreta, J., Real, F. X., de BolÃ³s, C. (2001). Mucins as Differentiation Markers in Bronchial Epithelium. *American Journal of Respiratory Cell and Molecular Biology, 24*(1), 22-29.

Lu, W., Zheng, J. (2013). The function of mucins in the COPD airway. *Current Respiratory Care Reports, 2*(3), 155-166.

Lugo-Villarino, G., Hudrisier, D., Benard, A., Neyrolles, O. (2013). Emerging trends in the formation and function of tuberculosis granulomas. *Front Immunol, 3*, 405.

Magi, B., Bargagli, E., Bini, L., Rottoli, P. (2006). Proteome analysis of bronchoalveolar lavage in lung diseases. *Proteomics, 6*(23), 6354-6369.

Mall, A., McLeod, H., Hickman, R., Kahn, D., Dent, D. (1999). Fragmentation Pattern of Mucins in Normal and Diseased Gastric Mucosae: A Glycoprotein Fractionates with Gastric

Mucins Purified from Mucosal scrapings of Cancer and Peptic Ulcer Patients. *Digestion, 60*, 216-226.

Marakalala, M. J., Guler, R., Matika, L., Murray, G., Jacobs, M., Brombacher, F., Rothfuchs, A. G., Sher, A., Brown, G. D. (2011). The Syk/CARD9-coupled receptor Dectin-1 is not required for host resistance to Mycobacterium tuberculosis in mice. *Microbes and Infection, 13*(2), 198-201.

Mayosi, B. M., Flisher, A. J., Lalloo, U. G., Sitas, F., Tollman, S. M., Bradshaw, D. (2009). The burden of non-communicable diseases in South Africa. *The Lancet, 374*(9693), 934-947.

Mehta, P. K., Raj, A., Singh, N., Khuller, G. K. (2012). Diagnosis of extrapulmonary tuberculosis by PCR. *FEMS Immunology & Medical Microbiology, 66*(1), 20-36.

Middleton, A. M., Chadwick, M. V., Nicholson, A. G., Dewar, A., Feldman, C., Wilson, R. (2003). Investigation of mycobacterial colonisation and invasion of the respiratory mucosa. *Thorax, 58*(3), 246-251.

Middleton, A. M., Chadwick, M. V., Nicholson, A. G., Dewar, A., Groger, R. K., Brown, E. J., Ratliff, T. L., Wilson, R. (2002). Interaction of Mycobacterium tuberculosis with human respiratory mucosa. *Tuberculosis (Edinb), 82*(2-3), 69-78.

Middleton, A. M., Chadwick, M. V., Nicholson, A. G., Dewar, A., Groger, R. K., Brown, E. J., Ratliff, T. L., Wilson, R. (2004). Inhibition of adherence of Mycobacterium avium complex and Mycobacterium tuberculosis to fibronectin on the respiratory mucosa. *Respiratory Medicine, 98*(12), 1203-1206.

Mizgerd, J. P. (2008). Acute Lower Respiratory Tract Infection. *New England Journal of Medicine, 358*(7), 716-727.

Morcillo, E. J., Cortijo, J. (2006). Mucus and MUC in asthma. *Curr Opin Pulm Med, 12*(1), 1-6.

Mukhopadhyay, S., Gal, A. A. (2010). Granulomatous Lung Disease: An Approach to the Differential Diagnosis. *Archives of Pathology & Laboratory Medicine, 134*(5), 667-690.

Neutra, M. R., Kozlowski, P. A. (2006). Mucosal vaccines: the promise and the challenge. *Nat Rev Immunol, 6*(2), 148-158.

Nicholas, B., Skipp, P., Mould, R., Rennard, S., Davies, D. (2006). Shotgun proteomic analysis of human-induced sputum. *Proteomics, 6*(15), 4390-4401.

Nie, S., Benito-Peña, E., Zhang, H., Wu, Y., Walt, D. R. (2013). Multiplexed Salivary Protein Profiling for Patients with Respiratory Diseases Using Fiber-Optic Bundles and Fluorescent Antibody-Based Microarrays. *Analytical Chemistry, 85*(19), 9272-9280.

Ong, C. W. M., Elkington, P. T., Friedland, J. S. (2014). Tuberculosis, Pulmonary Cavitation, and Matrix Metalloproteinases. *American journal of respiratory and critical care medicine, 190*(1), 9-18.

Pearson, J. P., Allen, A., Parry, S. (1981). A 70000-molecular-weight protein isolated from purified pig gastric mucus glycoprotein by reduction of disulphide bridges and its implication in the polymeric structure. *Biochemical Journal, 197*(1), 155-162.

Pelosi, P., Rocco, P., Negrini, D., Passi, A. (2007). The extracellular matrix of the lung and its role in edema formation. *Annals of the Brazilian Academy of Sciences, 79*(2), 285-297.

Perez-Vilar, J., Boucher, R. C. (2004). Reevaluating gel-forming mucins' roles in cystic fibrosis lung disease. *Free Radical Biology and Medicine, 37*(10), 1564-1577.

Plymoth, A., Löfdahl, C.-G., Ekberg-Jansson, A., Dahlbäck, M., Lindberg, H., Fehniger, T. E., Marko-Varga, G. (2003). Human bronchoalveolar lavage: Biofluid analysis with special emphasis on sample preparation. *Proteomics, 3*(6), 962-972.

Ramakrishnan, L. (2012). Revisiting the role of the granuloma in tuberculosis. *Nat Rev Immunol, 12*(5), 352-366.

Randell, S. H., Boucher, R. C. (2006). Effective Mucus Clearance Is Essential for Respiratory Health. *American Journal of Respiratory Cell and Molecular Biology, 35*(1), 20-28.

Ridley, C., Kouvatsos, N., Raynal, B. D., Howard, M., Collins, R. F., Desseyn, J.-L., Jowitt, T. A., Baldock, C., Davis, C. W., Hardingham, T. E., Thornton, D. J. (2014). Assembly of the respiratory mucin MUC5B: a new model for a gel-forming mucin. *The Journal of Biological Chemistry, 289*(23), 16409-16420.

Rose, M. C., Nickola, T. J., Voynow, J. A. (2001). Airway Mucus Obstruction: Mucin Glycoproteins, MUC Gene Regulation and Goblet Cell Hyperplasia. *American Journal of Respiratory Cell and Molecular Biology, 25*(5), 533-537.

Rose, M. C., Voynow, J. A. (2006). Respiratory tract mucin genes and mucin glycoproteins in health and disease. *Physiological Reviews, 86*(1), 245-278.

Rousseau, K., Byrne, C., Kim, Y. S., Gum, J. R., Swallow, D. M., Toribara, N. W. (2004). The complete genomic organization of the human MUC6 and MUC2 mucin genes. *Genomics, 83*(5), 936-939.

Rubin, B. K. (2010a). Mucus and mucins. *Otolaryngol Clin North Am, 43*(1), 27-34, vii-viii.

Rubin, B. K. (2010b). The role of mucus in cough research. *Lung, 188*(1), 69-72.

Sacchettini, J. C., Rubin, E. J., Freundlich, J. S. (2008). Drugs versus bugs: in pursuit of the persistent predator Mycobacterium tuberculosis. *Nat Rev Micro, 6*(1), 41-52.

Schauer, R. (2004). Sialic acids: fascinating sugars in higher animals and man. *Zoology, 107*(1), 49-64.

Schauer, R. (2009). Sialic acids as regulators of molecular and cellular interactions. *Current Opinion in Structural Biology, 19*(5), 507-514.

Schulz, B. L., Packer, N. H., Karlsson, N. G. (2002). Small-Scale Analysis of O-Linked Oligosaccharides from Glycoproteins and Mucins Separated by Gel Electrophoresis. *Analytical Chemistry, 74*(23), 6088-6097.

Scott, E. M., Carter, A. M., Findlay, J. B. C. (2005). The application of proteomics to diabetes. *Diabetes and Vascular Disease Research, 2*, 54-60.

Sharma, P., Dudus, L., Nielsen, P. A., Clausen, H., Yankaskas, J. R., Hollingsworth, M. A., Engelhardt, J. F. (1998). MUC5B and MUC7 Are Differentially Expressed in Mucous and Serous Cells of Submucosal Glands in Human Bronchial Airways. *American Journal of Respiratory Cell and Molecular Biology, 19*(1), 30-37.

Sheehan, J. K., Kirkham, S., Howard, M., Woodman, P., Kutay, S., Brazeau, C., Buckley, J., Thornton, D. J. (2004). Identification of molecular intermediates in the assembly pathway of the MUC5AC mucin. *Journal of Biological Chemistry, 279*(15), 15698-15705.

Sheehan, J. K., Thornton, D. J., Somerville, M., Carlstedt, I. (1991). Mucin structure. The structure and heterogeneity of respiratory mucus glycoproteins. *Am Rev Respir Dis, 144*(3 Pt 2), S4-9.

Silveyra, P., Floros, J. (2013). Genetic complexity of the human surfactant-associated proteins SP-A1 and SP-A2. *Gene, 531*(2), 126-132.

Sloane, A., Lindner, R., Prasad, S., Sebastuan, L., Pedersen, S., Robinson, M., Bye, P., Nielson, D., Harry, J. (2005). Proteomic analysis of sputum from adults and children with cystic fibrosis and from control subjects. *Am J Respir Crit Care Med, 172*(11), 1416-1426.

Sonawane, A., Mohanty, S., Jagannathan, L., Bekolay, A., Banerjee, S. (2012). Role of glycans and glycoproteins in disease development by Mycobacterium tuberculosis. *Critical reviews in microbiology, 38*(3), 250-266.

Streicher, E. M., Muller, B., Chihota, V., Mlambo, C., Tait, M., Pillay, M., Trollip, A., Hoek, K. G., Sirgel, F. A., van Pittius, N. C. G. (2012). Emergence and treatment of multidrug resistant (MDR) and extensively drug-resistant (XDR) tuberculosis in South Africa. *Infection, genetics and evolution, 12*(4), 686-694.

Swaminathan, S., Narendran, G. (2005). Extra-Pulmonary Tuberculosis. *Medicine*, 652.

Takahashi, M., Kuroki, Y., Ohtsubo, K., Taniguchi, N. (2009). Core fucose and bisecting GlcNAc, the direct modifiers of the N-glycan core: their functions and target proteins. *Carbohydrate Research, 344*(12), 1387-1390.

Takeuchi, K., Yuta, A., Sakakura, Y. (1995). MUC2 mucin expression in the nose and maxillary sinus. *Journal of Otolaryngology, 16*(6), 391-395.

Thornton, D., Howard, M., Devine, P., Sheehan, J. (1995). Methods for separation and deglycosylation of mucin subunits. *Analytical Biochemisty, 227*(1), 162-167.

Thornton, D. J., Carlstedt, I., Howard, M., Devine, P. L., Price, M. R., Sheehan, J. K. (1996). Respiratory mucins: identification of core proteins and glycoforms. *Biochem J, 316 (Pt 3)*, 967-975.

Thornton, D. J., Davies, J. R., Carlstedt, I., Sheehan, J. K. (1997a). Structure and biochemistry of human respiratory mucins. In *Airway Mucus: Basic Mechanisms and Clinical Perspectives* (pp. 19-39): Springer.

Thornton, D. J., Davies, J. R., Kraayenbrink, M., Richardson, P. S., Sheehan, J. K., Carlstedt, I. (1990). Mucus glycoproteins from 'normal' human tracheobronchial secretion. *Biochem J, 265*(1), 179-186.

Thornton, D. J., Howard, M., Khan, N., Sheehan, J. K. (1997b). Identification of two glycoforms of the MUC5B mucin in human respiratory mucus evidence for a cysteine-rich sequence repeated within the molecule. *Journal of Biological Chemistry, 272*(14), 9561-9566.

Thornton, D. J., Rousseau, K., McGuckin, M. A. (2008). Structure and Function of the Polymeric Mucins in Airways Mucus. *Annual Review of Physiology, 70*(1), 459-486.

Thornton, D. J., Sheehan, J. K. (2004). From mucins to mucus: toward a more coherent understanding of this essential barrier. *Proceedings of the American Thoracic Society, 1*(1), 54-61.

Tian, E., Ten Hagen, K. G. (2009). Recent insights into the biological roles of mucin-type O-glycosylation. *Glycoconjugate journal, 26*(3), 325-334.

Torrelles, J. B. (2012). *Broadening our view about the role of Mycobacterium tuberculosis cell envelope components during infection: a battle for survival*: INTECH Open Access Publisher.

Tytgat, K. M., Swallow, D. M., Van Klinken, B. J., Buller, H. A., Einerhand, A. W., Dekker, J. (1995). Unpredictable behaviour of mucins in SDS/polyacrylamide-gel electrophoresis. *Biochem J, 310 (Pt 3)*, 1053-1054.

van Zyl Smit, R. N., Pai, M., Yew, W. W., Leung, C. C., Zumla, A., Bateman, E. D., Dheda, K. (2010). Global lung health: the colliding epidemics of tuberculosis, tobacco smoking, HIV and COPD. *European Respiratory Journal, 35*(1), 27-33.

Vareille, M., Kieninger, E., Edwards, M. R., Regamey, N. (2011). The airway epithelium: soldier in the fight against respiratory viruses. *Clinical microbiology reviews, 24*(1), 210-229.

Varki, A. (2008). Sialic acids in human health and disease. *Trends in molecular medicine, 14*(8), 351-360.

Vinall, L. E., Fowler, J. C., Jones, A. L., Kirkbride, H. J., de Bolos, C., Laine, A., Porchet, N., Gum, J. R., Kim, Y. S., Moss, F. M., Mitchell, D. M., Swallow, D. M. (2000). Polymorphism of human mucin genes in chest disease: possible significance of MUC2. *Am J Respir Cell Mol Biol, 23*(5), 678-686.

Voynow, J. A., Gendler, S. J., Rose, M. C. (2006). Regulation of mucin genes in chronic inflammatory airway diseases. *Am J Respir Cell Mol Biol, 34*(6), 661-665.

Voynow, J. A., Selby, D. M., Rose, M. C. (1998). Mucin gene expression (MUC1, MUC2, and MUC5/5AC) in nasal epithelial cells of cystic fibrosis, allergic rhinitis, and normal individuals. *Lung, 176*(5), 345-354.

Wang, Y., Kuan, P. J., Xing, C., Cronkhite, J. T., Torres, F., Rosenblatt, R. L., DiMaio, J. M., Kinch, L. N., Grishin, N. V., Garcia, C. K. (2009). Genetic defects in surfactant protein A2 are associated with pulmonary fibrosis and lung cancer. *Am J Hum Genet, 84*(1), 52-59.

Wantanabe, K., Ohta, M., Yada, K., Komori, Y., Iwashita, Y., Kashima, K., Inomata, M. (2016). Fucosylation is associated with the malignant transformation of intraductal papillary mucinous neoplasms: a lectin microarray-based stufy. *Surgery Today*, 1-7.

Watson, A., Troxler, R., Pena, M., Kandil, A., Berger, J., Rose, M. (2003). Muc7 mucin glycoprotein is present in airway secretions of asthmatic, but not control, patients. *Am J Respir Crit Care Med, 167*, A465.

Wattiez, R., Hermans, C., Bernard, A., Lesur, O., Falmagne, P. (1999). Human bronchoalveolar lavage fluid: Two-dimensional gel electrophoresis, amino acid microsequencing and identification of major proteins. *Electrophoresis, 20*(7), 1634-1645.

Wattiez, R., Michel, O., Falmagne, P. (2007). Proteomics of Bronchoalveolar Lavage Fluid and Sputum. In V. Thongboonkerd (Ed.), *Proteomics of Human Body Fluids* (pp. 309-325): Humana Press.

WHO. (2010). Multidrug and extensively drug-resistant TB (M/XDR-TB) : 2010 global report on surveillance and response. 1-71.

WHO. (2015). Tuberculosis Fact Sheet N˚ 104.

Wickstrom, C., Davies, J. R., Eriksen, G. V., Veerman, E. C., Carlstedt, I. (1998). MUC5B is a major gel-forming, oligomeric mucin from human salivary gland, respiratory tract and endocervix: identification of glycoforms and C-terminal cleavage. *Biochemical Journal, 334*(3), 685-693.

Widdicombe, J. (1995). Relationships among the composition of mucus, epithelial lining liquid, and adhesion of microorganisms. *American journal of respiratory and critical care medicine, 151*(6), 2088-2092; discussion 2092-2083.

Woodward, H., Horsey, B., Bhavandan, V., Davidson, E. (1982). Isolation, purification, and properties of respiratory mucus glycoproteins. *Biochemistry, 21*(4), 694-701.

Yan, J., Packer, N. (2000). Amino Acid Analysis of Mucins. In A. Corfield (Ed.), *Glycoprotein Methods and Protocols* (Vol. 125, pp. 113-119): Humana Press.

Yilmaz, M. B., Zorlu, A., Dogan, O. T., Karahan, O., Tandogan, I., Akkurt, I. (2011). Role of CA-125 in Identification of Right Ventricular Failure in Chronic Obstructive Pulmonary Disease. *Clinical Cardiology, 34*(4), 244-248.